UNIVERSITÉ DE MONTRÉAL

THERMOPLASTIC ELASTOMER NANOCOMPOSITES BASED ON POLYPROPYLENE AND ETHYLENE PROPYLENE DIENE TERPOLYMER (PP/EPDM)

GHASEM NADERI

DÉPARTEMENT DE GÉNIE CHIMIQUE

ÉCOLE POLYTECHNIQUE DE MONTRÉAL

THÉSE PRÉSENTÉE EN VUE DE L'OBTENTION

DU DIPLÔME DE PHILOSOPHIAE DOCTOR

(GÉNIE CHIMIQUE)

Novembre 2006

Your file Votre référence
ISBN: 978-0-494-24545-3
Our file Notre référence
ISBN: 978-0-494-24545-3

UNIVERSITÉ DE MONTRÉAL

ÉCOLE POLYTECHNIQUE DE MONTRÉAL

Cette thèse intitulée :

THERMOPLASTIC ELASTOMER NANOCOMPOSITES BASED ON POLYPROPYLENE AND ETHYLENE PROPYLENE DIENE TERPOLYMER (PP/EPDM)

Présentée par: NADERI Ghasem

en vue de l'obtention du diplôme de : Philosophie Doctor

a été dûment acceptée par le jury d'examen constitué de :

M. SRINIVASAN Bala, Ph.D., président

M. LAFLEUR Pierre, Ph.D., membre et directeur de recherche

M. DUBOIS Charles, Ph.D., membre et codirecteur de recherche

M. AJJI Abdellah, Ph.D., membre

M. KAMAL Musa R., Ph.D., membre

Dedicated to my grand father, grand mother and my son "Navid"

ACKNOWLEDGEMENTS

I would like to express my heartfelt gratitude to my thesis director, Professor Pierre G. Lafleur for his kind guidance, and helpful suggestions throughout my Ph.D. research.

I would like to thank my research co-director Professor Charles Dubois for his patience during the numerous discussions that we had, which were helpful for my scientific formation.

I want to express appreciation to all the staff of the chemical engineering department for their help during the course of my Ph.D. at Ecole Polytechnique de Montreal University.

I would also like to show gratitude to all my colleagues of the research group for their good friendship, interesting discussions and comments.

I must acknowledge my family: my parents, my sisters, my brother, and my wife for their support during the four years of studies in Montreal.

I must thank God (Allah) for all his kindness to me and to mine.

RÉSUMÉ

Dans cette étude, des nanocomposites à base d'élastomères thermoplastiques vulcanisés dynamiquement (nanocomposites de TPVs) ont été préparés par un procédé de mélange à l'état fondu en trois étapes. Des nanocomposites à base d'élastomères thermoplastiques non vulcanisés (nanocomposites de TPEs) ont été également obtenus en utilisant un processus de mélange en une étape. Trois types de polypropylène (PP) avec différents indices de viscosité, le monomère de diène de propylène d'éthylène (EPDM), le polypropylène modifié par anhydride maléique (PPMA), à titre de compatibilisant, et un nanoargile modifié d'un intercalant (Cloisite 15A) ont été utilisés dans ce travail. Pendant la première étape du processus de préparation des TPVs, la poudre d'argile et des granules de PPMA ont été mélangés à l'état fondu pour obtenir un mélange maître où le rapport de PPMA/argile a été maintenu constant à 3:1. Dans la deuxième étape, le polyproplène et le nanoargile ont été ajoutés au mélange maître sec. Dans la troisième et dernière étape, le nanocomposite argile/polypropylène préparé à l'étape 2, le EPDM, l'oxyde de zinc (Zno) et l'acide stéarique (St.Ac.) ont été mélangés à l'état fondu. Trois à quatre minutes après la fonte du polypropylène, les additifs de catalyse et de vulcanisation, soient le bisulfure tétra-méthylique de thiuram (TMTD), le bisulfure de benzothiazyl (MBTS) et le soufre ont été incorporés au mélange. Les structures des nanocomposites ont été caractérisées par les techniques de diffraction de rayon X (XRD), microscopie à transmission (TEM) ou balayage électronique (SEM), calorimétrie, mesure des propriétés mécaniques et rhéologie.

Dans la première partie de ce travail, nous avons étudié l'effet de la viscosité du PP et du contenu en argile sur la microstructure et les propriétés mécaniques des nanocomposites TPV. L'évolution de la microstructure de nanocomposite pendant le processus de mélange a été également surveillée. Le couple mesuré sur l'arbre d'agitation était plus élevé pour des mélanges contenant du PPMA, indiquant ainsi une meilleure dispersion de l'argile. Les résultats de XRD ont montré que la crête d_{001} des nanocomposites de TPV basés sur PP/EPDM (40/60) a été décalée vers des angles inférieurs comparés aux organo-argiles brutes. On a constaté que la microstructure des nanocomposites est sensible à la différence de viscosité entre la phase thermoplastique et l'élastomère, et aussi à la teneur en argile. Avant la vulcanisation, les TPV préparés à partir de polypropylène de faible viscosité montraient une meilleure dispersion de l'argile dans le thermoplastique. L'analyse TEM d'un TPV contenant 60 % EPDM préparé avec du polypropylène de basse viscosité et 2 en % poids d'organo-argile a confirmé que le nano-argile était exfoliée et aléatoirement distribué dans la phase de polypropylène. Les photomicrographies de SEM des échantillons thermoplastiques dynamiquement vulcanisés d'élastomère ont préparé avec 60 % poids EPDM ont montré que les particules en caoutchouc ont été dispersées par le polypropylène dans la forme d'agrégats et leur taille accrue avec l'introduction de l'argile. L'addition d'argile a eu comme conséquence une amélioration significative du module en tension des nanocomposites TPV, une réduction du degré de cristallinité, une augmentation de la température de cristallisation de polymère et une réduction de la perméabilité à l'oxygène.

La deuxième partie de ce travail est consacrée à l'étude des propriétés rhéologiques et morphologiques des nanocomposites TPV. Les effets de la teneur en EPDM, PPMA et de la viscosité du polypropylène ont été considérés. Dans le cas des nanocomposites sans PPMA, l'absence d'agent de mouillage a empêché les chaînes de polypropylène de pénétrer efficacement entre les couches de silicate de l'argile. Cependant, la distance de couche intercalaire de l'argile a néanmoins été augmentée par le processus de vulcanisation, se qui s'est aussi traduit par une augmentation du module d'emmagasinement (G'). La dispersion de l'argile a été améliorée en incorporant le PPMA aux nanocomposites de PP et de TPV, principalement pour les compositions à base de PP de faible viscosité. Une augmentation importante du module G', de la contrainte seuil et une translation du plateau vers des plus basses fréquences ont été observés en comparaison de la matrice équivalente sans PMMA. L'agglomération de l'argile a diminué quand la concentration de la phase en caoutchouc a été augmentée. Les résultats de SEM ont montré que l'ampleur de la formation d'agglomérats dans les particules en caoutchouc était plus grande quand la taille de celles-ci, et donc la teneur en caoutchouc ont été augmentés. Le modèle de Carreau-Yasuda avec une contrainte seuil et un modèle viscoélastique linéaire, tenant compte de la fraction volumique maximale (ϕ_m), ont été utilisés pour décrire les propriétés viscoélastiques linéaires des nanocomposites TPV à l'état fondu. L'ajustement de ϕ_m aux données expérimentales a montré que celui-ci augmente avec l'augmentation du contenu d'EPDM.

Dans la troisième partie de cette étude, nous avons examiné la microstructure, la rhéologie, et les propriétés mécaniques des élastomères thermoplastiques de

nanocomposite (nanocomposites de TPE). Des teneurs en caoutchouc de 20, 40, et 60 % en poids ont été employées avec du polypropylène de différentes viscosités et de 3 % poids de nano-argile. L'analyse par XRD à montré une intercalation des nanoargiles pour toutes ces compositions. Dans les nanocomposites TPE faits à partir de PP de faible viscosité, l'intensité des pics de diffraction de rayon X a augmenté quand le contenu d'EPDM a été augmenté. Les résultats de TEM correspondants ont indiqué que l'argile a été dispersée principalement dans la phase en thermoplastique, alors que, pour le TPE nanocomposite utilisant un PP de haute viscosité, les feuillets de silicate s'avéraient être dispersées dans les phases d'EPDM et de PP. Les résultats de micrographie SEM ont montré que le diamètre moyen en volume (dv) des particules de caoutchouc dans les mélanges ayant 20, 40 ou 60 % d'EPDM diminuait avec l'augmentation de la viscosité de la phase PP. Les échantillons nano-argile-remplis provenant de LVP ont démontré une réduction de la taille des particules en caoutchouc comparées aux mélanges déchargés. La taille des gouttelettes en caoutchouc dispersées s'est avérée plus grande pour les mélanges nano-argile-remplis contenant 40 et 60 % EPDM préparés avec des HVP en comparaison des échantillons déchargés équivalents. Le TPE nano-argile-rempli a préparé avec LVP a illustré plus de perfectionnement dans le contrainte seuil comparé aux échantillons correspondants de HVP. L'augmentation du module et de la diminution de stockage de la pente terminale est avérée plus grande pour l'hybride de LVP en comparaison de l'échantillon équivalent de HVP. Les propriétés mécaniques étaient conformées à la structure morphologique trouvée par

SEM et TEM. Le module de tension a été amélioré pour tous les nanocomposites et a obtenu des pour cent plus élevés augmentent dans le cas des échantillons de LVP.

ABSTRACT

In this study, dynamically vulcanized nanocomposite thermoplastic elastomers (TPV nanocomposites) were prepared by a three-step melt mixing process. Uncured nanocomposite thermoplastic elastomers (TPE nanocomposites) were also prepared using a one-step melt mixing method. Three types of polypropylene (PP) with different melt flow index, an ethylene propylene diene monomer (EPDM), a maleic anhydride modified polypropylene (PPMA) as compatibilizer, and an organo-clay (Cloisite 15A) were employed in this work.

In the first part of this study, we prepared the dynamically-vulcanized nanocomposite thermoplastic elastomers (TPV nanocomposites) based on PP/EPDM (40/60, w/w) while investigating the effect of viscosity ratio of the plastic to the rubber and organo-clay content on their microstructure and mechanical properties. The evolution of the nanocomposite microstructure during the mixing process was also monitored.

The TPV nanocomposites exhibited higher steady-state value of the mixing torque in comparison with similar but unfilled TPVs prepared with PPMA. The XRD results revealed that the peak d_{001} of the clay in the TPV nanocomposites prepared with activators, accelerators, and sulfur was shifted toward lower angles compared with the original clay (Cloisite 15A). The first characteristic peak of the organo-clay disappeared for the TPV nanocomposites containing different viscosities of PP and 60 % EPDM when post processing was applied to these samples. It was found that the

microstructure of the prepared TPV nanocomposites is sensitive to the viscosity difference between the two phases (PP, and EPDM) and the clay content. The TEM image of the TPV nanocomposite prepared from low viscosity polypropylene (LVP) before curing stage (selectively reinforced PP-phase TPE nanocomposite) indicated that the silicate layers were dispersed throughout the PP matrix and could not penetrate into the EPDM phase during the mixing process. In the uncured TPV nanocomposites (before curing stage) based on high viscosity PP (HVP), however, the nanoclays were found to be dispersed in the continuous phase (PP) and partly agglomerated at interfacial boundary between the plastic and rubber phases. The TEM image of the TPV sample prepared from 60 % EPDM, and 40 % LVP at 2 wt % of the organo-clay showed that the silicate layers were nearly exfoliated and randomly distributed into the polypropylene phase. The SEM photomicrographs of the TPV samples prepared with 60 wt % of the elastomer revealed that the rubber particles were dispersed through the polypropylene matrix in form of aggregates and their size increased with the introduction of the clay. The nanoscale dimensions of the dispersed clay resulted in a significant improvement of the tensile modulus of the TPV nanocomposite from 20 to 90 % depending on the viscosity ratio of PP/EPDM and the clay content. Moreover, the oxygen permeability in the TPV nanocomposites based on PP/EPDM (40/60) at 2 wt % of the clay was found to be lower than in the unfilled but otherwise similar materials.

The second part of this work is devoted to study the rheological and morphological properties of the dynamically vulcanized nanocomposite thermoplastic elastomers (TPV nanocomposites), based on EPDM and PP containing 20, 40, and 60

wt % of the rubber at 2 wt % of the clay. The effects of composition, PPMA as compatibilizer, and different viscosities of polypropylene were also investigated.

The interlayer distance of the clay was increased in the TPV nanocomposites prepared from different viscosities of PP, but without PPMA, and containing 20, 40 or 60 % EPDM. In the TPV nanocomposite (without PPMA) the storage modulus curve significantly increased in comparison with the corresponding matrix. The agglomeration of the clay considerably decreased when the rubber content was increased. The yield stress of the prepared TPV nanocomposites, based on low viscosity PP, increased more than that for the hybrids having high viscosity PP. The TPV nanocomposites containing 20, 40 and 60 % EPDM exhibited strong elastic modulus that tends to plateau out at low shear rates. SEM results of the TPV samples showed that the agglomerate formation of the rubber particles was enhanced by the increased rubber aggregate size when the rubber content was increased. A Carreau-Yasuda law with a yield stress and a linear viscoelastic model, taking into account the maximum packing volume (ϕ_m), were used to describe the melt linear viscoelastic properties of the TPV nanocomposites. Considerable agreement was found between the linear viscoelastic model and the experimental data in the TPV nanocomposites, containing 60 % EPDM. In this model, the maximum packing volume increased with increasing the rubber content.

In the third part of this study, we examined the microstructure, rheology, and mechanical properties of the uncured nanocomposite thermoplastic elastomers (TPE nanocomposites) prepared by a one-step melt mixing process.

In the uncured TPE nanocomposites based on low viscosity PP (LVP), the intensity of the X-ray diffraction peaks increased when the rubber content was increased. However, the XRD peaks were almost similar in shape for the unvulcanized TPE samples prepared with medium viscosity PP (MVP) and different contents of the rubber. In contrary, the intensity of the XRD patterns decreased as the elastomer content was increased in the uncured TPE hybrids prepared from high viscosity PP (HVP). TEM results of the TPE nanocomposites prepared from LVP revealed that the silicate layers were mainly dispersed in the plastic phase, however, for the TPE nanocomposite based on HVP, the clay was found to be dispersed in both the EPDM and PP phases. The nanoclay-filled TPE samples prepared from LVP demonstrated a reduction in the size of the rubber particles compared with similar but unloaded blends. The size of the dispersed rubber droplets was shown to be larger for the nanoclay-filled blends prepared with HVP having 40 and 60 % EPDM in comparison with the equivalent samples without the clay. The nanoclay-filled TPEs prepared with LVP exhibited more enhancement in yield stress compared with the HVP based samples. The increase in the storage modulus and the decrease in the terminal zone slope of the elastic modulus curve were found to be larger in the LVP sample in comparison with the HVP hybrid. Mechanical properties were consistent with the morphological structure observed by SEM and TEM. The tensile modulus improved for all TPE nanocomposites and obtained higher percent increase in the case of LVP samples.

CONDENSÉ EN FRANÇAIS

Cette étude s'intéresse à la microstructure, la rhéologie, et les propriétés mécaniques des nanocomposites à base d'élastomères thermoplastiques vulcanisés dynamiquement (nanocomposites TPV) préparés par un procédé en trois étapes et des nanocomposites non vulcanisés (nanocomposites TPE) basés sur une matrice PP/EPDM et préparé par un procédé en une étape. Trois types de polypropylène (PP) d'indices de viscosité différents, le monomère de diène de propylène d'éthylène (EPDM), le polypropylène modifié par anhydride maléique (PPMA) comme compatibilisant, et l'organo-argile (Cloisite 15A) ont été utilisés dans ce travail.

Dans la première étape du processus de préparation des TPVs, la poudre d'argile et les granules de PPMA ont été mélangés à l'état fondu sous atmosphère d'azote pour obtenir un mélange maître en utilisant un mélangeur interne (Haake Rhemix 60). Le rapport de PPMA/argile a été maintenu constant à 3:1. Dans la deuxième étape, le mélange-maître sec a alors été mélangé avec des polypropylènes pour obtenir la composition désirée. Dans la troisième et dernière étape, l'EPDM, l'oxyde de zinc (ZnO) et l'acide stéarique (St.Ac.) sont ajoutés au nanocomposite de PP préparé à l'étape 2. Trois à quatre minutes après la fonte des nanocomposites de PP, du bisulfure tétra-méthylique de thiuram (TMTD), du bisulfure de benzothiazyl (MBTS) comme accélérateurs, et du soufre (S) sont finalement ajoutés au mélange.

Les nanocomposites TPV montrent une valeur plus élevée du couple observé sur l'arbre d'agitation en fin de mélange en comparaison avec des compositions TPV similaires mais sans argile. Le couple accru est une évidence indirecte d'une plus

grande interaction entre la matrice de TPV et le nano-argile. L'angle de diffraction (d_{001}) des plans des nanocomposites TPV basés sur PP/EPDM (40/60) comprenant des activateurs et des accélérateurs avant l'étape de vulcanisation décale vers des valeurs inférieures en comparaison de l'organo-argile brute, indiquant ainsi une structure intercalée. En outre, l'intensité du pic XRD caractéristique diminue après avoir ajouté le soufre (S) comme agent de vulcanisation. Ceci est explicable par le fait que la vulcanisation dynamique de la phase d'EPDM augmente la viscosité du mélange et par conséquent le niveau de contrainte de cisaillement imposés par la matrice pendant le mélange, ce qui facilite le procédé de dissolution des agglomérés d'argile. Le premier pic caractéristique de l'organo-argile disparaît pour les nanocomposites de TPV obtenus à partir de PP de différentes viscosités et 60 % d' EPDM quand une mise en forme ultérieure au procédé de mélange est appliqué à ces échantillons. L'absence de pic de diffraction suggère que le processus de compression des échantillons pourrait contribuer à une exfoliation supplémentaire des couches de silicate dans les nanocomposites TPV. La dispersion des couches de silicate au sein de la phase de polypropylène se produit avant la vulcanisation de la phase en caoutchoutique pour les nanocomposites TPV préparés à partir de PP de faible viscosité (LVP). Les silicates ne peuvent donc pas pénétrer dans la phase d'EPDM pendant le processus de mélange. Ceci se traduit par un renforcement sélectif de la phase thermoplastique, en raison de la faible viscosité du PP qui permet donc la dispersion de l'argile en début de procédé. Dans les compositions nanocomposites TPV non vulcanisés faits à partir de PP de haute viscosité (HVP), l'argile se disperse en partie dans la phase continue et s'agglomère en

partie à la frontière entre le polypropylène et les phases en caoutchouc. On constate que la microstructure des nanocomposites TPV est sensible au rapport de viscosité des deux phases et au contenu en nano-argile. L'argile est presqu' exfoliée et aléatoirement distribué dans la matrice de l'échantillon de TPV préparé avec LVP et contenant 60 % de caoutchouc et 2 % en poids d'argile. Les particules en caoutchouc se dispersent dans la matrice thermoplastique sous la forme d'agrégats et leur taille augmente avec l'introduction de l'argile dans les TPV préparés. L'augmentation de la dimension des particules de caoutchouc dans les nanocomposites de TPV est expliquée par l'évolution de la rhéologie des nanocomposites. On constate que la taille de la phase en caoutchouc dispersée dans les TPV ne contenant pas d'argile dépend du rapport de viscosité et des interactions entre les deux phases. Dans le cas des nanocomposites TPV, l'argile joue un rôle important pour déterminer la morphologie des échantillons. Au commencement, l'argile ne peut pas pénétrer dans la phase en caoutchouc mais après avoir ajouté des accélérateurs tels que le TMTD, la phase en caoutchouc devienne plus polaire, ce qui facilite la dispersion des silicates. Par conséquent, il est possible qu'une certaine fraction d'argile aille dans la phase d'EPDM avant la fin du cycle de mélange. Ceci change le rapport de viscosité entre les deux phases, et par conséquent, les augmentations de taille des particules en caoutchouc. Le module de tension des nanocomposites TPV ayant 60 % de caoutchouc s'améliore de manière significative (de 20 à 90 %) selon la concentration en organo-argile et la différence de viscosité entre le PP et l'EPDM. L'exfoliation de l'argile à 2 % dans les nanocomposites faits en PP de faible viscosité et ayant 60 % de caoutchouc, augmente le module de tension de 92 %,

alors que l'addition semblable de 2 % poids d'argile au TPV basé sur des résultats de PP de haute viscosité donne seulement une augmentation de 23 %. Ceci vient confirmer que la dispersion et l'exfoliation d'argile est mieux réalisée dans la composition à basse viscosité. L'exfoliation des silicates se traduit, dans la structure des nanocomposites correspondant, par une réduction du taux de cristallinité et une augmentation de la température de cristallisation du polymère. Les silicates dispersés d'argile agissent donc en tant qu'agents de nucléation. La perméabilité à l'oxygène des nanocomposites basés sur PP/EPDM (40/60) et 2 % poids d'argile diminue par près de 20 % par rapport au TPV primitif.

On constate que la distance intercalaire de l'argile dans les nanocomposites PP préparés avec des polypropylènes de différentes viscosités, mais sans PPMA, est semblable à celle de la Cloisite 15A originale. Ceci indique que le polypropylène ne peut pas pénétrer dans la couche intercalaire de l'organo-argile, malgré la présence de l'ion quaternaire. Cependant, la distance intercalaire de l'argile augmente dans les nanocomposites TPV préparés avec les mêmes PP, mais sans PPMA, et contenant 20, 40 ou 60 % d'EPDM. L'intensité des pics de XRD diminue à mesure que le contenu en caoutchouc augmente. Les nanocomposites de polypropylène préparés sans PPMA et contenant 2 % d'argile montrent des courbes du module d'emmagasinement G' très près des courbes correspondantes pour la matrice seule. Cependant, les courbes du module G' des nanocomposites de TPV sans PPMA et contenant 2 % poids d'argile augmentent de manière significative en comparaison de celles de la matrice équivalente. À mesure que la vulcanisation dynamique de la phase caoutchouteuse s'effectue les forces de

cisaillement imposées par la matrice augmentent, ce qui facilite la destruction des agglomérats d'argile. La dispersion de l'argile est améliorée par l'incorporation du PPMA dans les nanocomposites de PP et de TPV. La dispersion de l'argile a été améliorée en incorporant le PPMA aux nanocomposites de PP et de TPV, principalement pour les compositions à base de PP de faible viscosité. Une augmentation importante du module G', de la contrainte seuil et une translation du plateau vers les plus basses fréquences ont été observées en comparaison de la matrice équivalente sans PMMA. L'agglomération de l'argile a diminuée lorsque la concentration de la phase en caoutchouc a été augmentée. Dans le cas contraire, le matériau basé sur les HVP et l'argile de 2 % avec PPMA montre une courbe de module de stockage semblable à la matrice équivalente. Il semble donc que les LVP pénètrent plus aisément entre les couches de silicate en comparaison des HVP. Par conséquent, l'interaction de l'argile et de la matrice dans le nanocomposite de PP de LVP est plus grande que pour les composés utilisant des HVP. La contrainte seuil stress des nanocomposites de PP préparés à partir de PP de différentes viscosités augmente lorsque la viscosité de la matrice diminue. Ainsi, la contrainte seuil des nanocomposites de PP augmente à mesure que la distance des couches intercalaires de l'argile est augmentée. Dans les nanocomposites de TPV, l'intensité des pics de XRD des échantillons préparés avec le PPMA diminue en comparaison des échantillons semblables, mais sans PPMA. Ceci est dû au fait que la dispersion d'argile est améliorée en incorporant le PPMA dans la matrice du nanocomposite. La distance intercalaire des feuillets de silicate augmente également avec la teneur en caoutchouc.

On observe que les nanocomposites de TPV montrent un module élastique plus élevé et dont le plateau apparaît à des fréquences plus faible pour l'échantillon contenant 60 % d'EPDM. Ces résultats sont conformes aux observations en analyse XRD pour les nanocomposites de TPV. La contrainte seuil de la matrice à l'état fondu augmente de 2651 Pa pour le TPV contenant 20 % EPDM sans argile à 3665 Pa pour le nanocomposite de TPV sans PPMA et, enfin, à 5794 Pa pour le nanocomposite TPV avec PPMA. Ces résultats sont dus aux fortes interactions entre la matrice du TPV et l'argile, même sans PPMA. La contrainte seuil des nanocomposites de TPV augmente remarquablement quand le contenu en caoutchouc est augmenté. Ceci est attribuable à l'interaction plus forte entre l'argile et la matrice de nanocomposite ainsi qu'à l'existence d'une structure tridimensionnelle formée entre les particules de caoutchouc vulcanisées. L'ampleur de l'agglomération dans le caoutchouc est augmentée par la taille globale des particules, résultant de la plus grande concentration en caoutchouc dans les échantillons. La contrainte seuil du nanocomposite de TPV préparé à partir d'un PP de faible viscosité augmente plus que pour le cas d'une matrice faite à partir de PP de viscosité moyenne ou élevée, ce qui reflète une meilleure dispersion de l'argile. Les propriétés viscoélastiques linéaires de fonte des nanocomposites de TPV sont décrites par une loi de Carreau - de Yasuda et un modèle viscoélastique linéaire (modèle modifié de Palierne) considération le volume maximum d'emballage. Il y a un accord considérable entre les résultats des données expérimentales et le modèle modifié pour le nanocomposite de TPV à 60 % EPDM avec ϕ_m=0.64. Cependant, en nanocomposites de TPV à 40 % et 20 % d' EPDM, un meilleur ajustement est obtenu avec ϕ_m = 0.59 et

ϕ_m = 0.5. La diminution du volume maximum d'emballage dans les nanocomposites de TPV est due au fait que le degré de dispersion de nano-argile diminue dans les nanocomposites quand le contenu d'EPDM diminue.

On observe que les élastomères thermoplastiques non vulcanisés contenant 20, 40, et 60 % d'EPDM et 3 % poids de l'argile préparés par un mélange de fonte d'une étape à montré une intercalation des nanoargiles pour toutes ces compositions. Dans les nanocomposites TPE faits à partir de PP de faible viscosité, l'intensité des pics de diffraction de rayon X a augmenté quand le contenu d'EPDM a été augmenté. Les résultats de TEM correspondants ont indiqué que l'argile a été dispersée principalement dans la phase en thermoplastique, alors que, pour le TPE nanocomposite utilisant un PP de haute viscosité, les feuillets de silicate s'avéraient être dispersées dans les phases d'EPDM et de PP. Les résultats de micrographie SEM ont montré que le diamètre moyen en volume (dv) des particules de caoutchouc dans les mélanges ayant 20, 40 ou 60 % d'EPDM diminuait avec l'augmentation de la viscosité de la phase PP. Les échantillons nano-argile-remplis provenant de LVP ont démontré une réduction de la taille des particules en caoutchouc comparées aux mélanges déchargés. La taille des gouttelettes en caoutchouc dispersées s'est avérée plus grande pour les mélanges nano-argile-remplis contenant 40 et 60 % EPDM préparés avec des HVP en comparaison des échantillons déchargés équivalents. Le TPE nano-argile-rempli a préparé avec LVP a illustré plus de perfectionnement dans le contrainte seuil comparé aux échantillons correspondants de HVP. L'augmentation du module et de la diminution de stockage de la pente terminale est avérée plus grande pour l'hybride de LVP en comparaison de

l'échantillon équivalent de HVP. Les propriétés mécaniques étaient conformées à la structure morphologique trouvée par SEM et TEM. Le module de tension a été amélioré pour tous les nanocomposites et a obtenu des pour cent plus élevés augmentent dans le cas des échantillons de LVP.

TABLE OF CONTENTS

LIST OF TABLES

LIST OF FIGURES

NOMENCLATURE

English letters:

a	Yasuda parameter
Dn, dn	number average diameter
Dv, dv	volume average diameter
G′	storage modulus
G″	loss modulus
n	power law index
Mn	number average molecular weight
Mw	weight average molecular weight
t	time
Tc	crystallization temperature
Xc	degree of crystallinity

Greek letters:

$\dot{\gamma}$	shear rate
η^*	complex viscosity
η_0	zero shear viscosity

λ	time constant
σ_0	yield stress
ω	frequency

List of abbreviations

AFM	atomic force microscopy
AM	anhydride maleic
CEC	cation-exchange capacity
DSC	differential scanning calorimetry
EFM	elongational flow mixer
ENB	ethylidene norbornene
EPDM	ethylene-propylene-diene monomer
FIB	focused ion beam
HDPE	high density polyethylene
IPN	interpenetrating polymer network
MBTS	benzothiazyl disulfide
MMT	montmorillonite
NBR	Acrylonitrile-butadiene rubber
OMMT	organo montmorillonite

PEO	polyethylene oxide
PA6	polyamide 6
PCL	polycaprolactone
Phr	parts per hundred rubber
PP	polypropylene
PP-g-MAH	maleic anhydride grafted PP
PPMA	maleic anhydride modified polypropylene
PS	polystyrene
S	sulfur
SAXS	small-angle X-ray scattering
SEM	scanning electron microscopy
TEM	transmission electron microscopy
TMTD	tetra-methyl thiuram
TPE	thermoplastic elastomer
TPO	Thermoplastic olefin elastomer
TPV	thermoplastic vulcanizates
TSE	twin screw extruder
WAXD	wide angle X-ray diffraction
XRD	X-ray diffraction
ZnO	zinc oxide

CHAPTER 1

INTRODUCTION AND OBJECTIVES

1.1 Introduction

Thermoplastics can be formed and reprocessed at temperatures above their melting or softening point. In contrast, elastomers are amorphous polymers existing above their glass transition at room temperature and can never be re-melted. Thermoplastic elastomeric materials (TPEs) are an important family of plastics that enjoy many of the vulcanized rubber properties while being rapidly fabricated as thermoplastic materials.

TPEs can be processed using extrusion, injection or compression molding without the time-consuming cure step required with conventional vulcanizates. Another important reason for considering the TPEs is recycle-ability of scrap without the need for reclaiming [Coran *et al.,* 1978].

A special type of TPEs is obtained when the rubber is dynamically vulcanized during its blending process to give rise to a thermoplastic vulcanizates (TPVs). Dynamic vulcanization is a technique to obtain rubber particles fully dispersed throughout a thermoplastic matrix. The microstructure of this type of TPEs consists of a thermoplastic matrix (continuous phase) that contains very tiny dispersed cured rubber particles. Therefore, this structure enables the blend to be melt-processed similar to the

ordinary thermoplastic materials even though the rubber particles are crosslinked. Many commercial TPVs have been developed for various applications in automotive parts, cable insulation, footwear, packaging and medical industries due to their outstanding endurance, low density, and relatively low manufacturing costs. TPVs are commercially available from 45 A to 50 Shore D hardness.

Traditional microscale fillers have been incorporated in plastics and rubbers with the main objective of providing particular properties. The addition of fillers, such as glass fiber, carbon black, talc, and calcium carbonate to the TPV blends at high loading levels improve properties like stiffness, heat distortion temperature and dimensional stability. These fillers increase the weight of the TPV blends and cause an adverse effect especially for automotive and aerospace applications [Garces *et al.*, 2000]. Furthermore, macroscopic defects due to regions of high volume fraction of the filler are often the cause of breakdown or failure. Recently, a large window of opportunity has opened to overcome the limitations of classical micrometer-scale polymer composites.

Montmorillonite (Na^+–MMT) is a layered mica-type nanoclay mineral whose crystal lattice consists of a central octahedral sheet of alumina/magnesium sandwiched between two fused tetrahedral sheets. Montmorillonite has negative charges on the interlayer gallery walls and the galleries are normally occupied by cations such as Na^+, Ca^{2+}, and Mg^{2+}. The silicate layers have been modified to organo-montmorillonite (OMMT) by an aliphatic alkylammonium or alkyl phosphonium ion-exchange reaction in order to reduce the polar characteristic of the clay. This modification facilitates the

intercalation of polymer chains between the silicate layers by increasing the initial gallery spacing and improving the clay compatibility with non-polar polymers [Liu *et al.*, 2001; Xu *et al.*, 2003].

The potential use of a small amount of the clay (up to 5 wt %) has received a significant attention from scientists and engineers in recent years. This is mainly attributed to the nanoscale dimension of the silicate layers dispersed in the polymer matrix, which causes a strong interfacial interaction between silicate layers and polymer chains, leading to a dramatic change in the mechanical, thermal stability, barrier, optical, and fire resistance properties in comparison with pristine polymer [Hasegawa *et al.*, 2000]. For example, a volume fraction of only 0.04 clay increases the tensile modulus of a commercial TPV based on PP/EPDM by up to 170 % [Lee *et al.*, 2004]. Usuki and coworkers showed a 35% decrease in the gas permeability of EPDM prepared with 4 wt % clay in 2002. In addition, many of nanocomposites prepared with the clay maintain their excellent optical transparency [Nassar *et al.*, 2005].

The structure of nanocomposites depends on the structure of dispersed nanoclay particles in the polymer matrix, which can be classified as intercalated or exfoliated structure. In the intercalated state, the clay is dispersed as lamellar structures and polymer chains penetrate between the silicate layers of the clay but in the exfoliated structure, the clay is completely delaminated and the individual silicate layers are dispersed throughout the polymer matrix.

Polymer nanocomposites can be prepared using in situ polymerization method (penetration of a suitable monomer followed by polymerization) and by solution

method (intercalation of dissolved polymer from a solution). However, these two techniques (in situ polymerization and solution) can not be applied for preparation of nanocomposites based on nonpolar polymers such as poly-olefins. A suitable method for preparation of the hybrids (poly-olefin nanocomposites) is melt intercalation technique [Galgali *et a.,* 2001].

The structure of nanocomposites is characterized using X-ray diffraction (XRD) and transmission electron microscopy (TEM). Wide-angle X-ray diffraction (WAXD) can be used to determine the interlayer spacing of the clay in nanocomposites as well as the periodic arrangement of silicate layers in the virgin clay. A qualitative understanding of the microstructure of nanocomposites through direct visualization can be obtained using TEM. When the periodic arrangement of the clay is lost in nanocomposites (exfoliates structure), WAXD does not present definitive characterization concerning the structure of the nanocomposites. WAXD also suffers from problems of weak peak intensity and poor peak resolution. It should be noted that we can also use a small-angle X-ray scattering (SAXS) in order to characterize nanocomposite structures. Recently, Vaia and coworkers reported that the exfoliated structure of polycaprolactone-layered silicate nanocomposites has been characterized using SAXS.

1.2 Objectives

Nanocomposites based on polypropylene [Hesegawa *et al.,* 1998; Kyu-nam *et al.,* 2001; Svoboda *et al.,* 2002; Suprakas *et al.,* 2003; Lertwimolnun *et al.,* 2006] and

thermoplastic elastomers based on PP/EPDM [Coran *et al.*, 1982; Chung *et al.*, 1997; Baranov *et al.*, 2001; Goharpey *et al.*, 2003] have been prepared, and their properties and microstructure have been published. These studies reveal that a suitable compatibility between the clay and polymers as well as sufficient deformation rate applied during the process are essential to achieve an intercalated or exfoliated structure by using a simple melt mixing process.

The nanocomposites based on TPEs are emerging a new class of reinforced thermoplastic elastomers with generally improved mechanical and physical properties. Recently, Lee *et al.*, (2004) studied TPV/clay nanocomposite prepared by simple melt mixing a commercial TPV based on EPDM/PP with several types of clay without the use of a compatibilizing agent for the polyolefins. They reported that the mechanical properties of the TPV nanocomposite increased when the miscibility of the clay and polymer matrix was increased.

Although there have been a few studies on the preparation and properties of thermoplastic elastomer (TPE) nanocomposites [Mishra *et al.*, 2005], the area of dynamically vulcanized nanocomposite thermoplastic elastomers prepared using polypropylene of different viscosities, maleic anhydride grafted polypropylene (PPMA) as compatibilizer and sulfur as curing agent has remained uncharted.

Therefore, the main objective of this project was to prepare dynamically-vulcanized nanocomposite thermoplastic elastomers (TPV nanocomposites) based on PP/EPDM using a three-step melt mixing process and to study the parameters affecting their microstructure and properties. The microstructure, rheology and mechanical

properties of uncured thermoplastic elastomer nanocomposites (TPE nanocomposites) based on PP/EPDM prepared by a one-step melt mixing method were also studied.

For that purpose, we prepared the TPV and TPE nanocomposites while investigating the effect of PP/EPDM viscosity ratio, clay content, compatibilizer (PPMA), and composition on their microstructure. The evolution of the nanocomposites microstructure during the mixing process was also monitored.

In the forth chapter, we will prepare dynamically-vulcanized nanocomposite thermoplastic elastomers (TPV nanocomposites) based on PP/EPDM (40/60, w/w) using a three-step melt mixing process in an internal mixer. The effects of viscosity ratio, and nanoclay concentration on the microstructure and mechanical properties of the resulting PP/EPDM TPEs will be studied. We will also follow the microstructure change of the nanocomposite during the melt mixing process.

The fifth chapter is dedicated to examine the rheological and morphological properties of the TPV nanocomposites, based on EPDM and PP containing 20, 40, and 60 wt % of the rubber at 2 % clay. The effects of composition, maleic anhydride grafted polypropylene (PPMA) as compatibilizer, and different viscosities of polypropylene on the rheological behavior and morphological feature of the nanocomposites will be investigated as well.

The sixth chapter will seek the microstructure, rheology, and mechanical properties of the uncured TPE nanocomposites based on PP/EPDM prepared by a one-step melt mixing process. Three grads of polypropylene (with different viscosities) will

be compounded with 20, 40, and 60 % EPDM at 3 wt % of the clay in the mixer. The effects of PP/EPDM viscosity ratio and compositions will be also considered.

CHAPTER 2

LITERATURE REVIEW

2.1 Crystallography of layered silicates and their properties

The layered silicates are natural clays, which have been successfully used in the synthesis of polymer nanocomposites. The suggested crystallographic structure of the layered silicate is based on two tetrahedrally coordinated silicon atoms fused to an edge-shared octahedral sheet of aluminum or magnesium hydroxide. The layer thickness is 1nm and the lateral dimensions of these layers vary from 30 nm to several microns (high aspect ratio e.g. 10-1000) [Ajayan *et al.,* 2003].

One of the most commonly used layered silicates is montmorillonite (MMT) with a generally known structure and chemical formulation as shown in Figure 2.1, and in Table 2.1 respectively. Montmorillonite is discovered by Damour and Salvetat in 1847 [Damour *et al.,* 1847]. MMT could be formed by weathering of eruptive rock materials.

The montmorillonite has two important properties: it can be delaminated and dispersed into the polymer matrix, and also its surface can be treated by ion exchange reaction with organic and inorganic cations. The most common exchangeable cations are Na^+, Ca^2+, Mg^2+, K^+, and NH_4^+ [Kornmann., 2000; Suprakas *et al.,* 2003].

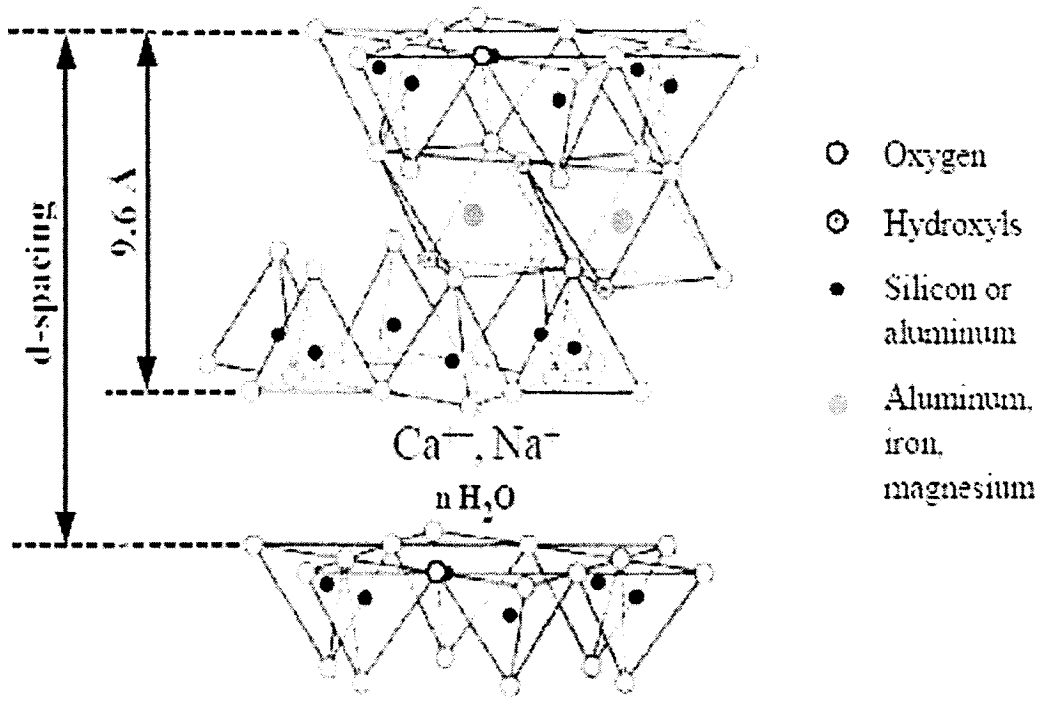

Figure 2.1: The structure of montmorillonite (2:1 phyllosilicates) [Kornmann. 2000].

Table 2.1: Chemical formulation and specification of montmorillonite [Suprakas *et al.*, 2003].

Layered silicates	chemical formulation	CEC (meqiv/100)	particle length (nm)
Montmorillonite	$M_x(Al_{4-x}Mg_x)Si_8O_{20}(OH)_4$	110	100-150

M, monovalent cation; x, degree of isomorphouse substitution (between 0.5 and 1.3)

CEC = cation exchange capacity

Layered silicates are inherently hydrophilic, but polymers tend to be hydrophobic. Compatibilizing agents allow the dispersion of the clay throughout polymers. Amino acids were among the first compatibilizers used in the synthesis of polyamide 6 nanocomposites [Usuki *et al.,* 1993].

Alkyl ammonium ions are the most popular compatibilizing agents, which can be intercalated easily between the layers of the clay. The alkyl ammonium ions allow the intercalation of the organic material with different polarities between the silicate layers by lowering the surface energy of the clay. Their basic formula is CH_3-$(CH_2)_n$-NH_3^+ in which n is between 1 and 18. The alkyl ammonium with chain length larger than eight carbon atoms favors the synthesis of delaminated nanocomposites. Alkyl ammonium ions based on secondary, tertiary, and quaternary amines have been also successfully used [Lan *et al.,* 1995; Wang *et al.,* 1998; Alexandre *et al.,* 2000].

2.2 Nanocomposite structures

Polymer nanocomposites are divided into three general types, which depend on the strength of the interfacial interactions between the polymer matrix and the layered silicate as well as the method of preparation as shown in Figure 2.2.

2.2.1 Intercalated structure

The first type of polymer nanocomposite structure is intercalated structure. This structure is formed by insertion of polymer chains into the layers of the clay. This provides an increased interlayer spacing while retaining the ordered layer structure of the layered silicate. Intercalated nanocomposites have properties similar to those of ceramic materials [Alexandre *e al.* 2000].

2.2.2 Flocculated structure

The flocculate structure is another type of polymer nanocomposite structures. In this structure due to the hydrophilic nature and edge-edge interaction of the silicate layers, the polymer chains face a hindrance to penetrate between the layers of the silicate particles. Except mentioned change above, the flocculated nanocomposites are conceptually similar to the intercalated nanocomposites [Suprakas *et al.*, 2003].

2.2.3 Exfoliated structure

In this structure a lower percentage of an organo layered silicate material is applied and the clay is completely delaminated, hence, monolayer silicates disperse

throughout a polymer matrix, and do not show any discontinuity in their arrangement [Suprakas *et al.*, 2003].

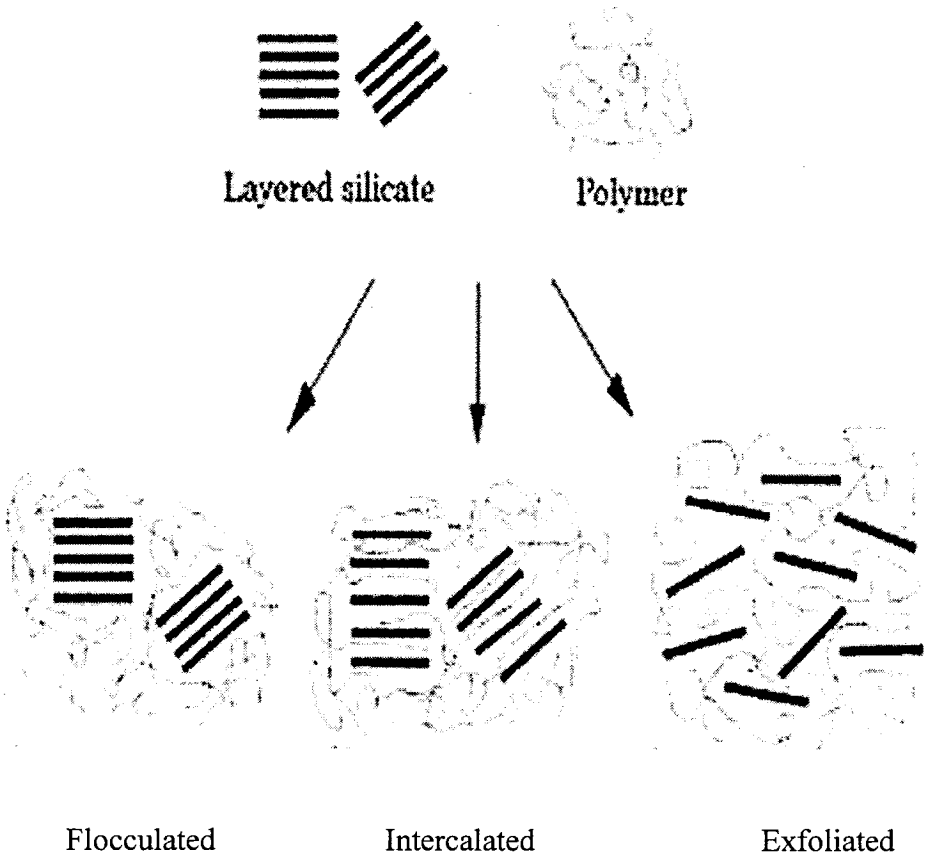

Figure 2.2: Schematic representation of different polymer layered silicate nanocomposites [Dennis *et al.*, 2001].

2.3 Synthesis of polymer nanocomposites

Three main methods can be used to prepare polymer-layered silicate nanocomposites as follow:

2.3.1 In situ polymerization method

In this technique, the layered silicate is swollen within a liquid monomer (or a monomer solution) therefore the polymerization can take place in between the intercalated sheets. In situ polymerization was the first method applied in the synthesis of polymer-clay nanocomposites based on polyamide 6 (PA6) [Usuki *et al.,* 1993].

In a study, Pantoustier and coworkers used this process for preparation of polycaprolactone (PCL) based nanocomposites in 2002. They reported that the modified montmorillonite is able to catalyze and control the polymerization of the caprolactone in term of its molecular weight distribution.

Nowadays, this technique is a conventional process used for synthesis of thermoset nanocomposites [Pantoustier et al. 2002].

2.3.2 Solution method

In this process, the organolayered silicate is first exfoliated in a polar solvent such as water or toluene in which the polymer is soluble. At the end the solvent is removed by evaporation under vacuum. Aranda and coworkers prepared nanocomposites based on polyethylene oxide (PEO) by solution method for the first time in 1992. They reported that the thermal stability of PEO was significantly improved by treating the clay with acetonitrile at room temperature for long periods of time [Aranda *et al.,* 1992]. Similar results were shown for nanocomposite prepared from high density polyethylene with the silicate layers dispersed within a mixture of xylene and benzonitrile [Jeon *et al.,* 1998].

The disadvantage of this method is the use of large quantity of solvent for preparation of nanocomposites. It should be noted that the solvent must be removed at the end of the process.

2.3.3 Melt intercalation method

In this technique, the clay is blended with the polymer matrix in the molten state. Driving force for this mechanism is the enthalpic contribution of the polymer/organo layered silicate interactions during the blending process. This method is compatible with industrial process, such as extrusion and injection molding and requires no chemical solvent. By using this method a wide range of nanocomposite structures can be achieved depending on the penetration degree of the polymer chains into the layered silicate [Vaia *et al.*, 1993; Makadia, 2000].

Polystyrene nanocomposites have been prepared for the first time by applying the melt intercalation method. Several layered silicates were utilized with different cation exchange capacity (80, 100 and 150 meq/100). It was found that an intercalated structure achieved when the cation exchange capacity (CEC) of the clay was increased from 80 to 120 meq/100 g. It was also shown that the time needed for PS intercalation was dependent on the molecular weight (M_w) of polystyrene. For instance, the PS intercalation at 160 °C occurred in 6 h for M_w of 30,000; in 24 h for M_w of 90,000, and in 48 h for M_w of 400,000 [Vaia *et al.*, 1997].

In a study, the melt intercalation method was used for preparing polyamide 6 nanocomposites using an organo-MMT in a twin screw extruder with different

nanoclay content (1 to 28 wt %). It was found that the nanocomposites prepared based on PA6 at low percent of the clay (up to 10 wt %) achieved an exfoliated structure [Liu *et al.,* 1999].

In another attempt, Forners and coworkers (2001) prepared nanocomposites based on PA6 with different molecular weights (low, medium, and high Mw of PA6) via melt intercalation method in a twin screw extruder at 240 ^{o}C with a screw speed of 280 rpm. The nanocomposites prepared based on low-molecular weight of PA6 obtained an intercalated structure; however, the PA6 hybrids from medium and high Mw achieved an exfoliated structure.

A HDPE/PA-66/modified clay (80/20/5 wt %) nanocomposite was prepared by melt intercalation technique using a co-rotating twin screw extruder at 280 ^{o}C. It was found that mixing time and post-processing can affect the degree of the clay exfoliation. It was also shown that the crystalline size of the nanocomposite decreased due to the fact that the clay acted as nucleating agent [Kamal *et al.,* 2003].

2.4 Polypropylene nanocomposites

Polypropylene (PP) is one of the most widely used polyolefin polymers for many applications. Since PP does not include any polar groups in its backbone, it was not believed that the homogeneous dispersion of polar silicate layers (clay) in polypropylene matrix would be possible. Takekoshi (1996) reported that the mechanical properties of PP nanocomposites increased when the interfacial affinity between the surface of the clay particle and polypropylene matrix was increased. As we

already mentioned, one of important properties of the clay is the ion exchange characteristic, therefore we are able to change the polarity of the nanofillers. In general, the clay is modified with alkylammonium to improve its interaction with polymer matrix because the alkylammonium modifies the hydrophilic nature of the clay surface to organophilic state. In order to achieve high mechanical properties of PP nanocomposites, researchers studied many parameters affecting the microstructure and morphology of the nanocomposites. The effect of important factors such as compatibilizer, organoclay, nanofiller content, and processing conditions on the final properties of the nanocomposites based on PP prepared by using melt intercalation method are reported below.

2.4.1 Effect of compatibilizer (PPMA) on microstructure and properties of PP nanocomposites

Nanocomposites based on polypropylene were prepared with several kinds of maleic anhydride polypropylene (PPMA) as compatibilizer to investigate the effect of the compatibilizers on the microstructure of the nanocomposites. It was found that the intercalation of the polymer into the layered silicate did not occur when the content of maleic anhydride (MA) in PPMA matrix was low (acid value = 7 mg KOH/g for Mw = 12,000), implicating a requirement for a minimal functionalization of the PP chains for intercalation to proceed. It was also shown that the penetration of polypropylene chains into the clay increased when the PPMA content was increased [Kato *et al.*, 1997].

In another attempt, Kawasumi and coworkers prepared polypropylene nanocomposites with different PPMA (compatibilizer) using a twin screw extruder at 200 °C. The exfoliated silicate layers and their homogeneous dispersion into the polypropylene matrix were proved by transmission electron microscopy (TEM) and x-ray diffraction (XRD) as illustrated in Figure 2.3. They reported that the microstructure of the samples was very sensitive to the compatibilizer concentration and maleic anhydride (MA) percent in PPMA. They showed that the clay is exfoliated into the matrix when the ratio of PPMA/clay = 3, acid value of PPMA = 26 mg KOH / g, and Mw of PPMA = 40,000. It was also found that the increase in the acid value of anhydride maleic polypropylene (e.g. acid value = 52 mg KOH/g) has no further effect on the increase in the interlayer spacing of the layered silicate [Kawasumi *et al.*, 1997; Hasegawa *et al.*, 1998].

In a study, Hernandez and coworkers showed that the mechanical properties of polypropylenes without clay decreased when the concentration of PP modified with maleic anhydride (PPMA) as compatibilizer was increased, however this was recovered with the addition of the clay [Hernandez *et al.*, 2002].

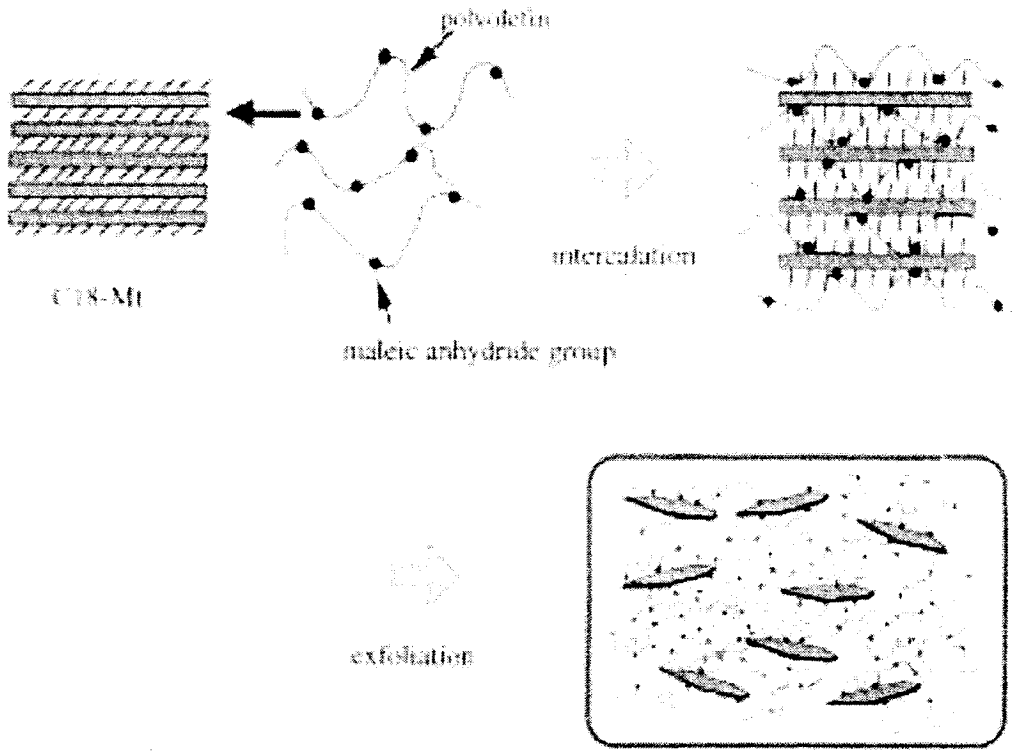

Figure 2.3: Schematic illustration of the process for dispersion of organo layered silicate in functionalized PP [Hasegawa *et al.*, 2000].

The effect of the compatibilizer concentration (PPMA) on the crystalline size and the mechanical properties of PP nanocomposites were studied by Xu *et al,* in 2003. The compounds were mixed using a roller mill at 180 °C for 15 min with 2 wt % of the clay (MMT). The content of the maleic anhydride grafted PP (PP-g-MAH) was increased from 0 to 30 wt % in the samples. They observed that the crystalline size of PP matrix in the nanocomposites decreased when PPMA content was increased. The maximum values of the tensile strength (40.2 MPa) and the impact strength (24.3 J/m) were obtained when the compatibilizer was 10 wt % and 20 wt %, respectively and also

the crystalline size of the nanocomposite was kept minimum at 20 wt % of the compatibilizer.

Polypropylene nanocomposites based on three different molecular weights of PPMA were prepared using a twin screw extruder via melt mixing method by Svoboda *et al.,* in 2002. They investigated the effect of Mw of PPMA (low, medium, and high Mw) on the morphology and the mechanical properties of the PP nanocomposites. The nanocomposites prepared with PPMA having high molecular weight (Mw = 330,000, MA = 0.5 wt %) presented the best overall mechanical properties. It was also observed that the impact strength of the samples was slightly increased with increasing the content of the clay [Svoboda *et al.,* 2002].

In another attempt, Darrel and coworkers produced PP nanocomposites by melt-mixing 5 wt % of organically modified layered silicates with varying acid number and molecular weight of maleated polypropylene compatibilizer. They reported that the acid number of PPMA alone could not be good predictor of the compatibilizer effectiveness, but the molar ratio of functional groups to compatibilizer chains was found to be a better factor for evaluating compatibilizers. The clay was more exfoliated with lower concentration of PPMA when the value of the molar ratio was increased [Darrell *et al.,* 2002].

In another study, the effect of Mw and % MA of PPMA on the dispersion of the clay in PP nanocomposites was studied by Ton-That and coworkers in 2003. It was found that the nanocomposites prepared with PPMA (Mw = 330,000, MA = 0.5 wt %) presented larger interaction between the clay and the matrix compared with the sample

containing PPMA (Mw = 9100, MA = 3.81 wt %). They reported that the degree of the intercalation and the homogenous dispersion of the clay in the PP nanocomposite can be affected by the molecular weight and the grafting content (MA %) of PPMA [Ton-That *et al.*, 2003].

2.4.2 Effect of organoclay on microstructure and properties of PP nanocomposites

New functionalized clay (epoxy propyl-methacrylate modified clay) was used by Liu *et al.* for preparing PP nanocomposite using a twin screw extruder with 180 rpm at 200 °C. They observed that the interlayer distance of the clay increased more than that of the ordinary organophilic clay prepared from alkyl ammonium. It was found that the dispersion of the clay through the polypropylene improved due to strong interactions between the clay and the matrix. It was also reported that a considerable improvement in the storage modulus (stiffness) and a decrease in the tan δ value of the PP nanocomposite were obtained with increasing the clay content [Liu *et al.*, 2001]. Similar results were observed by Wolf et al. in PP nanocomposites prepared with alkyl ammonium MMT, semi fluorinate surfactant, and ethylene glycol [Manias *et al.*, 2000; Wolf *et al.*, 1999; Kaempfer *et al.*, 2002].

Two modified clays known as tallow compound (cloisite 6A) and octadecylamine (nanocor) were used for preparing PP nanocomposite (PP/PPMA/clay, 84/12/4 wt %) by Brabender single screw extruder at 200 °C with 45 rpm. The crystalline morphology of the polypropylene nanocomposites did not exhibit spherulitic form and also the crystallites grew such as fibers which increased in diameter. The

tensile strength, modulus, and flexural modulus of the nanocomposites prepared with the clay (nanocor) increased more than those of the hybrid from Cloisite 6A [Kodgire *et al.*, 2001].

Weibing and coworker investigated the crystallinity of PP nanocomposite prepared via melt intercalation method in two roll mills at 180 °C by using several non isothermal crystallization kinetic equations. They reported that the crystalline size of the nanocomposite was smaller than that for pristine PP as well as Avrami equation modified by Jeziony could be used to describe the nonisothermal crystallization process of the nanocomposite, in addition the crystallization rate of the nanocomposite was faster than that of pure polypropylene [Weibing *et al.*, 2003].

Polypropylene calcium carbonate (~44 nm) nanocomposite was prepared by using Brabender mixer at 180 °C, 60 rpm, and 10 min via melt mixing method for investigating the mechanical properties of the sample. It was reported that the notched fracture toughness of the nanocomposite was higher than that of pure PP. The spherulite size and the crystallinity of PP were destroyed by $caco_3$ nanoparticles due to the fact that the nanofiller acted as nucleating agent [Chan *et al.*, 2002].

In a study, maleic anhydride grafted polypropylene/montmorillonite nanocomposite was prepared in Rheomix-600 mixer at 200 °C and 120 rpm for 10 min with clay content of 3 wt %. It was shown that the crystallization rate of polypropylene increased with the introduction of the clay and that the crystallization behavior of the nanocomposite followed Avrami equation, in addition, the nucleation activity of the

MMT was determined with the value of 0.84 by using Dobreva's method [Jian *et al.*, 2003].

The effect of the clay content on the viscoelastic properties of PP nanocomposites prepared with two grades of maleic anhydride grafted PP (1 & 0.65 % MA content) was examined by Hambir in 2002. It was shown that the storage modulus of the nanocomposites remarkably increased although the tan δ peak reduced when the clay content was increased [Hambir *et al.*, 2002].

In another attempt polypropylene nanocomposite was prepared via melt intercalation method in a co-rotating twin screw extruder (L/D = 30) at 210 °C. The effect of clay content on the tensile and fracture properties of the hybrid was studied. In the polypropylene nanocomposite, the tensile modulus increased and the toughness decreased when the clay content was increased [Shing *et al.*, 2002].

In a study, it was reported that the concentration of an organo MMT can change the microstructure of PP nanocomposites. The clay could be completely exfoliated in the polypropylene nanocomposite when the clay content was 2 wt %, however, an intercalated structure was achieved for the nanocomposite with increasing the nanofiller content (> 2 wt %) [Nam *et al.*, 2001].

2.4.3 Effect of processing conditions on microstructure and properties of PP nanocomposites

A formulation (PP/PPMA/clay, 80/15/5) was prepared using a co-rotating twin screw extruder to investigate the effect of processing conditions and screw profile on

the microstructure of the PP nanocomposite by lertwimolnun *et al.* in 2006. The exfoliation degree of the clay throughout the polypropylene matrix was estimated by rheological measurements. The results indicated that the dispersion of the clay into the matrix increased when the feeding rate was decreased. It was shown that no evolution of the intercalated structure was observed along the screw profile. They also reported that the exfoliation state of the clay in the nanocomposites seems to be dependent on the strain generated by the flow along the screws.

In another attempt, a PP nanocomposite was prepared via direct melt intercalation method in an internal mixer. It was shown that the interlayer spacing of the clay was not significantly affected by processing conditions, but increasing the shear stress, mixing time, as well as decreasing the mixing temperature improved the clay exfoliation throughout the polypropylene matrix. It was also reported that the yield stress value was directly correlated to the exfoliation degree of the nanocomposites [Lertwimolnun *et al.* 2005].

Than-Than and coworkers prepared nanocomposites based on polypropylene with direct and master-batch mixing process using a twin screw extruder. In the direct mixing process, PP, compatibilizer, and clay were dry mixed and fed into the extruder. In the master-batch method, a master-batch was first prepared by blending 10 wt % of the clay into the polypropylene. This master-batch was then dry-blended with PPMA and the mixture was passed through the mixer. Finally, they reported that the system prepared with master-batch method presented higher tensile strength, and modulus as

well as better exfoliation and intercalation of the clay in comparison with the direct mixing process [Ton-That *et al.*, 2003].

Dennis and coworkers investigated the effect of processing conditions on the formation of nanocomposites prepared from thermoplastics and organo-clays. They reported that excessive shear intensity or backmixing apparently cause poorer delamination of the MMT. It was also found that the excellent dispersion of the nanoclay throughout the matrix achieved with both co-rotating and counter-rotating, intermeshing types of extruders when the optimized screw configuration was used [Dennis *et al.*, 2001].

In a study, the effects of process conditions and twin screw extruder design on the dispersion of ultrafine $caco_3$ into PP matrix were investigated. It was found that the dispersion of the filler can be improved by increasing rotation speed and barrel temperature. The use of the gentle melting zone upstream from the feed port for mid-extruder feeding of $caco_3$ can improve the dispersion of the filler into the matrix. Some properties of the material such as impact resistance, tensile strength, and elongation at break decreased when the filler content was increased. The big agglomeration of the filler was observed with increasing the $caco_3$ concentration [Bories *et al.*, 1999].

Qin and coworkers studied the effect of shear stress on the dispersion of MMT in PP nanocomposites prepared with injection molding in 2003. To improve the dispersion of the clay through the matrix, the nanocomposite was further subjected to oscillating stress obtained by dynamic packing injection molding. The homogeneous dispersion of the clay in the matrix achieved when the shear stress was applied. A

transformation from an intercalated structure to an exfoliated structure was observed with increasing the shear stress [Qin *et al.*, 2003].

PPMA nanocomposite was prepared via melt blending in Brabender mixer under a flow of nitrogen or normal conditions in the presence of air with MMT mass fraction of 5 % at 453 K for 30 min, and 50 rpm/min. It was shown that the nanocomposite prepared in presence of nitrogen achieved an exfoliated structure and that a better efficiency of the clay in delaying the sample decomposition during the thermal oxidation in comparison with the sample prepared in the mixer under normal conditions [Tidjani *et al.*, 2003].

2.5 The rheological behavior of PP nanocomposites

The relationship between the rheological properties and the microstructure of the organoclay/polymer nanocomposites prepared with melt intercalation method was discussed by Young and coworkers. They reported that both the storage and loss moduli of the nanocomposites increased when the layered silicate content was increased. The strong interaction between the polymer chains and the clay was responsible for the improvement of the moduli. In the nanocomposites, a remarkable increase in the storage modulus with the onset of a plateau at low frequency observed when the clay was fully exfoliated in the polymer matrix [Yong *et al.*, 2001].

The effect of the compatibilizer (PPMA) and annealing time on the creep behavior of molten polypropylene organically modified clay nanocomposites prepared in an extruder were investigated. It was found that the creep resistance of the

nanocomposites significantly increased in the presence of the compatibilizer and further increased with increasing annealing time in comparison with the uncompatibilized hybrids. This was attributed to the exfoliation of the clay during extrusion and annealing. The zero shear viscosity of the compatibilized hybrids having 3 wt % of the clay was at least 3 times greater than that of the matrix resin and the uncompatibilized nanocomposites. It was also reported that the compatibilized polypropylene nanocomposites presented an apparent yield stress [Galgali *et al.*, 2001].

The melt-state linear and the nonlinear shear rheological behavior of polypropylene nanocomposites were investigated with different clay loading by Solomon *et al.* in 2002. The hybride materials exhibited apparent low-frequency plateaus in the linear viscoelastic moduli when the clay content was greater than 2 wt %. The chemistry of the amine exchanged into the clay could affect the hybride storage modulus. It was found that the amount of the stress overshoot observed in the flow reversal experiments increased when the rest time allowed between the reversals was increased. Similar results have been shown for PP nanocomposites by Li *et al.* in 2003.

Li and coworkers reported that the complex viscosity and the storage modulus (G′) of PP nanocomposites which exhibited an exfoliated structure were much greater than those for polypropylene hybrids with an intercalated structure. This was explained to be due to higher interaction of the clay and the polymer matrix [Li *et al.*, 2003].

In another attempt, Gu and coworkers studied the linear and nonlinear shear rheological properties of PP/organoclay prepared via melt intercalation method with PPMA as compatibilizer by ARES rheometer. The storage modulus (G′), loss moduli

(G″), and complex viscosity (η*) monotonically increased when the clay content was increased. Polypropylene showed pseudo-solid-like behavior in the presence of the nanoclay and PPMA. At low frequency (the terminal zone) the G′ was proportional to ω^2 (slop of 2 in a log-log plot) for pure PP, however, the dependence of the G′ and the G″ on ω showed no terminal linear viscoelastic behavior for the PP nanocomposites. At high shear rates, the nanocomposites presented greater shear thinning tendency than pristine polypropylene as a result of the preferential orientation of the silicate layers. It was also concluded that the polypropylene nanocomposites presented higher modulus as well as better processability compared with the pristine PP [Gu *et al.*, 2004].

2.6 Ethylene Propylene Diene Terpolymer (EPDM) nanocomposites

EPDM nanocomposites were first prepared using by melt mixing with EPDM and organophilic clay via a vulcanization process in 2002. The role of several accelerators and sulfur as curing agent were investigated by Usuki and coworkers. TEM image and XRD result showed an exfoliated structure for the EPDM-clay hybrid nanocomposite prepared with tetra-methyl thiuram monosulfide (TS) and zinc dimethyl dithiocarbamate (PZ) as accelerators. The gas permeability of the nanoclay-filled nanocomposite (4 wt % of the clay) decreased by 30 % in comparison with the unloaded EPDM. The tensile strength of the nanocomposite was 2 times higher than that of the unfilled rubber. The elongation at break of the EPDM-clay nanocomposite remarkably increased, but up to now its mechanism is unknown [Usuki *et al.*, 2002].

EPDM nanocomposites were prepared by a MMT modified with the octadecyl ammonium ion and low molecular weight of EPDM oligomer as compatibilizer via melt intercalation method. It was reported that the rubber chains were intercalated into the silicate layers effectively. A great enhancement in the tensile strength as well as the stiffness of the nanocomposite was observed in comparison with the unloaded rubber. The decrease of the tan δ and the shift of the Tg toward a higher temperature evidenced the strong interaction between the nanofiller and the matrix [Young *et al.*, 2002].

The effect of three different organo montmorillonite modified on the microstructure and the morphology of EPDM nanocomposites was investigated by Zheng *et al.* in 2004. It was reported that the clay grafted with tri-methyl-octadecylamine or dimethyl-benzyl-octadecylamine was intercalated and the MMT modified by methyl-bis (2-hydroxyethyl) coco-alkyl-amine was fully exfoliated throughout the matrix. The crosslink density of the nanocomposite also decreased as the organo-clay content increased. This was due to the retardation in the rate and the final state of the rubber cure [Zheng *et al.*, 2004].

In a study, Li and coworkers studied the mechanical properties of EPDM nanocomposites prepared with a maleic anhydride grafted EPDM oligomer as a compatibilizer via melt intercalation method. The exfoliation and uniformly dispersion of the OMMT throughout the EPDM matrix were confirmed by TEM image and XRD results. The mechanical properties of the samples showed a great improvement in both the tensile strength and the modulus of the samples. It was also reported that the solvent

resistance of the nanocomposites remarkably increased in comparison with the unfilled rubber [Li *et al.*, 2004].

EPDM/organoclay nanocomposites were prepared with two kinds of the cure system (sulfur and peroxide) by Hua et al. in 2004. The clay was exfoliated into the EPDM matrix when the rubber cured with the sulfur curing agent. An intercalate structure was obtained for the elastomer vulcanized by peroxide. The mechanical properties of the sulfur based nanocomposite increased more than those of the samples vulcanized with peroxide system. The crosslink density of the EPDM rubber cured with sulfur decreased in comparison with the unfilled sample. However, the cure state of the nanocomposite prepared with peroxide curative was virtually unchanged by the addition of the OMMT [Hua et al. in 2004].

The effects of processing conditions and formulation on the microstructure and the mechanical properties of EPDM nanocomposites based on sulfur curing system were shown by Konstantinos *et al.* in 2004. They reported that the mechanical performance of the rubber nanocomposite increased when the temperature of the shear mixing was increased. The microstructure of the compounds prepared by an open mill at room temperature exhibited a micro-composite structure with big silicate agglomerates [Konstantinos *et al.* 2004].

The MMT modified by primary (PRIM) and quaternary amine were used for the nanocomposite formation in an ethylene/propylene/diene rubber (EPDM) with sulfur and zinc dimethyldithiocarbamate (ZDEC) as vulcanization agents. It was shown that the modifiers of the clay play a crucial role to promote the intercalation or the

exfoliation of the nanoclay. It was found that the nanocomposite prepared based on PRIM illustrated de-intercalation of the clay (collapse of the layers) [Konstantinos *et al.* 2005].

In another attempt, a MMT was modified with maleic anhydride (MA) in order to increase the d-spacing of the clay and preparing EPDM nanocomposite in the presence of benzyl peroxide. It was shown that the MA acted as curing agent for EPDM matrix and compatibilizer for the elastomer and the MMT. It was also reported that the tensile strength and the modulus of the sample significantly increased due to the fully exfoliation of the grafted MMT [Liu *et al.*, 2006].

2.7 Thermoplastic elastomers based on PP/EPDM

Thermoplastic elastomers (TPEs) exhibit the functional properties of conventional thermoset rubbers but can be processed by using thermoplastic fabrication techniques. Polyolefins (e.g. polypropylene) and elastomers (e.g. EPDM) can be melt-mixed to prepare the TPEs [Fisher *et al.,* 1974; Coran *et al.,* 1980].

Dynamic vulcanization was first used for preparing high impact plastic via partially vulcanization of a polyisobutylene and PP by Gessler in 1962. Dynamic vulcanization is a process which initially forms cross-linked or three dimensional polymer structures as with static curing. However, these structures are broken down and also the micron size of the rubber particles can be fully dispersed throughout the thermoplastic matrix. The process needs to be carried out under high shear mixing and temperature to complete the vulcanization of the elastomer. Therefore, dynamic curing

is a technique for achieving the vulcanized rubber in the thermoplastic matrix. Thermoplastic elastomers prepared by using dynamic vulcanization method are so-called thermoplastic vulcanizates (TPVs). It was shown that the necessary crosslinks can be generated by dynamic vulcanization of the rubber as well as a static cure [Gessler *et al.,* 1962].

Theoretical and experimental studies indicate that the microstructure of the TPEs can be affected by mixing conditions, viscosity ratio of polymers, critical capillary number, flow field type and its intensity, thermal history, dynamic interfacial interaction between two phases, curing agent, crosslink density, and additives (fillers, plasticizers, etc) [Karger-Kocsis *et al.,* 1984; Utracki *et al.,* 1992]. Therefore we explain the effects of the important parameters on the microstructure and the mechanical properties of the thermoplastic elastomers prepared based on PP/EPDM as discussed below.

2.7.1 Effect of dynamic vulcanization on microstructure and mechanical properties of PP/EPDM

The mechanical properties of TPVs were reported in comparison with uncured thermoplastic elastomers (TPEs) by Coran *et al.* in 1978. It was found that the mechanical properties of the materials significantly increased (tensile strength, elastic recovery, properties retention at elevated temperatures, flex fatigue resistance, and consistence processability) when the rubber phase was dynamically vulcanized. They

also showed that the mechanical properties of the TPVs improved with decreasing the rubber particle size [Coran *et al.*, 1982, 1987].

PP/EPDM based TPEs were dynamically cured using dimethylol octyl phenol as curing agent by Abdou-Sabet *et al.* in 1982. The effect of different vulcanization agents (sulfur, Phenol, peroxide) on the mechanical properties of the TPVs was studied. They reported that the compression set, oil resistance, and processing characteristics of the blends prepared with phenolic curative improved in comparison with the sample vulcanized by sulfur curing agent. It was also shown that the heat resistance properties of the TPVs cured with semi efficient or efficient curing systems (accelerators / sulfur $\geq$ 1) increased more than that of the TPVs prepared with conventional systems (accelerators / sulfur $<$ 1). The mechanical properties of the TPVs based on peroxide curative were not favorable due to the degradation of the polypropylene chains [Abdou-Sabet *et al.*, 1991].

The morphology of PP/EPDM blends containing 80 % rubber was studied by Abdou-Sabet *et al.* in 1996. In the uncured blends, polypropylene was the minor component and dispersed in the EPDM matrix. However, the morphology of the TPVs showed that in the initial step of the dynamic vulcanization of the rubber phase, two co-continuous phases were first produced and, as the vulcanization degree of the rubber increased, the continuous rubber phase became elongated more and more and then broke up into EPDM droplets. When the rubber droplets were forming, the polypropylene grew to be the continuous phase [Abdou-Sabet *et al.*, 2000].

Dynamically vulcanized TPVs based on PP/EPDM were prepared using a twin extruder by Toshio *et al.* in order to investigate the dynamic vulcanization effect of the rubber phase on the microstructure and the mechanical properties of the blends. It was shown that the impact strength of the samples increased when the rubber phase was dynamically cured and more increased with increasing the EPDM content. They also reported that the morphology of the samples were essentially the same before and after the elastomer vulcanization. The cured rubber particles acted as nucleating agent leading a decrease in the crystalline size of PP phase [Toshio et al., 1995]. Similar results have been published by Jain *et al.* (2000) and Neeraj *et al.* (2000) in the TPVs based on PP/EPDM prepared by phenolic curing agent.

In another attempt, Goharpey and coworkers prepared TPEs and TPVs based on PP/EPDM (40/60 w/w) in order to study the dynamic vulcanization effect of the rubber phase on the interfacial tension coefficient of the blends in 2001. It was found that the interfacial interaction between the two phases increased when the rubber phase of the samples was dynamically cured [Goharpey *et al.*, 2001].

2.7.2 Effects of viscosity ratio and filler content on microstructure and mechanical properties of PP/EPDM

Danesi and Porter prepared uncured TPEs based on high molecular weight of EPDM and PP in order to study the morphology of the blends in 1978. They presented bicontinuous morphology with 50 % of EPDM and also the minor phase dispersed in

the major phase by means of optical microscopy. Similar results were reviewed by Kresge for the morphology of PP /EPDM thermoplastic elastomers [Kresge, 1978].

It was reported that the morphology of the unvulcanized PP/EPDM blends was dependent on the interfacial tension between the two phases, processing conditions, elastic ratio, viscosity ratio, composition, and ethylene content of rubber. The fine dispersion of the rubber particles can be achieved when the ethylene content and the number average molecular weight of the rubber are low and also the rubber/plastic viscosity ratio value is near unity. Coalescence effect after mixing was shown to be very important in the morphology study of the uncured blends. The morphology of the blends changed when the hot batch of the samples was cooled by cold press. Laminar phase morphology was formed when the hot batch of the blends was cold pressed. The morphology of the blends having similar concentrations of both the rubber and the plastic showed a random co-continuous structure when the samples were prepared via compression molding [Avgeropoulos *et al.*, 1976; Karges-Kocsis *et al.*, 1987; Wu, 1987; Chung *et al.*, 1997].

Goharpay and coworkers studied the morphology development of PP/EPDM (40/60, w/w) during mixing. Samples were taken from a hot running mixer and rapidly quenched in liquid nitrogen before and after the onset of the rubber vulcanization. They illustrated that the rubber particles were dispersed throughout the polypropylene matrix for the unvulcanized but frozen samples, however, the unfrozen blends showed a particulate co-continuous morphology. It was also shown that the cured rubber particles

dispersed into the plastic matrix for the dynamically vulcanized blends [Goharpey *et al.*, 2001].

In another attempt, TPVs blends were prepared with different viscosity ratio of PP/EPDM. The decrease of the rubber particle size with decreasing the viscosity difference between the elastomer and the plastic was evidenced by using scanning electron microscopy (SEM). It was also shown that the mixing torque and the tensile strength increased as the viscosity difference between two phases were decreased. This was due to the small size of the rubber particles as well as the high interfacial adhesion of the elastomer phase with the polypropylene matrix [Goharpey *et al.*, 2003].

Some properties of dynamically vulcanized thermoplastic elastomers based on PP/EPDM such as hardness, ultimate tensile, modulus and tension set increased with introduction of carbon black. The processability and the elastic recovery of the blends improved when the oil content was increased. It was also shown that the crosslink density of the TPV materials increased by using the EPDM rubber with the high moony viscosity [Coran *et al.*, 1982; Abdou-Sabet *et al.*, 1996].

In a study, the morphology and the mechanical properties of carbon black-filled blends based on PP/EPDM (50/50 to 20/80, w/w) were investigated and compared with similar but unfilled samples. It was shown that the rubber particles were dispersed in the thermoplastic matrix (PP) for the dynamically cured samples at all ratios. It was found that the rubber particles size of the loaded blends increased more than that of the unfilled samples. This was due to the fact that carbon black has a tendency to stay in the rubber phase leading to increase in the viscosity difference between the two phases

and therefore, increase in the rubber particle size. The tensile strength and the rupture energy of the blends improved when the carbon black content was increased [Katbab *et al.* 2000].

The effect of silica fillers on the microstructure and the morphology of dynamically vulcanized TPVs based on PP/EPDM (40/60, w/w) with different filler content was examined by Bazgir *et al.* in 2004. The vulcanized blends containing 10 or 30 % silica presented the lower viscosity and consequently the better processability compared with the unfilled samples. It was shown that increasing the silica concentration led to increase the size of the rubber particles dispersed into the polypropylene matrix. The silica-loaded blends presented a reduction in the tan δ and also an enhancement in the storage modulus in comparison with the similar unloaded blends. The tensile strength and the elongation at break of the silica-filled cured blends increased when the content of the filler was increased [Bazgir *et al.,* 2003, 2004].

TPV nanocomposites were prepared using a commercial TPV with different kinds of clay without any compatibilizer by Lee and Goettler in 2004. They reported that the interlayer distance and the dispersion of the clay in the TPV materials were strongly dependent on the miscibility of the clay and the polymer matrix, as already mentioned in single polymer system. They also prepared uncured EPDM/PP based nanocomposites having 30, 50, and 70 % EPDM at 6 % wt of the clay without any compatibilizer. Silicate layers distribution in each phase was found to be dependent upon the mixing condition and route of the clay feeding. The uncured nanocomposites (selectively reinforced plastic phase) showed higher tensile modulus in comparison

with the unvulcanized samples prepared with the nanoclay-filled rubber phase. The tensile strength of the nanocomposites decreased when the nanoclay content was increased [Lee *et al.*, 2004].

Thermoplastic olefin nanocomposites (TPOs) based on PP/EPDM (70/30, w/w) were made with different clays loading in order to study the morphology of the nanocomposite by using atomic force microscopy (AFM). The reduction in the size of the rubber particles was observed with increasing the clay concentration as a result of the increase in the melt viscosity of the nanocomposite. In the nanocomposites, the un-notched (Izod) impact strength increased when the clay content was increased. On the contrary, the notched (Izod) impact strength decreased with increasing the layered silicate concentration [Mehta *et al.*, 2004].

A new TPV/organoclay nanocomposite was prepared with MMT modified by glycidyl methacrylate in the presence of dicumyl peroxide during melt mixing. TEM image and XRD results showed an intercalated structure for the TPV nanocomposite. The tensile modulus of the nanocomposite reinforced with 5 % of the clay was higher than that of the micro-composite filled with 20 wt % talc. Dynamic mechanical analysis revealed that the Tg of the PP phase of the nanoclay-filled samples increased in comparison with the pristine TPV, however, this was unchanged for EPDM phase [Mishra *et al.*, 2004].

In a study, Mishra and coworkers prepared TPO/nanoclay nanocomposites having PP/EPDM (75/25, w/w) with maleic anhydride modified polypropylene (PPMA) as compatibilizer at different clay content using a one-step melt mixing

process. It was found that the silicate layers were dispersed into the polypropylene phase and could not diffuse into the rubber phase. It was also reported that the tensile strength and modulus of the nanocomposites considerably improved when the clay content was increased [Meshra *et al.,* 2005].

2.8 The rheological behavior of dynamically vulcanized TPVs, EPDM/PP blends and their nanocomposites

Han and White reported that polypropylenes exhibit a Newtonian viscosity at low shear rates and stress however, the shear viscosity of dynamically vulcanized TPVs based on PP/EPDM increases indefinitely in the low shear stress. It was also found that the uncured PP/EPDM blends present rheological behavior close to the PP and may demonstrate a zero shear viscosity. The TPVs show a yield value in shear flow and the storage modulus goes asymptotically to a finite value as frequency goes to zero. Moreover, the complex viscosity of the TPVs is much greater than the shear viscosity. They reported that the elongational viscosity of polypropylene is roughly constant but for the TPVs, it is decreasing functions of deformation rate. In the uncured PP/EPDM blends, the storage modulus tends to go to zero at low frequency, the normal stresses are very low, and the complex viscosity is higher than the shear viscosity except at low shear rates or frequencies where they are equal. The rheological behavior and viscoelastic properties of the TPVs are similar to those found in ABS resins and polymer systems filled with small particles [Han *et al.,* 1995].

In another attempt, the rheological properties of unvulcanized and dynamically crosslinked polypropylene/ethylene-propylene elastomer blends in the melt state were compared by Krulis and Fortelny. They found that the rheological behavior of both the uncured blends and the dynamically vulcanized TPVs were strongly dependent on the rubber/plastic ratio. It was shown that a physical network between rubber particles was formed when the EPDM percentage was more than 30 % in the TPV samples. The rheological and the morphological feature of both the TPVs and the TPE blends were similar at low concentration of the EPDM phase (up to 20 %). The rubbery plateau exhibited in the storage modulus of the dynamically vulcanized blends at low frequencies was explained to be due to the long-lived entanglements among touching crosslinked rubber particles [Krulis *et al.*, 1997].

Rheological and morphological properties of TPVs based on PP/EPDM containing 20, 40, and 60 wt % of EPDM were investigated by Goharpey and coworkers. They observed a significant viscosity upturn and a strong storage modulus that tended to plateau at low shear rates for the TPVs. These results were attributed to the network structure resulting from agglomerates formed between the cured rubber particles as evidenced by the morphological features of the blends. It was shown that the sample prepared with 60 % the EPDM rubber presented multiple elastic responses in terms of the relaxation time distribution ($H(\lambda)$) suggesting apart from the contribution of flow-induced molecular orientation of the PP matrix, there may also exist some elastic response induced by the agglomerates formed between the cured rubber particles. They also reported that a linear viscoelastic model similar to the

Pelerine model for dilute suspension, taking into account the maximum packing volume, can be applied to describe the rheology of the TPVs materials [Goharpey *et al.*, 2005].

2.9 Conclusions of the literature review

Some of the main conclusions of the literature review can be summarized as follow:

1. The direct melt intercalation method offers a convenient technique for preparation of nonpolar polymer nanocomposites (poly-olefin hybrids).

2. The intercalation of polypropylene chains into the organo-clays does not occur when the acid value of PPMA as compatibilizer is low (acid value $\leq$ 7 mg KOH/g).

3. Increasing the acid value of PPMA (acid value $\geq$ 52 mg KOH/g) has no further effect on increasing the interlayer spacing of the layered silicates.

4. The crystalline size of PP nanocomposites decreases with increasing PPMA content.

5. The mechanical properties of PP nanocomposites increase when the molecular weight of PPMA is increased.

6. In PP nanocomposites, the storage modulus increases and the tan δ decreases with increasing the organo-clay content.

7. The crystalline size of polypropylene nanocomposites is smaller than that for pristine PP.

8. The interlayer spacing of the organo-clays is not significantly influenced by processing conditions; however, increasing shear stress, mixing time, and decreasing mixing temperature increase the exfoliation degree of the clay in polypropylene nanocomposites.

9. PP nanocomposites prepared with master-batch method (M.B) present higher tensile strength, and modulus in comparison with direct mixing process (D.M). Moreover, the degree of exfoliation and intercalation of the clay in M.B. is much better than that of D.M.

10. Both the storage and loss moduli in PP nanocomposites (melt state) increase and also, the frequency dependence decrease when the silicate layer content is increased. The strong interaction between polymer chains and the clay is responsible for the improvement of both the moduli.

11. The yield stress value is directly correlated to the exfoliation degree of the clay in polypropylene nanocomposites.

12. The plateau-like behavior of the storage modulus at low frequency is observed for the clay fully exfoliated in polypropylene matrix.

13. In PP nanocomposites, the amount of stress overshoot observed in flow reversal experiments increase when the rest time allowed between the reversals is increased.

14. PP nanocomposites present a greater shear thinning tendency than pristine polypropylene at high shear rates as a result of the preferential orientation of the silicate layers.

15. In EPDM nanocomposites, the curatives play a crucial role to promote the intercalation or exfoliation of the clay. EPDM-clay hybrid nanocomposites prepared with tetra-methyl thiuram monosulfide (TS) and zinc dimethyl dithiocarbamate (PZ) as accelerators achieve an exfoliated structure.

16. The crosslink density of EPDM nanocomposites decreases when the concentration of the organo-clay was increased. This is due to the retardation in the rate and final state of cure.

17. The mechanical properties of TPEs significantly increase (tensile strength, elastic recovery, properties retention at elevated temperatures, flex fatigue resistance, and consistence processability) when the rubber phase is dynamically vulcanized. The mechanical properties of TPVs improve with decreasing the rubber particle size.

18. The impact strength of TPEs increases when the rubber phase is dynamically cured. The cured rubber particles act as nucleating agent, which lead to decrease in the crystalline size of the plastic phase.

19. In TPEs, the interfacial interactions between two phases (PP and EPDM) increase as the rubber phase of the blends is dynamically vulcanized.

20. In uncured PP/EPDM (40/60) blends, the rubber droplets are dispersed throughout polypropylene matrix during melt mixing, however, the blend show a particulate co-continuous morphology at room temperature. Two-phase morphology is observed for the dynamically vulcanized blends (TPVs) in which the cured rubber particles are dispersed in the thermoplastic matrix (PP).

21. In TPVs based on PP/EPDM, the rubber particle size decreases with decreasing the viscosity difference between the elastomer and plastic phases.

22. In uncured PP/EPDM (70/30) blends, the size of the dispersed rubber particles reduces with the introduction of the clay.

23. TPVs show a yield stress in shear flow as well as a strong elastic modulus goes asymptotically to a finite value as frequency goes to zero.

CHAPTER 3

ORGANIZATION OF THE ARTICLES

In the first paper, we prepare dynamically-vulcanized nanocomposite thermoplastic elastomers (TPV nanocomposites) based on 60 % EPDM and 40 % polypropylene using a three-step melt mixing process in an internal mixer. The effects of clay concentration and viscosity ratio of the rubber to the plastic are also discussed in this paper. Furthermore, the evolution of the nanocomposite microstructure during the mixing process is monitored.

To achieve the aforementioned objectives we chose three types of polypropylene (PP) with different melt flow index and one grade of EPDM [Mooney viscosity ML (1+4, 125) = 55]. The rheological properties of polypropylenes and EPDM are obtained using a stress controlled rheometer. It is shown that there is approximately a five-fold difference in zero shear viscosity between high and medium-viscous PP and, also, a fifteen-fold difference between high and low viscosity polypropylene.

In the first step of the TPVs process, the clay powder (Cloisite 15A) and PPMA as compatibilizer (PPMA/clay = 3) are melt mixed under nitrogen to obtain a master batch. The master batch is then melt-blended with different polypropylenes to achieve PP nanocomposites. In third and final step, PP nanocomposites prepared from step2, EPDM, Zinc oxide (Zno) and stearic acid (St.Ac.) as activators are melt mixed. Three

to four minutes after the melting of the PP nanocomposites, tetra-methyl thiuram disulfide (TMTD), benzothiazyl disulfide (MBTS) as accelerators, and sulfur (S) as curing agent are introduced to the mixer.

The dispersion of the clay through the TPV matrix is evaluated by an X-ray diffraction (XRD) at room temperature. It is found that the first characteristic peak of the clay disappears for the TPV nanocomposites based on different viscosities of PP at 2 wt % of the clay. The nanostructure of the clay in the hybrids is observed by a transmission electron microscopy (TEM). The TEM image of the TPV sample prepared with low viscosity polypropylene (LVP) confirm that the clay is nearly exfoliated and randomly distributed throughout the polypropylene phase. In order to study the morphology of the TPV nanocomposite samples using scanning electron microscopy (SEM), cryogenically fractured surfaces of the samples are etched by hot xylene. The morphology results demonstrate that the rubber particles are dispersed through the polypropylene in form of aggregates and their size increase with the introduction of the clay. The stress-strain properties of the nanocomposites are determined in accordance with the test procedures set forth in ASTM D 412. The nanoscale dimensions of the dispersed clay cause a significant improvement in the tensile modulus of the TPV nanocomposite samples from 20 to 90 % depending on the clay content and the viscosity ratio of PP/EPDM. The crystallization of the nanocomposites is studied using a differential scanning calorimeter (DSC) under a nitrogen atmosphere. The degree of crystallinity decreases and the crystallization temperature increases in the nanocomposites as the clay content is increased.

In the second paper, the rheological and morphological properties of the dynamically vulcanized nanocomposite thermoplastic elastomers (TPV nanocomposites), based on EPDM and PP containing 20, 40, and 60 wt % of the rubber and 2 wt % of the clay are examined. The effects of PPMA as compatibilizer, composition, and different viscosities of polypropylene are also considered.

In uncompatibilized TPV nanocomposites (without PPMA) prepared with PP of different viscosities having 20, 40, 60 % EPDM, the polypropylene chains penetrate between the silicate layers of the clay, consequently the interlayer distance of the clay increase. The exfoliation degree of the clay improves by incorporating PPMA in the TPV nanocomposites. The agglomeration of the clay considerably decreases when the concentration of the rubber phase is increased in the TPV samples. The storage modulus (G′) of the TPV hybrids (without PPMA) containing 20, 40, and 60 % rubber significantly increases in comparison with similar but unfilled samples and also a further increase in the G′ from the incorporation of the PPMA in the TPV nanocomposites. The TPV nanocomposites exhibit strong storage modulus that tends to become increasingly independent of frequency (plateau) at low frequencies with the highest extent for the sample containing 60 % of EPDM. In the TPV nanocomposites, the size of the rubber particles increases as the elastomer content increases. The yield stress of the TPV nanocomposite prepared based on low viscosity PP increases more than that for the hybrid having high viscosity PP. A Carreau-Yasuda law with a yield stress and a linear viscoelastic model, taking into account the maximum packing volume, are used to describe the melt linear viscoelastic properties of the TPV

nanocomposites. The maximum packing volume increases with increasing EPDM content.

In the third paper, "The influence of matrix viscosity and composition on the morphology, rheology and mechanical properties of thermoplastic elastomer nanocomposites (TPE nanocomposites) based on PP/EPDM" is studied.

Papers 1 and 2 provide comprehensive knowledge of the microstructure, rheological, and mechanical properties of the TPV nanocomposites (selectively reinforced plastic phase) prepared by a three-step melt mixing process, containing 20, 40, and 60 % EPDM with different viscosities of PP at different contents of the clay. The morphological features of the TPV hybrids were examined both before and after curing the rubber phase. The morphological results of the TPV samples prepared from low and high viscosity PP (LVP and HVP) before the vulcanization of the EPDM phase (selectively reinforced plastic-phase TPE nanocomposites) revealed that the silicate layers were dispersed through the PP phase and could not penetrate into the rubber phase during the mixing process. These results were explained due to the initial placement of the clay in the polypropylene phase (selectively reinforced plastic phase).

One of the important factors affecting the mechanical properties of nanoclay-reinforced TPEs is feeding routes. On the other hand, the final phase morphology of the TPE nanocomposites significantly depends on the phase location of the clay reinforcement, whether it lies in the dispersed rubber phase or in the continuous plastic matrix.

In this work, we study the microstructure, rheology, and mechanical properties of the uncured TPE nanocomposites prepared by a one-step melt mixing process in a small laboratory mixer. EPDM contents of 20, 40, and 60 % are compounded with different viscosities of polypropylene at 3 wt % of the clay. The effect of viscosity ratio of PP to EPDM and different compositions are also investigated.

It is found that the unvulcanized nanocomposites (TPE nanocomposites) prepared from different viscosities of PP and 20, 40, 60 % rubber show an intercalated structure. The clay tends to disperse into the low viscosity polypropylene (LVP) phase in the TPE samples having 20, 40, and 60 % EPDM. In the uncured TPEs based on medium viscosity polypropylene (MVP), the clay disperses into the PP phase but some silicate layers diffuse into the EPDM phase with increasing the rubber content. The organo-clay disperses through both the PP and EPDM phases in the TPE hybrids prepared from high viscosity PP (HVP). The volume average diameter (dv) of the dispersed rubber droplets in the unloaded blends having 20, 40 and 60 % EPDM decreases with increasing the viscosity of PP phase. The nanoclay-filled sample prepared with LVP exhibits a reduction in the size of the dispersed rubber particles compared with similar but unfilled blend. The size of the dispersed rubber droplets is shown to be larger for the nanoclay-filled blends prepared with HVP containing 40 and 60 % EPDM in comparison with the similar but unloaded samples. The nanoclay-filled TPEs prepared with LVP show more enhancement in yield stress compared with the equivalent samples from HVP. The increase in the storage modulus and the decrease in the terminal zone slope of the elastic modulus curve are found to be larger for the LVP

blend in comparison with the HVP sample. Mechanical properties are consistent with the morphological structure observed by SEM and TEM. The tensile modulus improved for all TPE nanocomposites and obtained higher percent increase in the case of LVP samples.

CHAPTER 4

Microstructure-Properties Correlations in Dynamically Vulcanized Nanocomposite Thermoplastic Elastomers Based on PP/EPDM

The objective of this first paper is to prepare dynamically-vulcanized nanocomposite thermoplastic elastomers (TPV nanocomposites) based on PP/EPDM and study on parameters affecting microstructure and their properties. In this paper, we will prepare the dynamically-vulcanized nanocomposite thermoplastic elastomers based on PP/EPDM (40/60, w/w). The effect of viscosity ratio of two phases, and nanoclay concentration on the microstructure and the mechanical properties of the resulting PP/EPDM TPEs will be studied. We will also follow the microstructure change of the nanocomposites during the mixing process. In order to evaluate the dispersion of the clay through the polymer matrix, an X-ray diffraction (XRD) was performed at room temperature. The nanostructure of the clay was observed by a transmission electron microscopy (TEM). A thin section of each specimen was prepared by using a focused ion beam (FIB) and a cryo-microtom equipped with a diamond knife at -100 ^{o}C. To study the morphology of the TPV nanocomposite samples, cryogenically fractured surfaces of the samples were etched by hot xylene. Treated samples were then coated with gold-palladium alloy and viewed with a scanning electron microscope (SEM). The

stress-strain properties of the composites were determined in accordance with the test procedures set forth in ASTM D412. Crystallization was studied using a differential scanning calorimeter (DSC) under a nitrogen atmosphere. The permeability was also evaluated as the volume of the oxygen permeated per unit area of the TPV sample sheet for 24h.

This paper is accepted by the Journal of Polymer Engineering & Science (in press, 2006).

Microstructure-Properties Correlations in Dynamically Vulcanized Nanocomposite Thermoplastic Elastomers Based on PP/EPDM

Naderi Ghasem, Lafleur Pierre G., and Dubois Charles*

Center for Applied Research on Polymers and Composites, CREPEC, Department of Chemical Engineering, Ecole Polytechnique de Montreal, 2900 Edouard Montpetit, P.O. Box 6079, Station Centre-Ville Montreal, QC, Canada, H3C 3A7

Abstract

Thermoplastic vulcanized nanocomposites (TPV nanocomposites) were prepared in a laboratory mixer using EPDM, polypropylene of different viscosities, maleic anhydride modified polypropylene (PPMA), organo-nanoclay (Cloisite 15A) and an appropriate sulfur curing system. Based on the obtained results from X-ray diffraction (XRD), transmission electron microscopy (TEM), scanning electron microscopy (SEM), differential scanning calorimeter (DSC), and mechanical properties, the microstructure of the prepared nanocomposites is sensitive to the viscosity difference between the two phases and the clay content. X-ray diffraction results and TEM images of the TPV nanocomposites showed that the clay was nearly exfoliated and randomly distributed into the polypropylene phase. The SEM photomicrographs of the dynamically vulcanized thermoplastic elastomer samples showed the rubber particles were dispersed through the polypropylene matrix in form of aggregates and their size increased with the introduction of clay. The nanoscale

*Corresponding author. Tel.: +1 514 340 4711 ex 4893; fax: +1 514 340 4159
Email address: Charles.Dubois@polymtl.ca (C. Dubois).

dimensions of the dispersed clay resulted in a significant improvement of the tensile modulus of the TPV nanocomposite samples, from 20 to 90 % depending on the clay content and the viscosity ratio of PP/EPDM. In the PP nanocomposites, the clay layers act as nucleating agents, resulting in higher crystallization temperature and reduced degree of crystallinity. Moreover, the oxygen permeability in the TPV nanocomposites was found to be lower than in similar but unfilled materials.

Keywords: Nanocomposite thermoplastic elastomers, Dynamic vulcanization, PP/EPDM, TPV nanocomposites, Viscosity ratio of PP/EPDM.

4.1 Introduction

Thermoplastic elastomers (TPEs) constitute a unique class of polymers that offers many of the positive attributes of vulcanized rubbers, such as low compression set and high flexibility, while being processed using conventional thermoplastic fabrication techniques, without the time-consuming cure step usually required with vulcanizates. A special type of TPEs is obtained when the rubber is dynamically vulcanized during its blending process to give rise to a thermoplastic vulcanizates (TPVs). The microstructure of this type of TPEs consists of a thermoplastic matrix (continuous phase) that contains a dispersed cured rubber phase [1-2].

Many commercial TPVs have been developed for various applications in automotive parts, cable insulation, footwear, packaging and medical industries because of their excellent weather-ability, low density, and relatively low cost [3-5].

The addition of fillers, such as glass fiber, carbon black, talc, and calcium carbonate to the TPV blends at high loading levels improve properties like stiffness, heat distortion temperature and dimensional stability. These fillers increase the weight of the TPV blends and cause an adverse effect especially for automotive and aerospace applications [6, 7].

The potential use of a small amount of clay (up to 5 wt %) has received a significant attention from scientists and engineers in recent years [8]. This is mainly attributed to the nanoscale dimension of silicate layers dispersed in the polymer matrix, which causes a strong interfacial interaction between silicate layers and polymer chains, leading to a dramatic change in the mechanical, thermal stability, barrier, optical, and fire resistance properties in comparison with pristine polymer [9].

Montmorillonite (Na^+–MMT) is layered mica-type clay mineral. Its crystal lattice consists of a central octahedral sheet of alumina/magnesium sandwiched between two fused tetrahedral sheets. Montmorillonite has negative charges on the interlayer gallery walls and the galleries are normally occupied by cations such as Na^+, Ca^{2+}, and Mg^{2+}. The silicate layers are often modified to organo-montmorillonite (OMMT) by an aliphatic alkylammonium or alkyl phosphonium ion-exchange reaction in order to reduce the polar characteristic of the clay. This modification facilitates the intercalation of polymer chains between the clay layers by increasing the initial gallery spacing and improving the clay compatibility with non-polar polymers [10-11].

The structure of nanocomposites depends on the structure of dispersed clay particles in the polymer matrix, which can be classified as intercalated or exfoliated

structure. In the intercalated state, the clay is dispersed as lamellar structures and polymer chains penetrate between silicate layers of clay but in the exfoliated structure, clay is completely delaminated and the individual silicate layers are dispersed throughout the polymer matrix.

Nanocomposites based on polypropylene [12-16] and thermoplastic elastomers based on PP/EPDM [17-19] have been prepared, and their properties and microstructure have been published. These studies reveal that a suitable compatibility between the clay and the polymers and also sufficient deformation rate applied during the process are essential to achieve intercalated or exfoliated structure by using a simple melt mixing process.

The nanocomposites based on TPEs are a new class of reinforced thermoplastic elastomers with generally improved mechanical and physical properties compared to their unfilled counterparts. Recently, Lee and Goettler [20] studied TPV/clay nanocomposite prepared by simple melt mixing a commercial TPV with several types of clay without the use of a compatibilizing agent for the polyolefin. They reported that the mechanical properties of the TPV nanocomposite increased when the miscibility of the clay and polymer matrix increased.

Although there have been a few studies on the preparation and properties of thermoplastic elastomer (TPE) nanocomposites [21], the area of dynamically vulcanized nanocomposite TPEs prepared using polypropylene of different viscosities, maleic anhydride grafted polypropylene and sulfur as curing agent has remained uncharted.

The main objective of this project was to obtain dynamically-vulcanized nanocomposite thermoplastic elastomers based on PP/EPDM and to study the parameters affecting their microstructure and properties. For that purpose, we studied dynamically-vulcanized nanocomposite TPEs while investigating the effect of PP/EPDM viscosity ratio and clay concentration on their microstructure and mechanical properties. The evolution of the nanocomposite microstructure during the mixing process was also monitored.

4.2 Experimental

4.2.1 Materials

The basic specifications of EPDM and the three grades of polypropylene (Basell Co.) employed in this study are reported in Table 4.1. The EPDM rubber (Buna EP T 6470) was based on ethylene norbornene (ENB) as a termonomer, and was supplied by Bayer Co.

The clay used was Cloisite 15A from Southern Clay Products; a natural montmorillonite modified with a dimethyl dehydrogenated tallow quaternary ammonium having a cation-exchange capacity (CEC) at 125 meq/100g and a specific gravity of 1.66.

The maleic anhydride-modified polypropylene (PPMA) Epolene G3015 (Acid Number = 15, mol of MA/mol of PPMA = 6.3, AM % ~ 1) was obtained from Eastman Chemical.

Table 4.1: Basic specification of PP and EPDM

Materials	Characteristics	
PP (P1)	MFI	14 gr/10 min
	Density	0.91 g/cm^3
	Tm	>160 ^{oC}
	η_0	1818 Pa.s
PP (P2)	MFI	4 gr/10 min
	η_0	5000
PP (P3)	MFI	0.5 gr/10 min
	η_0	27100
EPDM	Mooney Viscosity ML (1+4), 125°C	55
	Ethylene Content	68 %
	Termonomer Content	4.5 % ENB
	Density	0.86 g/cm^3

The curing of TPV nanocomposites was achieved with benzothiazyl disulfide (MBTS), tetra-methyl thiuram disulfide (TMTD), and sulfur (S), obtained from Bayer Company.

4.2.2 Sample Preparation

TPV nanocomposite samples were prepared by a three step melt mixing process in an internal mixer (Haake Rhemix 600).

In the first step of the TPV process, the clay powder and PPMA pellets were dry-mixed in a bag to ensure that the materials were well dispersed at the macro-scale level. The mixture was then melt-mixed at 180 °C under nitrogen to obtain a master batch using the mixer at a rotor speed of 150 rpm for 10 min. For all master batches, the PPMA/clay ratio was kept constant at 3:1.

In the second step, the master batch was then dry-blended with polypropylene to give the desired composition (see Table 4.2), and fed to the mixer in applying the same previous processing conditions.

In the third and final step, PP nanocomposite (from step 2), EPDM, Zinc oxide (Zno) and stearic acid (St.Ac.) were mixed at 180 °C and 100 rpm. Three to four minutes after the melting of the PP nanocomposite, the TMTD and MBTS curing agents were added to the mixer and after 60 seconds of mixing, the sulfur (S) was introduced and followed by a continuous mixing for four minutes.

Prepared compounds were compression-molded by hot press at 200 °C for 10 min to obtain suitable samples for testing.

The ratio of PP/EPDM was kept constant at 40:60 (wt %) and the vulcanizing system was based on 100 phr EPDM, 5 phr Zno, 1 phr stearic acid, 1 phr TMTD, 0.3 phr MBTS, and 1 phr S.

For comparison purposes, unfilled but otherwise similar TPVs were also compounded as reference materials. In all instances, clay had been dried at 80 °C for 24 h prior to processing.

Table 4.2: Samples code and compositions

Sample Code	PP	PPMA	Clay
NP11	P1=96	3	1
NP12	P1=92	6	2
NP13	P1=88	9	3
NP15	P1=80	15	5
NP21	P2=96	3	1
NP22	P2=92	6	2
NP23	P2=88	9	3
NP25	P2=80	15	5
NP31	P3=96	3	1
NP32	P3=92	6	2
NP33	P3=88	9	3
NP35	P3=80	15	5
PP21	P2=97	3	-

4.2.3 Characterization

In order to evaluate the dispersion of the clay in the polymer matrix, X-ray diffraction (XRD) was performed at room temperature using an X-ray diffractomer (Philips model X'Pert) in the low angle of 2θ. The X-ray beam was a Cu-K_α radiation (λ=1.540598 A°) using a 50 kV voltage generator and a 40 mA current. The basal spacing of silicates was estimated from the position of the plane peak in the WAXD intensity profile using the Bragg's law, $d = \lambda / (2 \sin\theta_{max})$. Specimens for X-ray diffraction were obtained by compression-molded sheets of 2 mm in thickness.

The nanostructure of the clay was observed by a transmission electron microscopy (JEM-2100F, JEOL) with an accelerator voltage of 200 kV. The surface of the samples was first coated with gold and then a thin section of each specimen was prepared by using a focused ion beam (FIB, FB-2000A, Hitachi) and also a cryo-microtom equipped with a diamond knife at -100 °C.

To study the morphology of the TPV nanocomposite samples, cryogenically fractured surfaces of the samples were etched by hot xylene. Treated samples were then coated with gold and viewed with a scanning electron microscope model JSM-840 made by JEOL company.

The rheological characterization of polypropylenes and EPDM were carried out using a stress controlled rheometer (SR 5000). The experiments were performed in parallel-plate geometry with a diameter of 25 mm under a nitrogen atmosphere at a temperature of 220 °C and in the range of 0.01-80 Hz frequency.

The stress-strain properties of the composites were determined in accordance with the test procedures set forth in ASTM D 412 using an Instron model 4201 at cross-head speed of 50 mm/min.

Crystallization was studied using a Pyrist1 (Perkin Elmer) differential scanning calorimeter under a nitrogen atmosphere. Samples were heated from 50 ^{o}C to 200 ^{o}C at a rate of 10 ^{o}C/min and they were then cooled from 200 ^{o}C to 50 ^{o}C at the same rate after holding at 200 ^{o}C for 5 minutes to erase any thermal history effects.

Oxygen permeability was measured by using an OX-TRAN model 2/21, Mocon Co. The 1 mm thick sample specimens were prepared by using hot press with standard mold at 200 ^{0}C. The permeability was evaluated as the volume of oxygen permeated per unit area of the TPV sheet for 24h.

4.3 Results and discussion

Figure 4.1 shows the elastic modulus (G′) and complex viscosities (η^*) of EPDM and polypropylenes with different viscosities (P1, P2, and P3) as a function of angular frequency.

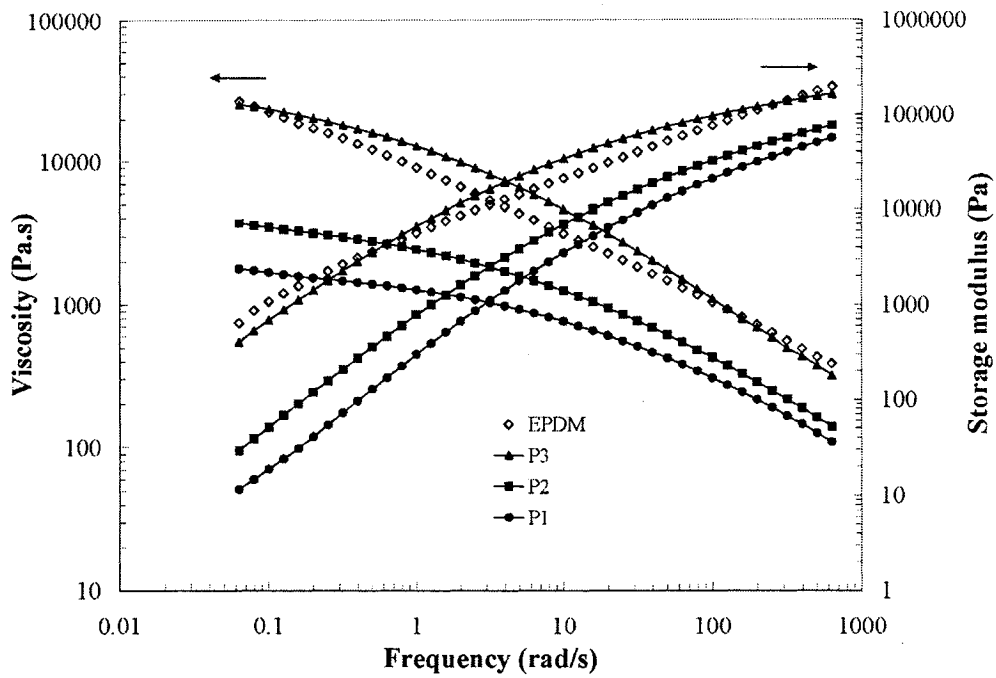

Figure 4.1: Complex viscosity and storage modulus of EPDM and three different polypropylenes versus angular frequency.

Since it was observed that the pure materials follow the Cox-Merz [22] relation, $[\eta^*(\omega = \gamma) = \eta(\gamma)]$, the simplified Carreau-Yasuda model [23] was used to fit the

complex viscosity data of the pure polymers from oscillatory shear measurements. The Carreau-Yasuda (C.Y) model is given by:

$$\eta^*(\omega) = \frac{\eta_0}{(1+(\omega\tau)^a)^{1-n/a}} \quad \text{(4.1)}$$

Where η^* is complex viscosity, η_0 is the zero shear viscosity, a is dimension less parameter which specifies the transition from Newtonian to shear thinning behavior, τ is in general close to the average of the melt relaxation time and n is the so-called power law index. The zero shear viscosity of three different viscosities of PPs, as reported in Table 4.1, was estimated by fitting equation (4.1) to experimental data.

The evolution of torque during the compounding of a multiphase reactive formulation often brings evidences of the time dependent mixture state. Figure 4.2 shows torque traces for unfilled TPV based on PP21/EPDM (40/60 w/w) and TPV nanocomposites prepared from NP21/EPDM (40/60 w/w). As shown in this figure, a higher steady-state value of the mixing torque is obtained for a TPV nanocomposite prepared from NP21/EPDM, in comparison with that of the unfilled TPV. The chemical reactions involved in the vulcanization of the unfilled TPV are reported by Coran and coworkers [1].

We have noticed that for formulations with similar clay contents (not shown in Figure 4.2), a simple indicator of the extent of clay exfoliation within the TPV matrix is the steady-state torque recorded during melt mixing. An increased torque value is an indirect evidence of a larger interaction between the TPV matrix and the clay [24].

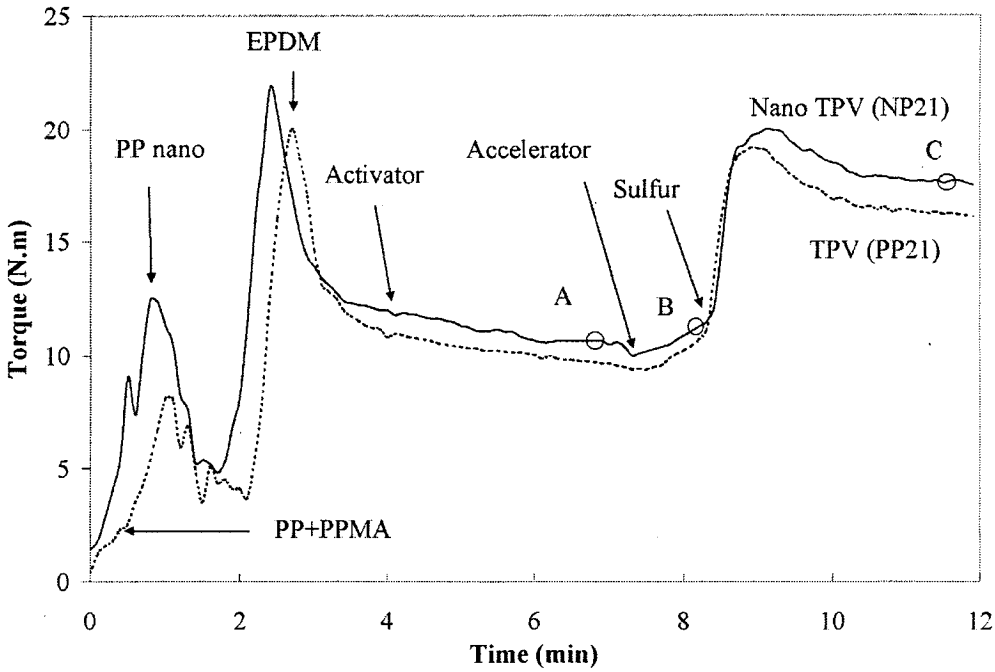

Figure 4.2: Comparison of mixing torque recorded for unfilled TPV prepared by PP21/EPDM (40/60, w/w) and TPV nanocomposite based on NP12/EPDM (40/60,w/w).

The structure and morphology of the nanocomposites were characterized by using X-ray diffraction analysis and TEM imaging of samples taken after the observed maximum in the mixing torque, as discussed previously.

In preliminary experiments assessing the effect of PPMA content, low viscosity polypropylene (P1) was used to prepare 2 % wt clay nanocomposites with PPMA/clay weight ratio of o, 1, 2, and 3. The X-ray diffraction results of corresponding samples are shown in Figure 4.3. It can be seen from curves (a) and (b) that the diffraction peak corresponding to the (001) plane of clay appears at 2.9 °, while the diffraction peak of the uncompatibilized system (PP/PPMA/clay, 98/0/2) appears at a higher angle (2θ = 3 °, d = 29.42 Á). These results reveal that polypropylene can not intercalate between the layers of the clay modified by a dimethyl dehydrogenated tallow quaternary ammonium [25]. On the contrary, the XRD peaks of the samples prepared using master batch with different ratios of PPMA/clay show an increase in the interlayer spacing as a result of the intercalation of polypropylene. The interlayer distance of the clay (d = 33.31 Á) in the nanocomposite prepared with a PPMA/clay ratio of 2 (PP/PPMA/clay, 94/4/2) is higher than that of the sample with PP/PPMA/clay (96/2/2), (d = 31.3 Á) as shown in curves (c), and (d) respectively. From the results in (e), it is shown that the position of the clay characteristic XRD peak of the sample with PPMA/clay = 3 remains relatively constant. However, an important difference is observed in the decrease of the peak intensity, in comparison with the similar nanocomposite based on a PPMA/clay ratio of 2. These results are in consistent with the recent work of Vergnes [25]. The PPMA/clay ratio was therefore maintained constant at 3 for this work, but the role of PPMA concentration on nanocomposites morphology would need to be further investigated in the future. The concentration range and type of PPMA used for this work were similar

to the conditions reported in [25, 26] and therefore, miscibility of the polymers was assumed.

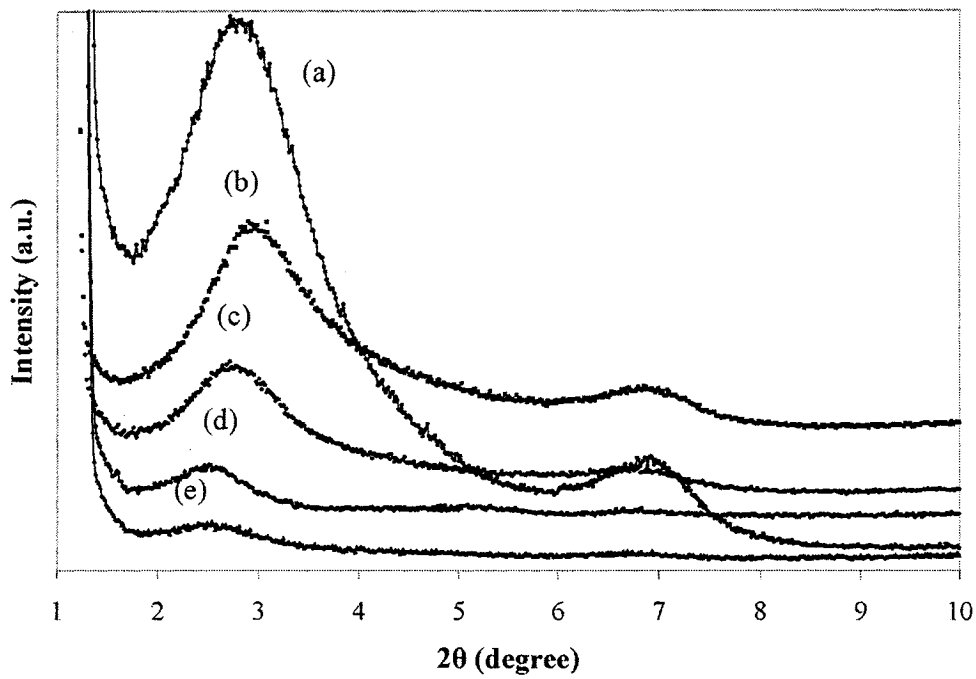

Figure 4.3: X-ray diffraction patterns of (a) clay, and 2 % clay P1 nanocomposites prepared with (b) PPMA=0, (c) PPMA/clay=1, (d) PPMA/clay=2, and (e) PPMA/clay=3.

The x-ray diffraction results of the clay itself, PPMA/clay =3 master batch and nanocomposites based on 2 wt % of clay respectively prepared with polypropylene of three different viscosities (P1, P2, and P3) are shown in Figure 4.4.

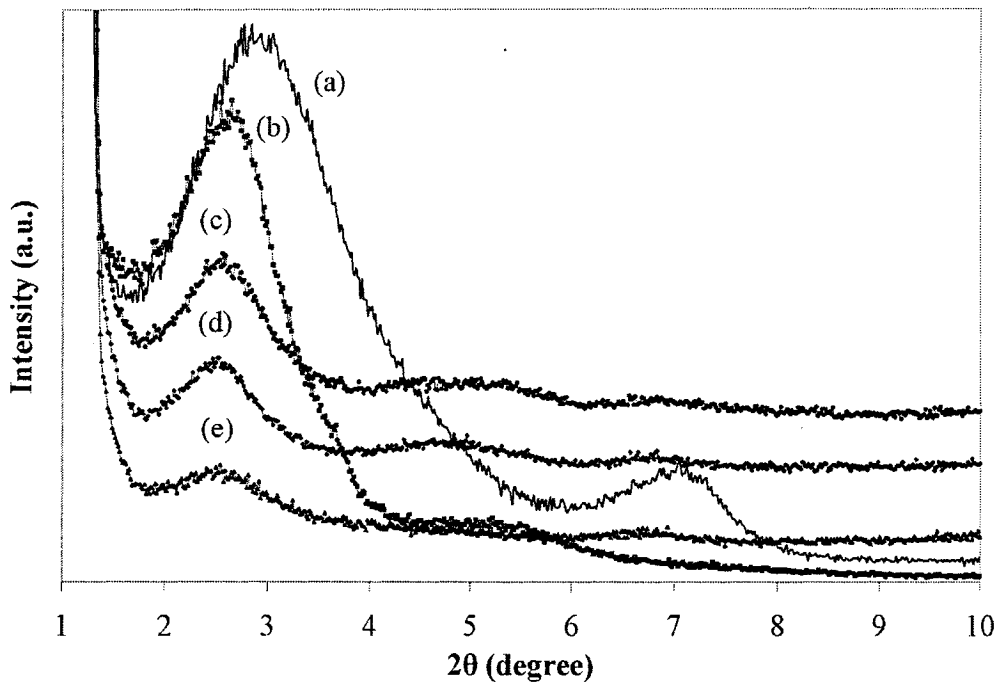

Figure 4.4: X-ray diffraction patterns of (a) clay, (b) master batch (PPMA/clay = 3), (c) NP32, (d) NP22, (e) NP12.

It is observed that the diffraction peak corresponding to the (001) plane of the clay appears at 2.9 °, while the diffraction peak of the master batch appears at a lower angle (2θ = 2.75°, d = 32.10 Á) than that of clay, which indicates an increase in the interlayer distance of the clay.

It has been reported that PPMA can penetrate into the silicate layers of the clay during melt mixing and induces an expansion of the gallery distance [27].

The interlayer distance of the nanocomposite based on P1 with 2 wt % of clay is about 33.65 Á, larger than the original interlayer spacing of Cloisite 15 A and the master batch, which implies the polypropylene can intercalate into the clay. The interlayer distance of P3 nanocomposite for the 2 wt % clay formulation (d=32.25 Á) is less than that of the similar nanocomposite based on P1 with the same clay content. It should also be noted that the intensity of the diffraction peak in the nanocomposite based on P1 decreases and also the peak is broader than its counterpart in nanocomposites based on P2 and P3 of identical clay content.

The decrease in the intensity and the broadening of the peaks indicate that the stacks of layered silicates become more intercalated or partially exfoliated; hence, the nanocomposite obtained from low viscosity polypropylene yields a more disordered structure (better clay dispersion). This is explained by the fact that polypropylene molecules with high MFI (low viscosity) need a lesser level of attractive Flory-Huggins interactions to penetrate between the silicate layers consisting of PPMA with low molecular weight in comparison with high viscosity propylene products [16]. This entropic effect is found to be more important than the increased stress level imparted to the clay particles by polypropylenes of higher viscosity [16].

In Figure 4.5, we present the XRD patterns of PP nanocomposites based on 5 wt % of clay respectively prepared with polypropylene of three different viscosities (P1, P2 and P3).

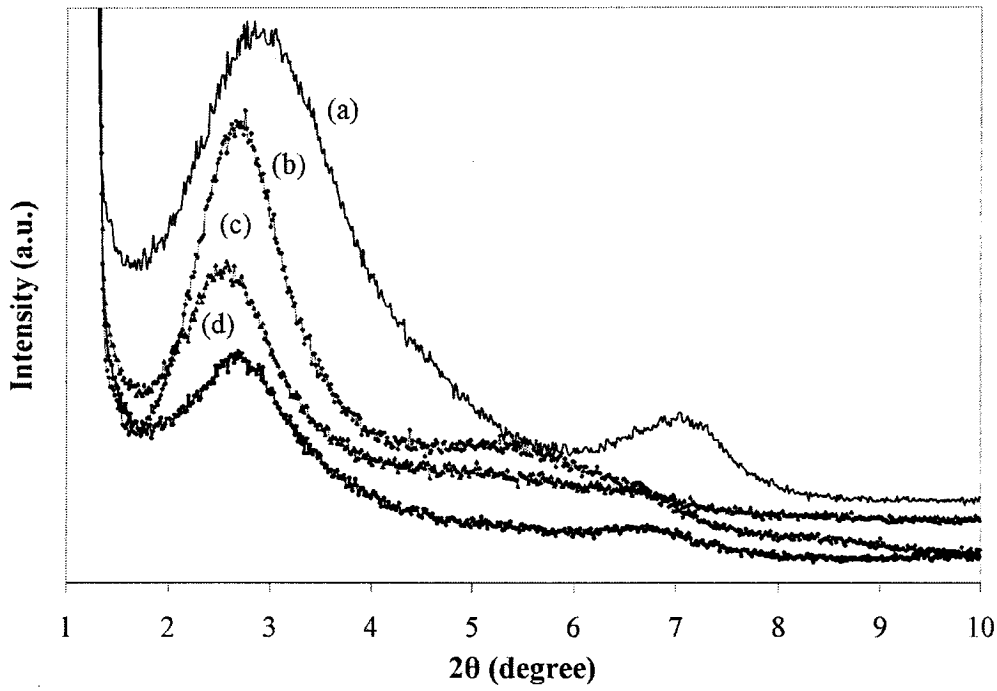

Figure 4.5: X-ray diffraction patterns of (a) clay (b) NP35, (c) NP25, and (d) NP15.

It can be seen that the intensities of the peaks increased in comparison with the nanocomposites prepared with 2 wt % of the clay. This is due to the influence of the packing density, rending more difficult the penetration of the polymer chains between the silicate layers. X-ray diffraction patterns of the clay and TPV nanocomposite prepared based on NP15/EPDM (40/60 w/w) are presented in Figure 4.6 at different mixing stages (A, B, C as shown in Figure 4.2).

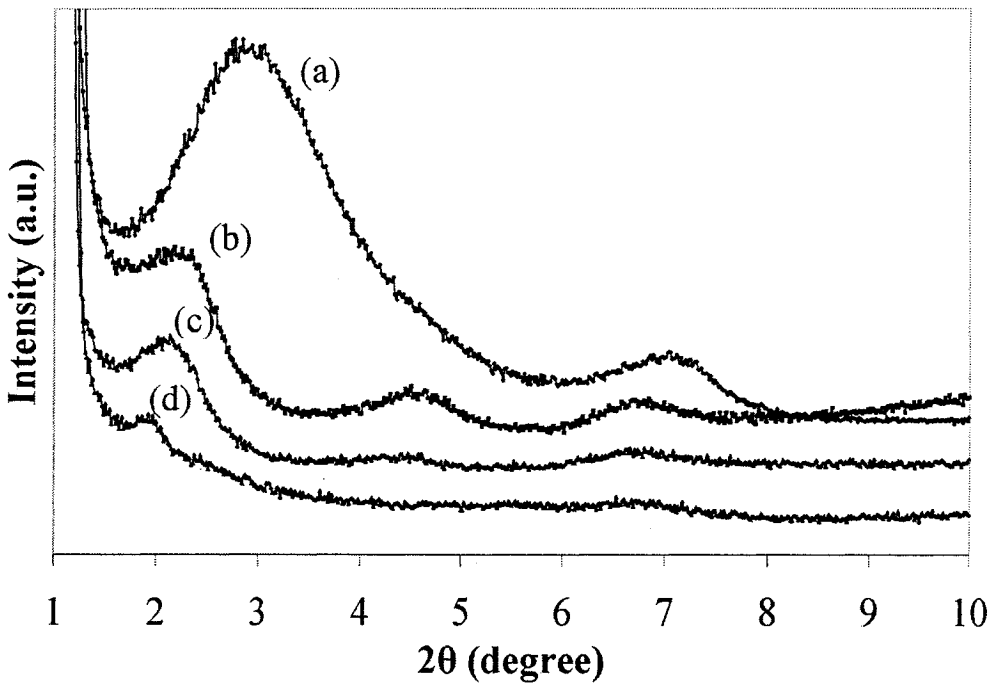

Figure 4.6: X-ray diffraction patterns of (a) clay and TPV nanocomposite based on NP15/EPDM (40/60) at different mixing stages, (b) stage A, (c) stage B, (d) stage C.

The diffraction peak corresponding to the (001) plane of the nanocomposite with activators (stage A) appears at 2.5 ° (d = 35.35 Á), while the nanocomposite with activators and accelerators (stage B) shows a peak at a lower angle (2θ = 2.2 °, d = 40.12 Á) as shown in figures 4.6-b and 4.6-c respectively. The peak d_{001} of the TPV

nanocomposite prepared by NP15/EPDM (40/60 w/w) with activators, accelerators, and sulfur (stage C) is also shifted toward lower angles ($2\theta = 1.9^{\circ}$, d = 46.31 Å). It is also seen that the intensities of the XRD peaks decreased.

Similar trends were observed for TPV nanocomposites prepared based on NP25/EPDM and NP35/EPDM (40/60 w/w).

This can be explained by the fact that the dynamic vulcanization of the EPDM phase increased the viscosity of the blend and hence the shear stress imposed by the matrix during mixing is also increased, which facilitates the break-up process of the clay agglomerates.

Figure 4.7 shows the effect of post-processing (compression molding) on the x-ray diffraction patterns of the TPV nanocomposites based on NP15/EPDM, NP25/EPDM and NP35/EPDM (40/60). It can be seen that the first characteristic peak of the clay disappeared for all TPV nanocomposites based on different viscosities of PP (PP3, PP2, and PP1) when post processing is applied to these samples as shown in Figures 4.7-b, c, and d respectively. The absence of the diffraction peak suggests that the compression molding process could contribute to the further exfoliation of the silicate layers in the TPV nanocomposites.

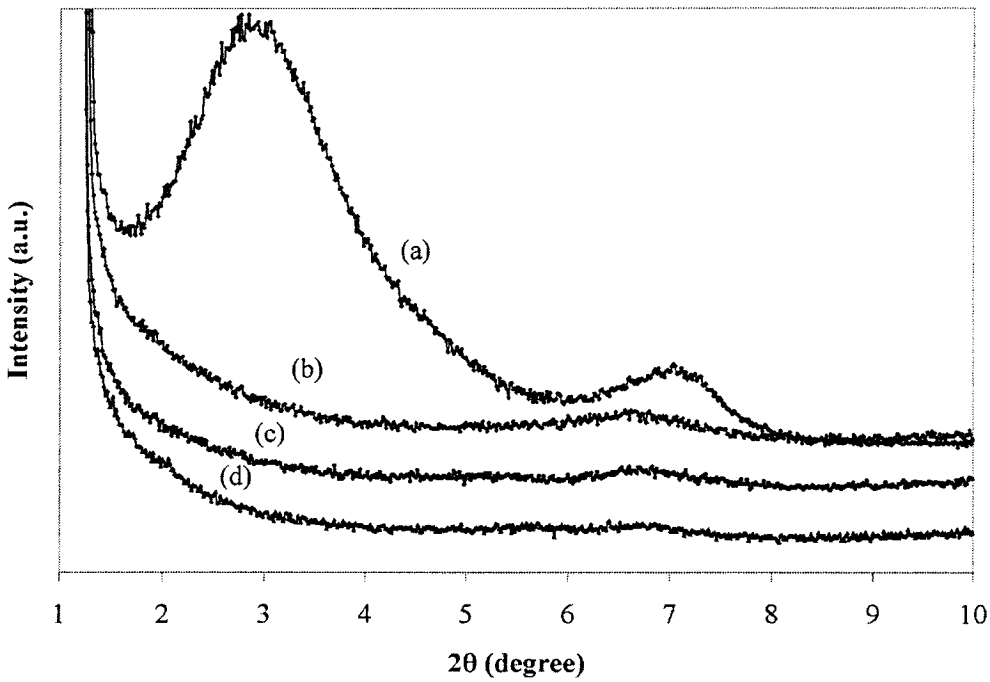

Figure 4.7: X-ray diffraction patterns of (a) clay and TPV nanocomposites prepared with (b) NP35/EPDM (40/60), (c) NP25/EPDM (40/60), (d) NP15/EPDM (40/60).

It should be noted that X-ray diffraction pattern of the clay shows two peaks, the second peak appeared at $2\theta=7.1°$ which may be because of diffraction from a second silicate layer (d_{002}), since 2θ of second peak is about twice the d_{001} peak of the clay. The second peak of clay may also come from the portion of the clay that is not modified

[28]. On the other hand, for the X-ray diffraction patterns of the TPV nanocomposites, the second peak of the clay appears at lower 2θ (6.7°).

In order to get a better insight of the clay dispersion, TEM images where taken from these PP nanocomposites and TPVs as illustrated in Figures 4.8-4.10. The TEM image of the PP nanocomposites prepared by using low viscosity of polypropylene (P1) shows silicates agglomeration at 2 and 5 wt % of the clay as shown in Figures 4.8-a, 4.8-b respectively.

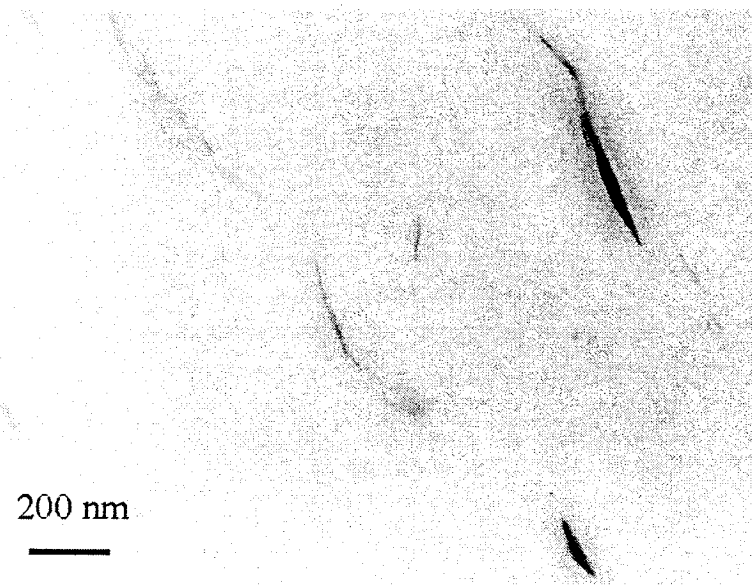

(a)

Figure 4.8: TEM image of PP nanocomposite prepared by (a) P1 with 2 wt % of clay.

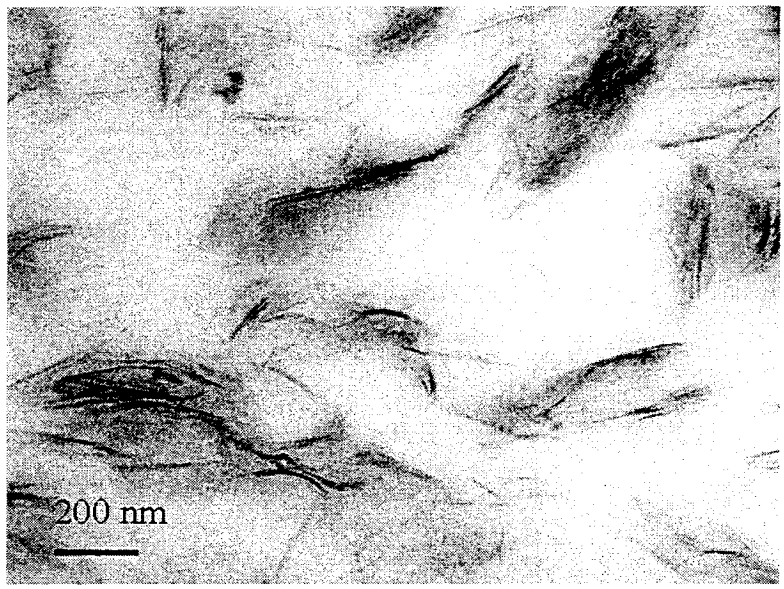

(b)

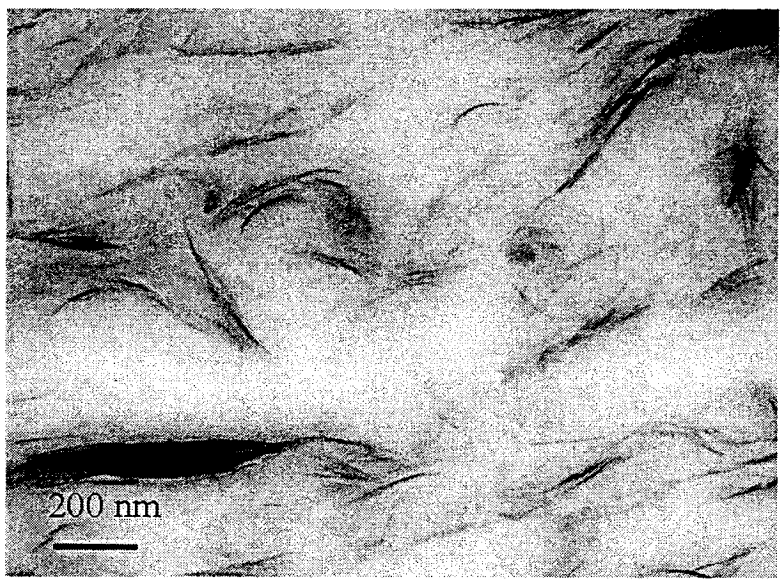

(c)

Figure 4.8: TEM image of PP nanocomposites prepared by (b) P1 with 5 wt % (c) P3 with 5 wt % of clay.

It can be seen that the size of the stacks increased at higher clay content. We also observed the agglomeration of the clay for the nanocomposite prepared from high viscosity polypropylene (P3) at 5 wt % of clay as shown in Figure 4.8-c.

A TEM image of the TPV nanocomposite prepared from low viscosity polypropylene (P1) before curing stage (stage A) is showed in Figure 4.9-a.

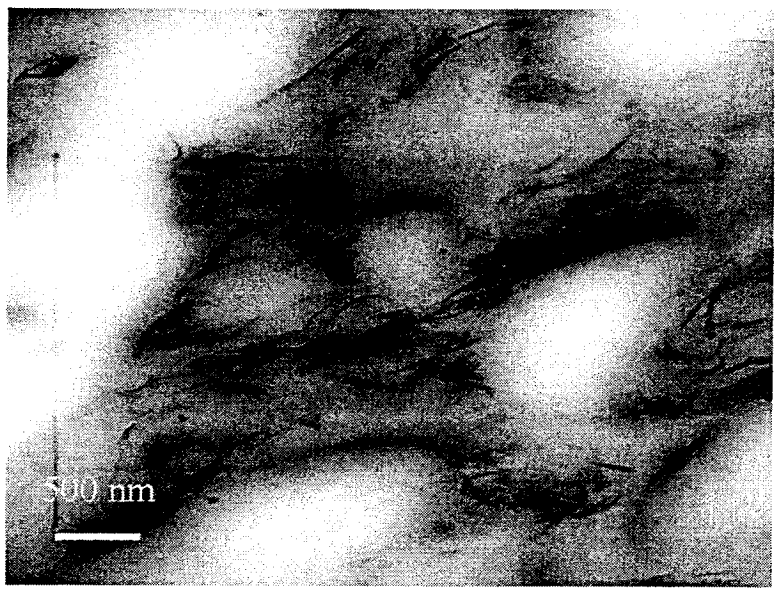

(a)

Figure 4.9: TEM image of TPV nanocomposite before curing stage (stage A) prepared by (a) NP15/EPDM (40/60 w/w).

It indicates that silicate layers are dispersed through the PP matrix and cannot penetrate into the EPDM phase during the mixing process. The rubber phase is white in color, and silicate layers appear as black lines in the darker polypropylene phase. Also at stage A of the mixing process, in the TPV nanocomposites based on high viscosity PP the clays were found to be dispersed in the continuous phase but partly agglomerated at interfacial boundary between the polypropylene and rubber phases, as shown in Figure 4.9-b.

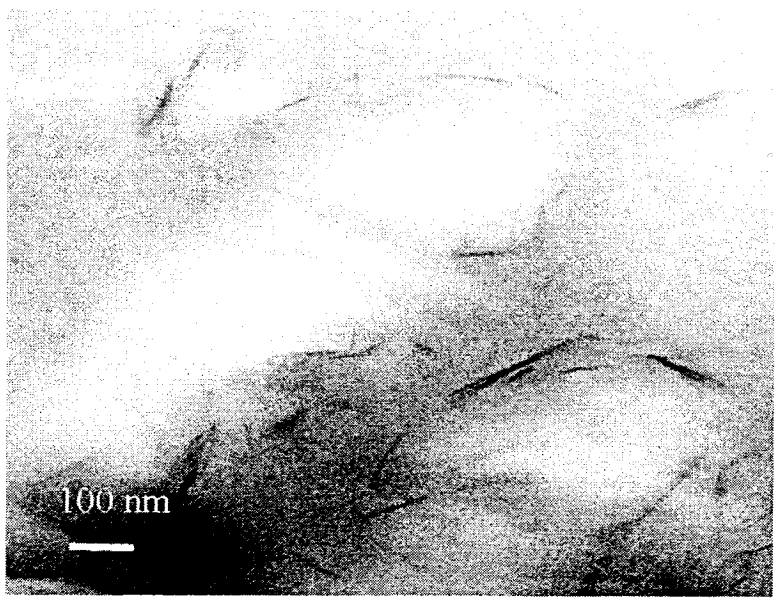

(b)

Figure 4.9: TEM image of TPV nanocomposite before curing stage (stage A) prepared by (b) NP35/EPDM (40/60 w/w).

TEM images of TPV nanocomposites prepared from NP15/EPDM (40/60), and NP35/EPDM (40/60) are presented in Figure 4.10-a, and 4.10-b respectively. For both nanocomposites, XRD results suggested a nearly completely exfoliated structure.

For the low viscosity polypropylene formulation, it can be seen that a significant fraction of the silicate layers are exfoliated in the PP matrix, while a slight amount remained in a more clustered state. The latter is more pronounced for the high viscosity PP based TPV (Figure 4.10-b). The existence of the small peak around $2\theta=7°$ in the X-ray diffraction patterns should therefore be associated to these un-exfoliated silicates.

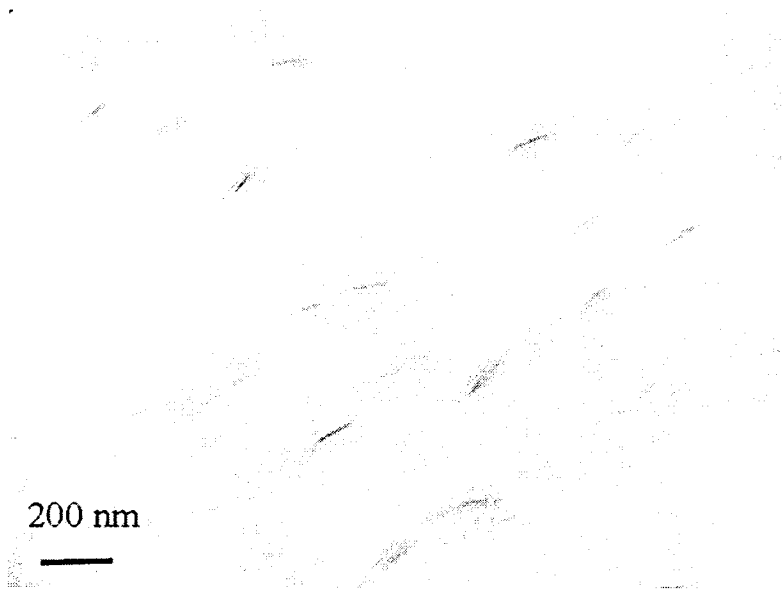

(a)

Figure 4.10: TEM image of TPV nanocomposites prepared by (a) NP15/EPDM (40/60 w/w).

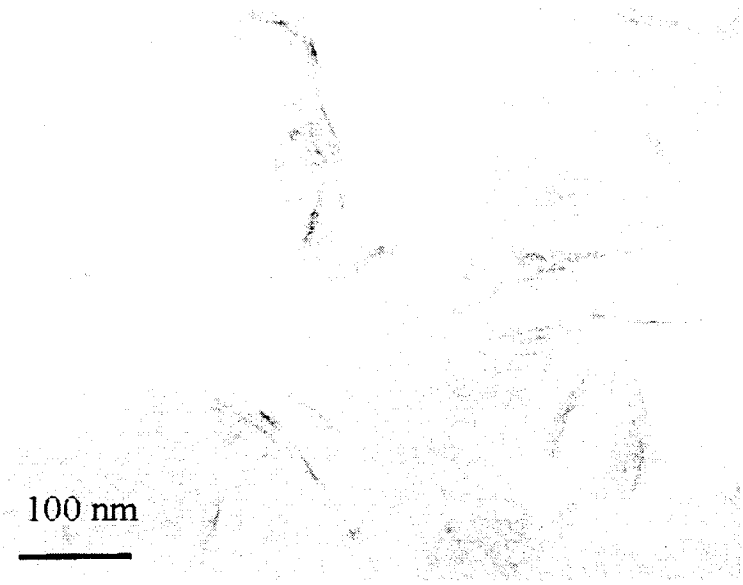

(a)

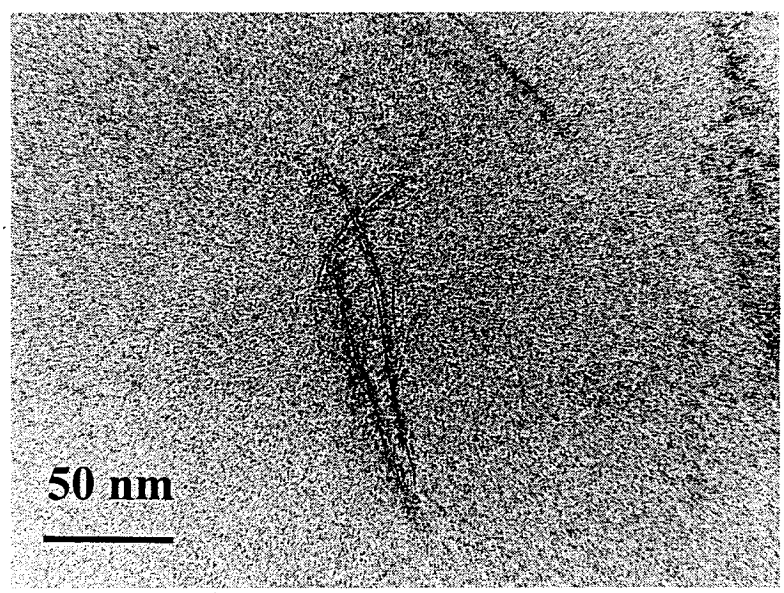

(a)

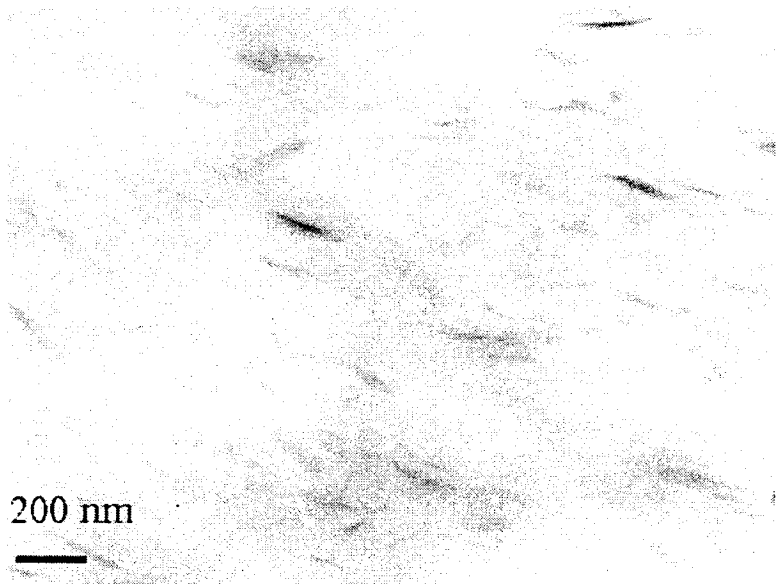

(b)

Figure 4.10: TEM image of TPV nanocomposites prepared by (a) NP15/EPDM (40/60 w/w) with different magnifications (b) NP35/EPDM (40/60 w/w).

Further insights on the morphology of these materials are found in Figure 4.11 where SEM images of cryogenically fractured and etched TPV samples based on P2/EPDM with and without clay are reported. In spite of the higher concentration of the rubber phase, it is clearly seen that the rubber particles are dispersed throughout the polypropylene in form of aggregates and the size of the rubber particles is less than 2 μ in the unfilled TPV sample of Figure 4.11-a. This behavior is attributed to the viscoelasticity of the rubber phase as reported by Wu et al. [29].

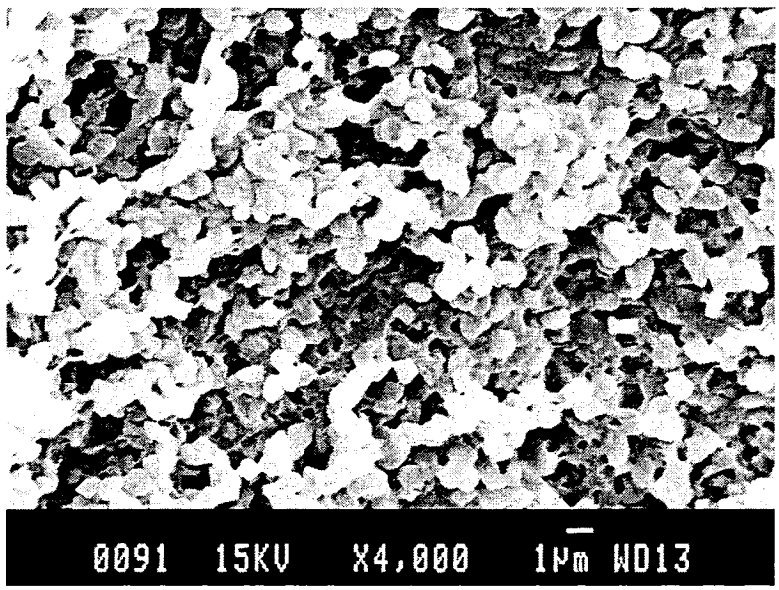

(a)

Figure 4.11: SEM photomicrograph of TPV based on (a) P2/EPDM (40/60 w/w) without clay.

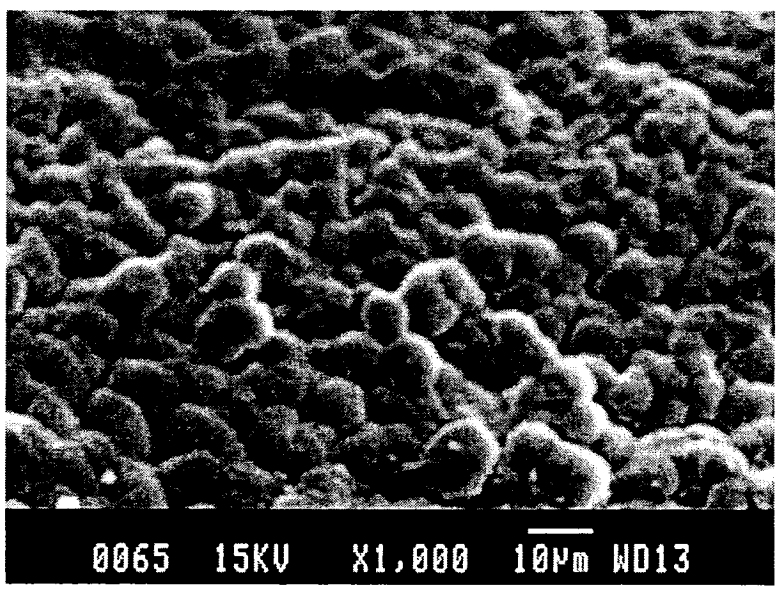

(b)

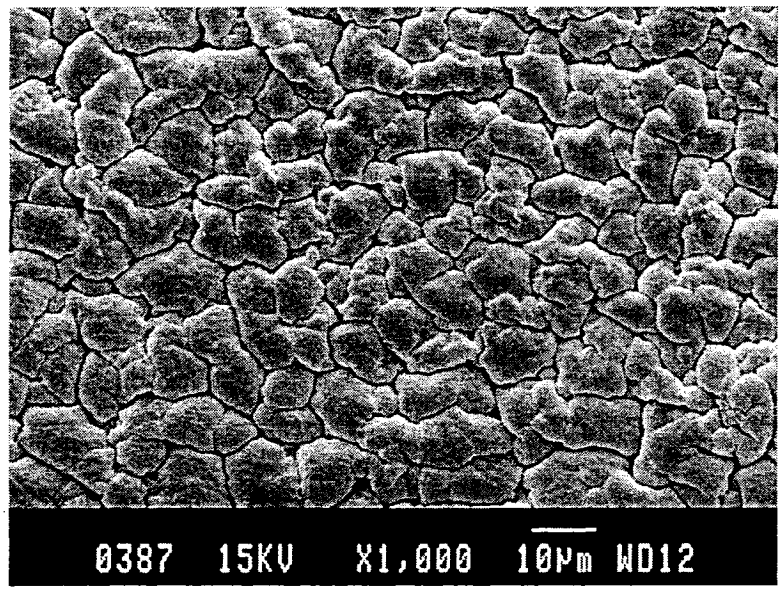

(c)

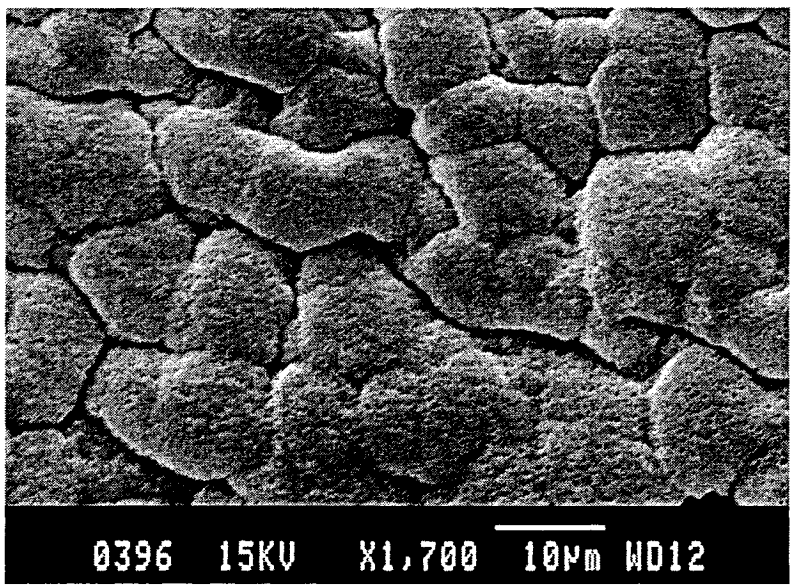

(d)

Figure 4.11: SEM photomicrograph of TPV nanocomposites based on (b) NP22/EPDM (40/60 w/w), (c) NP23/EPDM (40/60 w/w) and (d) NP25/EPDM (40/60 w/w).

It should be noted that the crosslinked rubber particles are covered by a layer of polypropylene and attached together via a joint shell mechanism [18]. As shown in Figure 4.11-d the solvent has not been able to wash out these shells, but they developed a porous structure after the extraction process. It can also be observed in Figures 11 (b), (c) and (d) that the size of rubber particles has been increased by the introduction of the clay. The increase in the rubber phase of the TPV nanocomposites is explained by the modified rheology of the nanocomposites. It is accepted that the size of the dispersed rubber phase in unfilled TPV materials based on PP/EPDM (without clay) depends on the viscosity ratio and interfacial interactions between two phases (Goharpey et al. 2003, [18]). In the case of the TPV nanocomposites, the clay plays an important role to determine the morphology of the samples. Initially, the nanoclay can not penetrate into the rubber phase but after adding curing accelerators such as TMTD, the rubber phase become more polar [30]. Therefore, it is possible that some nanoclay goes to EPDM phase before the completion of the curing cycle. This changes the viscosity ratio between the two phases, and consequently, the size of the rubber phase increases. Figures 4.10 a2 and 4.10 b also confirm the presence of some nanoclay in EPDM phase.

In further characterization of these materials, mechanical properties and oxygen transmission rate for the TPVs and TPV nanocomposites have been obtained and are reported in Table 4.3.

Table 4.3: Mechanical properties and gas permeability of TPV nanocomposites and pristine reference samples

Sample Code	Tensile Modulus (MPa)	Elongation at Break (%)	Tensile Strength (MPa)	Oxygen Transmission Rate (cm^3/m^2.day)
Pristine TPV P1	19.10	740.3	12.2	540
TPV NP11	25.15	694.3	11.1	
TPV NP12	30.82	623.5	10.2	
TPV NP13	34.12	532.7	9.3	
TPV NP15	36.70	459.9	8.5	428
Pristine TPV P2	21.93	790.5	13.5	514
TPV NP21	25.77	760.2	12.8	
TPV NP22	28.54	700.3	12.1	
TPV NP23	31.14	645.9	11.4	
TPV NP25	37.32	560.2	10.0	415
Pristine TPV P3	27.51	880.2	17.1	495
TPV NP31	27.91	817.1	16.7	
TPV NP32	29.54	711.9	15.9	
TPV NP33	30.98	660.1	14.8	
TPV NP35	33.75	621.6	14.1	405

It is observed that the tensile strength and modulus of the pristine TPV reference samples without clay increase when the viscosity of polypropylene phase increases. This is due to the fact that the decrease in the viscosity difference between the two phases leads to formation of smaller rubber particles with higher specific surface area; therefore, the level of interactions between two phases (PP and EPDM) improves [18].

In TPV nanocomposites, the tensile modulus of samples increased from 20 to 90 % depending on clay content and the viscosity ratio of PP/EPDM. For example, the exfoliation of 2 wt % clay in a low viscosity PP based TPV nanocomposite (NP15/EPDM, 40/60) increased the tension modulus by 92 %, while the similar addition of 2 wt % clay to TPV based on high viscosity PP (NP35/EPDM, 40/60) resulted in only a 23 % increase in tension modulus over unfilled pristine TPV. This would tend to confirm that the clay dispersion and exfoliation is better achieved in the former composition.

It is also observed that the tensile strength of the TPV nanocomposites decreases with increasing nanofiller content as reported in Table 4.3.

The improvement in the mechanical properties of a filled system not only depends on the filler type and extent, but also on the crystallinity of polymer matrix [24].

Figure 4.12 shows the crystallinity and crystallization temperature of polypropylene nanocomposites prepared with different melt flow index and different loading levels. It is seen that the degree of crystallinity of the nanocomposites decreases with the increasing clay content as shown in Figure 4.12-a. This decrease is due to

interaction between the polymer matrix and the clay, which reduces the mobility of crystallizeable chain segments [31]. We note that the reduction in the crystallinity of the nanocomposites may be correlated the decrease in tensile strength.

As can be seen in Figure 4.12-b, the peak crystallization temperatures (Tc) of all compositions increase with the clay content because the nanoscale particles acted as nucleating agents, also causing a reduction of the size of the crystalline domains [32].

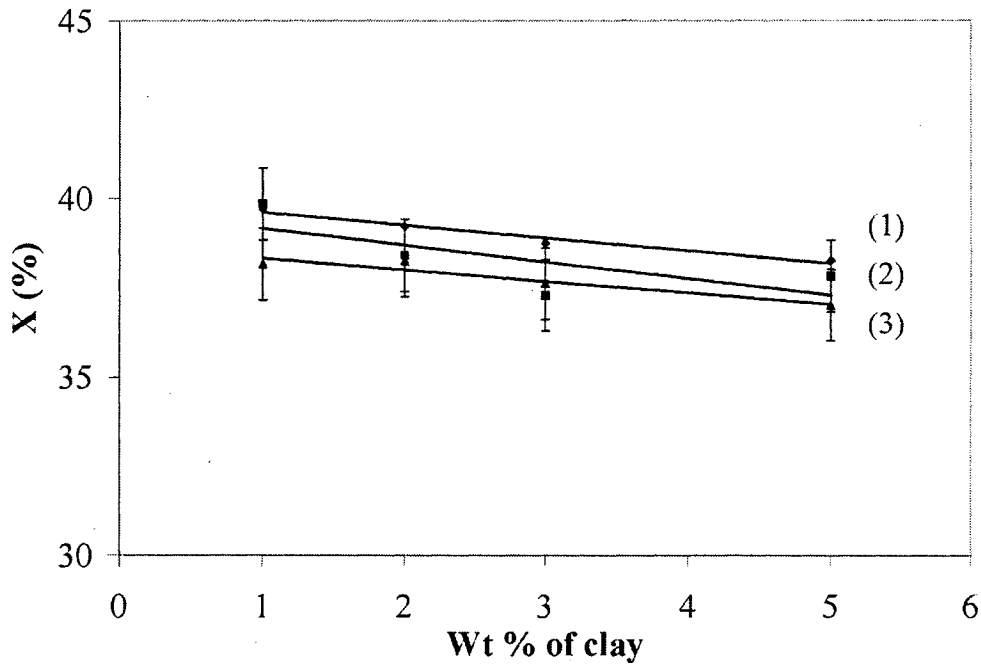

Figure 4.12: (a) Crystallinity of PP nanocomposites prepared with [(1) MFI = 14, (2) MFI =4, (3) MFI = 0.5].

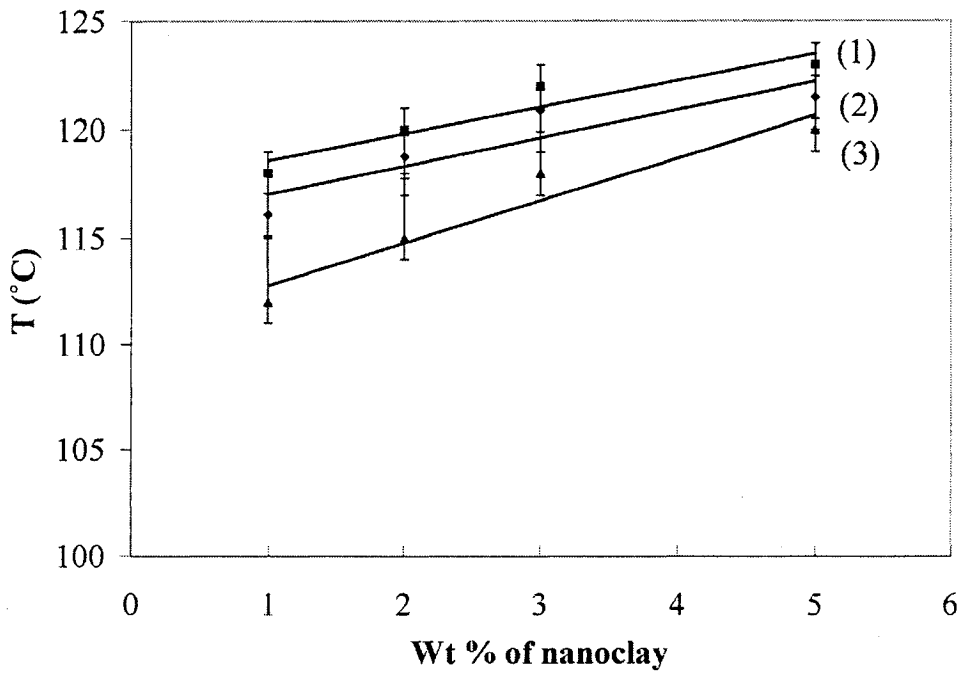

Figure 4.12: (b) Crystallization temperature of PP nanocomposites prepared with [(1) MFI = 14, (2) MFI = 4, (3) MFI = 0.5].

Another important feature of the TPV nanocomposites is their barrier properties such as oxygen permeability. The oxygen permeability results of the pristine TPVs and TPV nanocomposites are reported in Table 4.3. The oxygen permeability of all TPV nanocomposites decreases with introduction of the clay, indicating an improved gas-barrier property of the TPV nanocomposites. In the TPV nanocomposites prepared with

polypropylene of different viscosity at 2 wt % of clay, the oxygen permeability decreased by 20 % as compared with the pristine TPVs.

4.4 Conclusion

TPV nanocomposites have been prepared in a melt compounding process by dynamically vulcanizing thermoplastic elastomers based on PP/EPDM. The compounding process itself was found to be instrumental in the final dispersion state of the layered silicates. The interlayer distance is first increased by the incorporation of the filler in the PPMA to obtain a master batch. This preliminary blend is then compounded with the PP, where the PPMA fraction acts as a compatibilizer for the non-polar PP. Further intercalation and partial exfoliation is finally achieved by the shear stress developed during the vulcanization of EPDM due to the viscosity increased. The microstructure of the TPV nanocomposites was found to be sensitive to the viscosity ratio of PP/EPDM and clay content.

In the TPV nanocomposites prepared with low viscosity polypropylene, an almost complete exfoliation and random distribution of clay in the thermoplastic phase was confirmed by X-ray diffraction analysis and TEM images.

In all TPVs, the rubber particles were dispersed through the polypropylene in the form of agglomerates and the rubber particles size increased with the introduction of clay as evidenced by the morphological features of the dynamically vulcanized nanocomposite samples.

In the TPV nanocomposite based on low viscosity polypropylene, tensile modulus increased by 90 % at 2 wt % of clay.

The exfoliated structure resulted in a reduction of the degree of crystallinity and an increase of the polymer crystallization temperature because the dispersed clay silicate acted as nucleating agents.

Moreover, the oxygen permeability of the TPV nanocomposite samples prepared from polypropylene of different viscosities decreased in comparison with the pristine TPVs.

Acknowledgments

This research was supported by the Natural Sciences and Engineering Research Council of Canada (NSERC). The authors acknowledge the generous assistance given by Bayer and Eastman Chemical Products companies in connection with the supply of materials used in this research.

References

1. A.Y. Coran and R. P. Patel (Monsanto Co.), U.S. Patent 4,130,535 (1978).

2. S. Abou-sabet and M.A. Fath, U.S. Patent 4,311,628 (1982).

3. G. Naderi and M. Razavi Nouri, *Iran. Polym. J.*, **8**, 37, (1999).

4. A.K. Bhowmick and T. Inoue, *J. Appl. Polym. Sci.*, **49**, 1893, (1993).

5. M.H.R. Ghoreishy, M. Razavi-Nouri and Gh. Naderi, *Plas. Rubber. and Comp.*, **29**, 5, (2000).

6. A.A. Katbab, H. Nazockdast and H. Bazgir, *J. Appl. Polym. Sci.*, **75**, 1127, (2000).

7. J. Graces, D. Moll, J. Bicerano, R. Fibiger, *Adv Mater*, **12**, 1835, (2000).

8. S. Hambir, N. Bulakh and P. Jog, *Polym. Eng. Sci.*, **42,** 1800, (2002).

9. N. Hasegawa, H. Okamoto, M. Kawasumi, M. Kato, A. Tsukigase and A. Usuki, *J. Appl. Polym. Sci.*, **78**, 11, 1918, (2000).

10. X. Liu and Q. Wu, *Polymer,* **42**, 10013, (2001).

11. W. Xu, G. Liang, W. Wang, S. Tang, P. He and W. Pan, *J. Appl. Polym. Sci.*, **88**, 3225, (2003).

12. S. R. Suprakas and O. Masami, *Prog. Polym. Sci.*, **28**, 1539, (2003).

13. N. Hesegawa, M. Kawasumi, M. kato, A. Usuki, A. Okada, *J. Appl. Polym. Sci.*, **67**, 87, (1998).

14. M. Alexandre and P. Dubois, *Mater. Sci. Eng.*, **28**, 1, (2000).

15. P. Svoboda, C. Zeng, H. Wang, L. J. Lee and D. L. Tomasko, *J. Appl. Polym. Sci.*, **85**, 1562, (2002).

16. K. Kyu-nam, K. Hyungsu and L. Jae-wook, *Polym. Eng. Sci.*, **41**, 1963, (2001).

17. O. Chung, and A. Y. Coran, *Rubber. Chem. Tech.*, **70**, 781, (1997).

18. F. Goharpey, A. A. Katbab and H. Nazockdast, *Rubber Chem. Tech.*, **76**, 1, (2003).

19. A.O. Baranov, N.A. Erina, T.I. Medintseva, S.A. Kuptsov and E.V. Prut, *Polym. Sci., Ser. A*, **43**, 11, 1177, (2001).

20. Y. Lee Keun and A. Goettler Lloyd, *Polym. Eng. Sci.*, **44,** 6, 1103, (2004).

21. J.K. Mishra, K. Hwang, C. Ha, *Polymer*, **46**, 1995, (2005).

22. W. P. Cox and E. H. Merz, J. Polym. Sci. 28, 619, (1958).

23. Carreau P. J., De Kee D., Chhabra R. P., Rheology of polymeric systems: Principles and applications" Munich, Hanser Publishers, (1997.

24. T.G. Gopakumar, J.A. Lee, M. Kontopoulou and J.s. Parent, *Polymer*, **43**, 5483, (2002).

25. W. Lertwimolnun, and B. Vergnes, *Polymer*, **46**, 3462, (2005).

26. M. Darrell, and J. Krishnamurthy, *Ind. Eng. Chem. Res.*, **41**, 6402, (2002).

27. M. Kawasumi, N. Hasegawa, M. Kato, A. Usuki and A. Okada, *Macromolecules*, **30**, 6333, (1997).

28. M. Mehrabzadeh and M.R. Kamal, *Polym. Eng. Sci.*, **44,** 6, 1152, (2004).

29. S. Wu, *Polym. Eng. Sci.*, **27,** 335, (1987).

30. A. Usuki, A. Tukigase, and M. Kato, *Polymer*, **43**, 2185, (2002).

31. J. Ma., S. Zhang, Z. Qi. Y. Hu., *J. Appl. Polym. Sci.*, **83**, 1978, (2002).

32. J. Li, C. Zhou, Z. Chixing, and W. Gang, *Polym. Tes.*, **22**, 217, (2003).

CHAPTER 5

Dynamically Vulcanized Nanocomposite Thermoplastic Elastomers Based on EPDM/PP (Rheology & Morphology)

The main object of this second paper is to study the rheological and morphological properties of dynamically vulcanized nanocomposite thermoplastic elastomers (TPV nanocomposites), based on Ethylene Propylene Diene Terpolymer (EPDM) and Polypropylene (PP) containing 20, 40, and 60 % rubber at 2 wt % of clay. The effects of composition, maleic anhydride grafted polypropylene (PPMA) as compatibilizer, and different viscosities of polypropylene were also investigated.

The melt linear viscoelastic behavior of the samples was studied by a stress controlled rheometer at a temperature of 220 °C. We performed morphological studies on the samples using scanning electron microscopy (SEM), and transmission electron microscopy (TEM).

A Carreau-Yasuda law with yield stress and a linear viscoelastic model taking into account the maximum packing volume were used to describe the melt linear viscoelastic properties of the TPV nanocomposites.

This article is submitted to the Journal of International Polymer Processing.

Dynamically Vulcanized Nanocomposite Thermoplastic Elastomers Based on PP/EPDM (Rheology & Morphology)

Naderi Ghasem, Lafleur Pierre G., and Dubois Charles[†]

Center for Applied Research on Polymers and Composites, CREPEC, Department of Chemical Engineering, Ecole Polytechnique de Montreal, 2900 Edouard Montpetit, P.O. Box 6079, Station Centre-Ville Montreal, QC, Canada, H3C 3A7.

Abstract:

This study examined the rheological and morphological properties of dynamically vulcanized nanocomposite thermoplastic elastomers (TPV nanocomposites) based on PP/EPDM. Rubber contents of 20, 40, and 60 % were used with polypropylene of different viscosities at 2 wt % of clay.

We performed the rheological and morphological characterizations on the nanocomposites using X-ray diffraction (XRD), transmission electron microscopy (TEM), scanning electron microscopy (SEM) and rheometry in small amplitude oscillatory shear.

The effects of polypropylene viscosity, maleic anhydride grafted polypropylene (PPMA), and composition were also investigated.

The storage modulus (G') of the TPV nanocomposites (without PPMA) containing 20, 40, and 60 % rubber significantly increased in comparison with similar but unfilled samples and also a further increase in the G' from the incorporation of the

[†]Correspondence to: Charles Dubois
Email address: Charles.Dubois@polymtl.ca

PPMA in the samples. The agglomeration of the clay considerably decreased when the rubber content was increased in the TPV nanocomposites.

The yield stress of the prepared TPV nanocomposite, based on low viscosity PP, increased more than that of the sample from high viscosity PP. The TPV nanocomposites containing 20, 40 and 60 % EPDM exhibited a strong elastic modulus that tends to level off (Plateau) at low shear rates. These results were attributed to strong interfacial interactions between the silicate layers and the TPV matrix and, also, the existence of the physical three-dimensional network structure formed between the cured rubber particles, as evidenced by the morphological features of the samples.

A Carreau-Yasuda law with yield stress and a linear viscoelastic model, taking into account the maximum packing volume (ϕ_m) were used to describe the melt linear viscoelastic properties of the TPV nanocomposites. In this model, the maximum packing volume increased when the rubber content was increased.

Keywords: TPV Nanocomposite, Dynamic vulcanization, Viscosity ratio of PP/EPDM, Maximum packing density, Rheological behavior, Morphological feature.

5.1. Introduction

Thermoplastic vulcanizates (TPVs) are a unique class of polymers with the physical and mechanical properties of vulcanized rubbers, such as a low compression set, high flexibility, resistance to fatigue and heat, and chemicals resistance, while at the same time being processed by conventional fabrication techniques, including extrusion

and injection molding. TPVs have a wide application in automotive parts, cable insulation, footwear and the packaging industry because of their outstanding endurance, low density and relatively low manufacturing costs [1-3].

In recent years, the addition of a small amount of modified clays has been shown to be an effective strategy for achieving improved rigidity (stiffness) without incurring a significant loss of impact strength, while simultaneously yielding enhanced barrier properties, reduced flammability and the enhanced biodegradability of a biodegradable polymer [4-8].

Combination of these two complementary technologies to form TPV/clay nanocomposites generates potentially synergistic properties.

Besides these mechanical properties, the rheological properties of nanocomposite materials in the molten state are very important in determining the use of these nanocomposites, and they also suggest a potential method for directly evaluating the dispersion state of the clay in the nanocomposites [9-11].

While considerable attention has been paid to the rheological properties of PP nanocomposites [12-13], few efforts have been devoted to the study of the rheological properties of dynamically crosslinked PP/EPDM blends [14-15]. Furthermore, no studies regarding the effect of matrix viscosity, composition and compatibilizer (PPMA) on the rheology of PP/EPDM dynamically vulcanized nanocomposite thermoplastic elastomers have yet been published.

Very recently, we successfully prepared dynamically vulcanized nanocomposite TPEs based on PP/EPDM containing 60 % of EPDM at different nanoclay loading [16].

We demonstrated that the silicate layers achieve a nearly exfoliated structure and randomly distributed through the polypropylene phase of the TPV nanocomposites.

In this article we studied the rheological and morphological properties of the TPV nanocomposites, while investigating the influence of composition, viscosity ratio of PP/EPDM, and compatibilizer (PPMA) on the rheology of the dynamically vulcanized nanocomposite thermoplastic elastomers.

5.2 Experimental

More extensive details on preparation methods are explained in our earlier publication (Naderi et al., journal of Polymer Engineering and science in press, 2006) and should be referred to accordingly.

5.2.1. Materials

The specifications of EPDM and the three grades of polypropylene (Basell Co.) employed in this study are reported in Table 5.1. The EPDM rubber (Buna EP T 6470) was based on ethylene norbornene (ENB) as a termonomer, and was supplied by Bayer Co.

The nanoclay used was Cloisite 15A procured from Southern Clay Products. It was a natural montmorillonite modified with a dimethyl dehydrogenated tallow quaternary ammonium having a cation-exchange capacity (CEC) at 125 meq/100g and a specific gravity of 1.66.

Epolene G3015 (Acid Number = 15, mol of MA/mol of PPMA = 6.3) as maleic anhydride-modified polypropylene (PPMA) was obtained from Eastman Chemical.

The curing of TPV nanocomposites was achieved with benzothiazyl disulfide (MBTS), tetramethyl thiuram disulfide (TMTD), and sulfur (S) obtained from Bayer Company.

Table 5.1: Basic specification of PP and EPDM

Materials	Characteristics	
PP (P1)	MFI	14 gr/10 min
	Density	0.91 g/cm^3
	Tm	>160 ^{oC}
	η_0 [1]	1818 Pa.s
PP (P2)	MFI	4 gr/10 min
	η_0 [1]	5000
PP (P3)	MFI	0.5 gr/10 min
	η_0 [1]	27100
EPDM	Mooney Viscosity ML (1+4), 125°C	55
	Ethylene Content	68 %
	Termonomer Content	4.5 % ENB
	Density	0.86 g/cm^3

1- Zero shear viscosity is obtained by C. Y. model $\eta^*(\omega) = \eta_0((1+(\omega\lambda)^a)^{(m-1)/a}$

5.2.2. Preparation of Blends

TPV nanocomposite samples were prepared by a three steps melt mixing process in an internal mixer (Haake Rhemix 600). At first, the nanoclay powder and PPMA pellets were dry-mixed in a bag to ensure that the materials were well dispersed. The mixture was then melt-mixed at 180 °C under nitrogen to obtain a master batch using the mixer at a rotor speed of 150 rpm for 10 min. For the master batch, the PPMA/nanoclay weight ratio was kept constant at 3:1. In the second step, the master batch was then dry-blended with polypropylene to give the desired composition (see Table 5.2), and fed to the mixer in applying the same previous processing conditions. In the third and final step, PP nanocomposite, EPDM, Zinc oxide (Zno) and stearic acid (St.Ac.) were mixed at 180 °C and 100 rpm. Three to four minutes after the melting of the PP nanocomposite, the TMTD and MBTS curing agents were added to the mixer and after 60 seconds of mixing, the sulfur (S) was introduced and followed by a continuous mixing for four additional minutes.

The clay content was kept constant at 2 wt % for all nanocomposites and also the weight ratios of PP/EPDM were 80/20, 60/40 and 40/60. Prepared compounds were compression-molded by hot press at 200 °C for 10 min to obtain suitable samples for X-ray diffraction test.

The vulcanizing system was based on 100 phr EPDM, 5 phr ZnO, 1 phr stearic acid, 1 phr TMTD, 0.3 phr MBTS, and 1 phr S.

In all instances, the clay had been dried at 80 °C for 24 h prior to processing.

Table 5.2: Code and composition of samples.

Sample Code	PP	PPMA	Nanoclay	EPDM
NP12	P1=92	6	2	-
NP22	P2=92	6	2	-
NP32	P3=92	6	2	-
PP12	P1=98	-	2	-
PP22	P2=98	-	2	-
PP32	P3=98	-	2	-
TPV1 20 P	P1=78	-	2	20
TPV1 20 N	P1=72	6	2	20
TPV1 20	P1=80	-	-	20
TPV1 40	P1=60	-	-	40
TPV1 60	P1=40	-	-	60
TPV1 40 N	P1=52	6	2	40
TPV1 60 N	P1=32	6	2	60
TPV2 60 N	P2=32	6	2	60
TPV3 60 N	P3=32	6	2	60

5.2.3. Characterization

In order to evaluate the dispersion of the clay in the polymer matrix, X-ray diffraction (XRD) was performed at room temperature using an X-ray diffractomer (Philips model X'Pert) in the low angle of 2θ. The X-ray beam was a Cu-K_α radiation (λ=1.540598 A°) using a 50 kV voltage generator and a 40 mA current. The basal spacing of silicates was estimated from the position of the plane peak in the WAXD intensity profile using the Bragg's law, $d = \lambda / (2 \sin\theta_{max})$. Specimens for X-ray diffraction were obtained from compression-molded sheets of 2 mm in thickness.

The nanostructure of the clay was observed by a transmission electron microscopy (JEM-2100F, JEOL) with an accelerator voltage of 200 kV. The surface of the samples was coated with gold and then a thin section (ca. 100 nm) of each specimens was prepared by using a focused ion beam (FIB, FB-2000A, Hitachi) and a cryo-microtome equipped with diamond knife at low temperature (-100 °C).

To study the morphology of the TPV nanocomposite samples, cryogenically fractured surfaces of the samples were etched by hot xylene. Treated samples were then coated with gold and viewed with a scanning electron microscope (SEM) model JSM-840 made by JEOL company.

Rheological properties of PP, and TPV nanocomposite samples were carried out using a stress controlled rheometer (TA Instruments, AR 2000). The experiments were performed in parallel-plate geometry with a diameter of 25 mm under a nitrogen atmosphere at a temperature of 220 °C, using a 0.01-80 Hz frequency range.

5.3. Results and discussion

5.3.1-Effects of PPMA and the viscosity of polypropylene in PP nanocomposites

Figure 5.1 shows the X-ray diffraction patterns of the original Cloisite 15A, master batch (PPMA/clay, 3/1), uncompatibilized P1 nanocomposite (PP12), and the nanocomposites prepared with, respectively, polypropylene of different viscosities (NP32, NP22 and NP12). The concentration of the nanoclay was kept constant at 2 % wt.

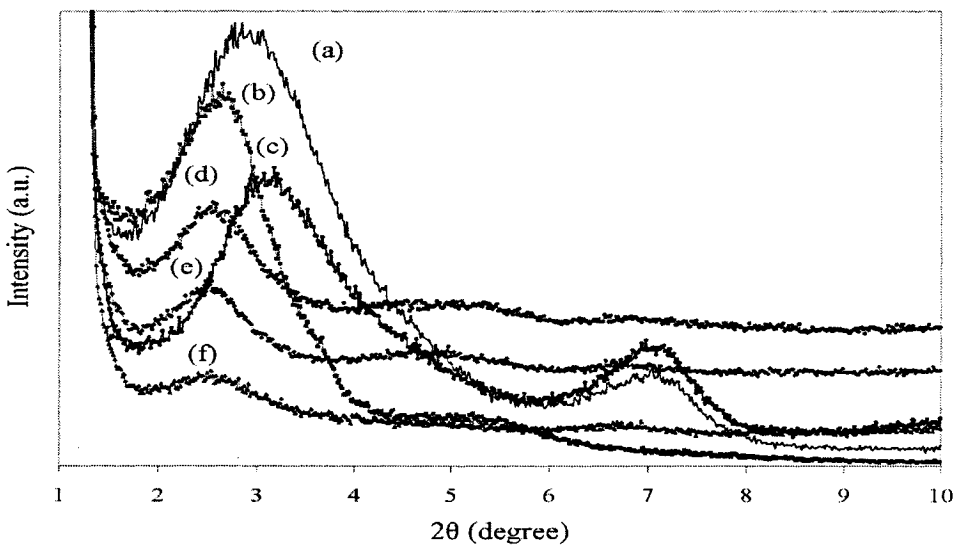

Figure 5.1: X-ray diffraction patterns of (a) Cloisite 15A, (b) PPMA/Clay, (c) PP12, (d) NP32, (e) NP22, (f) NP12.

The diffraction peak corresponding to the (001) plane of the clay appeared at 2.9 ° (d = 30.44Å) before compounding. For the uncompatibilized P1 nanocomposite (PP12), the XRD result shows a peak at $2\theta = 3^{o}$, corresponding to a d-spacing of 29.42 Å. This indicates that the polypropylene could not penetrate into the interlayer of the clay, even when modified by a dimethyl dehydrogenated tallow quaternary ammonium at the shear stress imposed by the matrix. Similar trends were observed for the PP nanocomposites prepared from P2 and P3 without PPMA.

In the polypropylene nanocomposites prepared with PPMA, an intercalated structure was achieved for P1 and P2 because the X-ray diffraction peaks were shifted to a lower angle, indicating the interlayer spacing of the silicate layers was increased by the intercalation of P1 and P2 chains in comparison with the master batch. The results of the interlayer spacing are summarized in Table 5.3. It can be seen that the interlayer distance of the NP32 is less than that for the NP12. This shows that the penetration of the polypropylene chains between the silicate layers, consisting of low-viscous PPMA, is more difficult for high viscosity polypropylene (HVP) in comparison with low viscosity polypropylene (LVP) [17]. It should be noted that the intensity of the X-ray diffraction peak in the P1 nanocomposite with PPMA (NP12) decreases and, furthermore, the peak becomes broader in comparison with NP32. The decrease in the intensity and the broadening of the XRD peak indicate that the stacks of the layered silicates have become yet more disordered or partially exfoliated [17-18]. Likewise, the PP nanocomposite prepared with low-viscous PP yields a more disordered structure compared with the high-viscous PP nanocomposite.

Table 5.3: Interlayer spacing for nanocomposite samples.

Sample Code	d-spacing (Å)
Cloisite 15A	30.44
PP12	29.42
Master batch	32.10
NP32	32.25
NP22	33.30
NP12	33.65
TPV1 20 P	37.61
TPV1 20 N	37.61
TPV1 40 N	38.40
TPV1 60 N	-

It is believed that the rheological studies of nanocomposites can be used to evaluate the dispersion state of clays in the molten state since the rheological properties of nanocomposites are sensitive to the structure, particle size, shape and surface modification of the dispersed phase [10].

We conducted amplitude sweep experiments at ω = 1 rad/s to determine the linear viscoelasticity region. Figure 5.2 shows the storage modulus as a function of the strain amplitude obtained for the polypropylene (P1), PP12 and NP12. The linear viscoelastic range in P1 and PP12, where the storage modulus remains constant with respect to the strain amplitude, is very wide. However, the linear viscoelastic range decreases in the PPMA modified P1 nanocomposite (NP12).

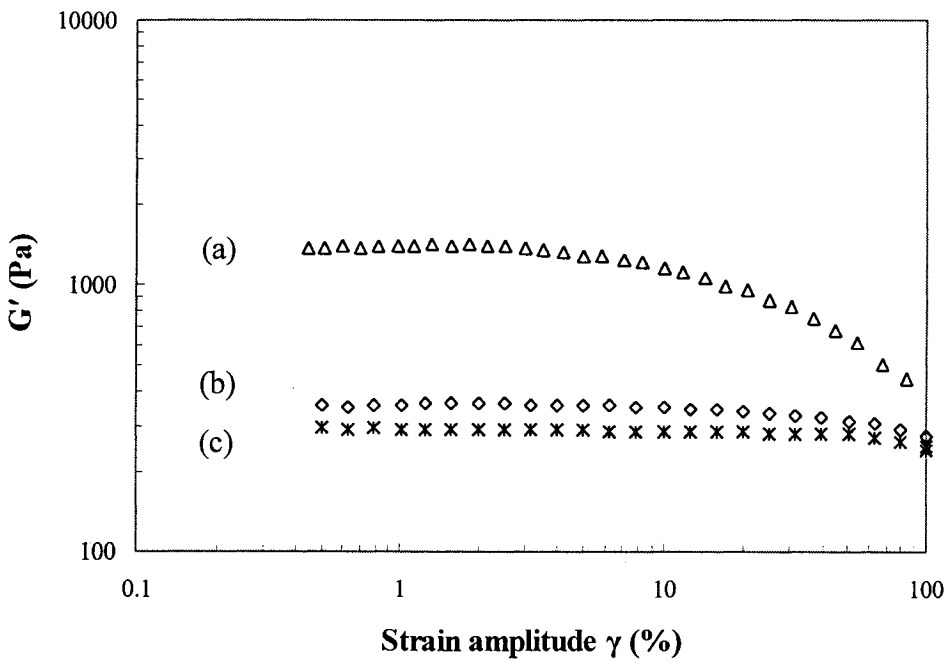

Figure 5.2: Storage modulus as a function of strain amplitude for (a) NP12, (b) PP12,and (c) P1.

Since the amount of clay in the polypropylene nanocomposites is the same, the decrease in the linear viscoelastic range of the nanocomposite can be attributed to the

difference in the state of dispersion. It should be noted that the low viscous PPMA has mainly an effect of dilution on the viscosity of PP [18].

The result of the storage modulus, and the complex viscosity as a function of the frequency for polypropylenes and their nanocomposites both with and without PPMA, are shown in Figures 5.3 a, b, c.

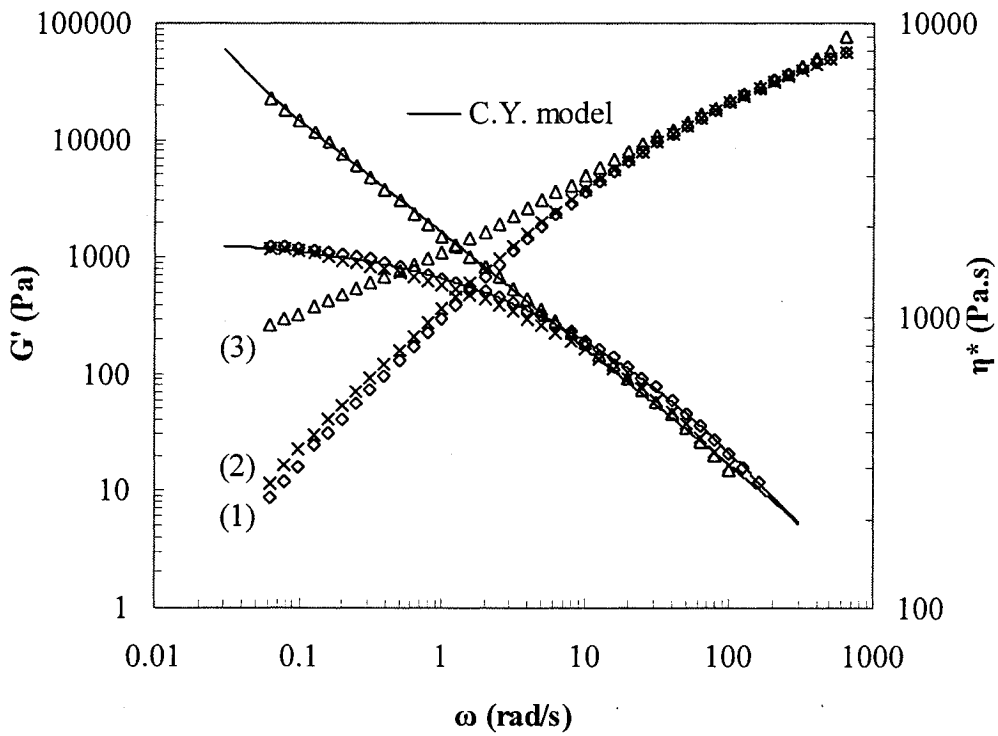

Figure 5.3 (a): Storage modulus and complex viscosity as a function of frequency for (1) P1, (2) PP12 and (3) NP12

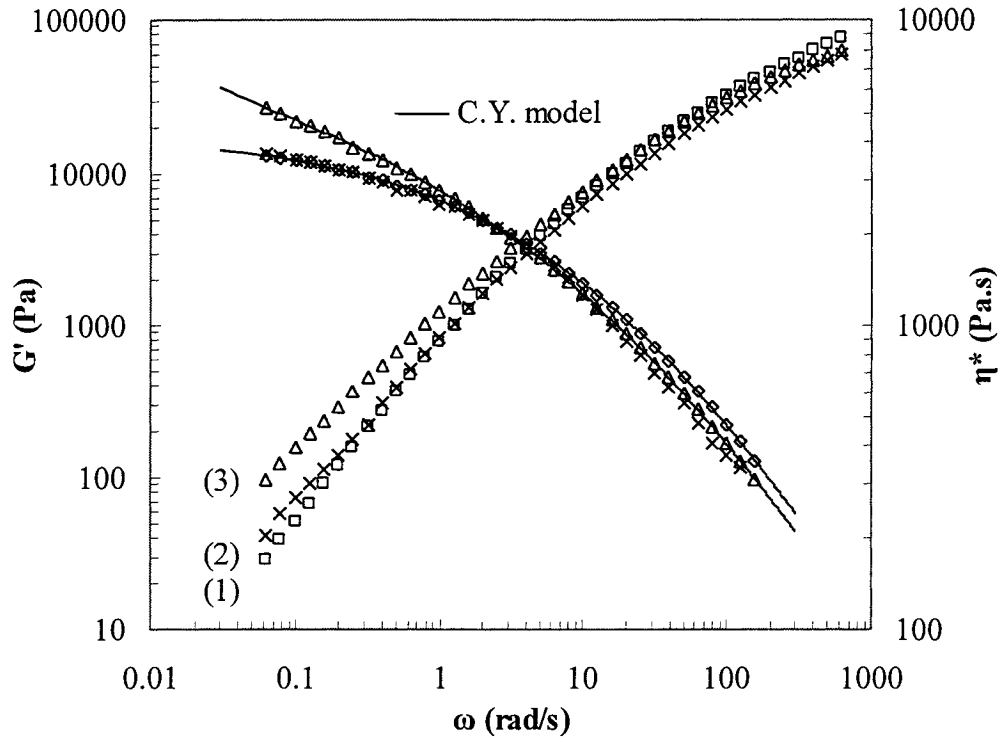

Figure 5.3 (b): Storage modulus and complex viscosity as a function of frequency for (1) P2, (2) PP22 and (3) NP22.

The PP nanocomposites prepared without PPMA containing P1, P2, and P3 at 2 wt % of the clay demonstrate the storage modulus curves very close to those of the corresponding matrix as shown in Figures 5.3 a, b, c respectively. Figure 5.3 (a)-3 also shows a dramatic increase in the storage modulus of the PP nanocomposite based on NP12 with the onset of a plateau at a low frequency. However, the sample containing polypropylene of high viscosity (NP32) exhibits a storage modulus curve very close to the corresponding matrix storage modulus curve, as shown in Figure 5.3 (c)-3.

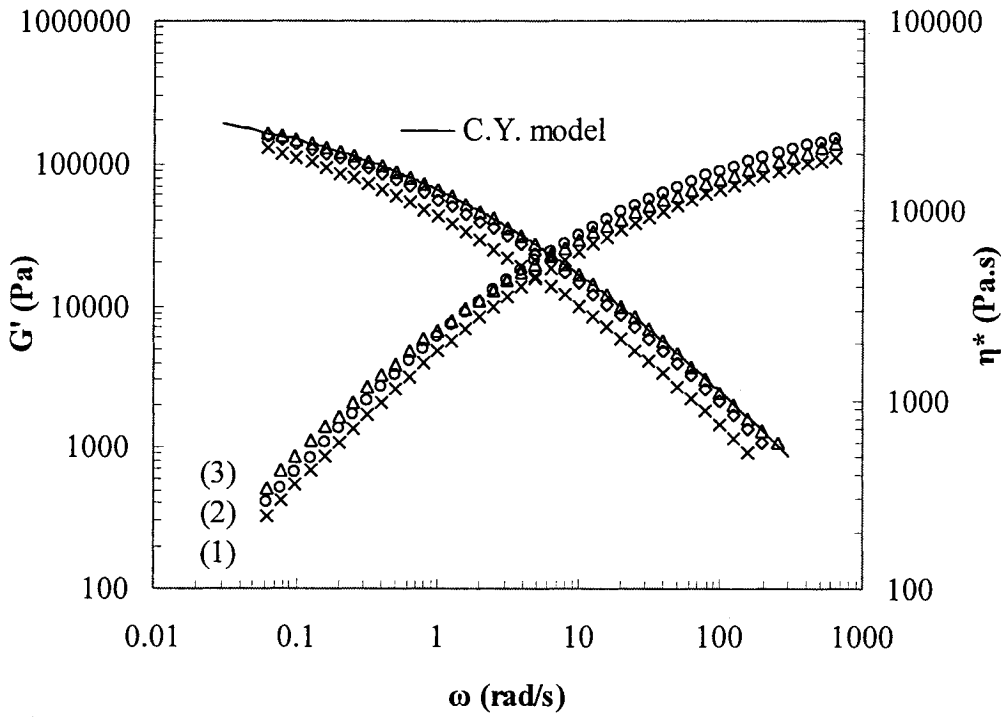

Figure 5.3 (c): Storage modulus and complex viscosity as a function of frequency for (1) P3, (2) PP32 and (3) NP32.

Inspection of these Figures reveals a significant difference between the nanocomposites, particularly at low-level frequencies. It has been widely reported that the consistent behavior of nanocomposites at low frequency, which is quite different from that observed in the polymer matrix, could be attributed to the existence of a percolated network microstructure [11].

Therefore, it is reasonable to say that the low viscosity polypropylene can more readily penetrate between the silicate layers, thus the nanoclay-PP interactions in the nanocomposite prepared with LVP and PPMA are greater than in the hybrid based on

HVP and PPMA. These results are in agreement with the decrease in the intensity and the broadening peak observed in the x-ray diffraction patterns of the nanocomposites (Fig.5.1).

Similar trends are observed in the complex viscosity of the PP nanocomposites, as shown in Figures 5.3 a, b, c. The solid-like behavior of the nanocomposites at low frequency is comparable to those reported for the block copolymer and the highly concentrated particulate composites exhibiting a yield stress. A Carreau-Yasuda model [18, 19] with a yield stress can be used to describe the behavior of the polypropylene nanocomposite as follows:

$$\eta_{(s)}(\omega) = \frac{\sigma_0}{\omega} + \eta_0[1 + (\lambda\omega)^a]^{(m-1)/a}$$

.....(5.1)

Where σ_0 is the yield stress, η_0 is the zero shear viscosity, λ is the time constant, a is the Yasuda parameter and m is the dimensionless power law index. Figure 5.4 shows the yield stress obtained by Eq. (5.1) and the interlayer spacing of silicate layers from Table 5.3 for the polypropylene nanocomposites prepared using PP12, NP12, NP22 and NP32.

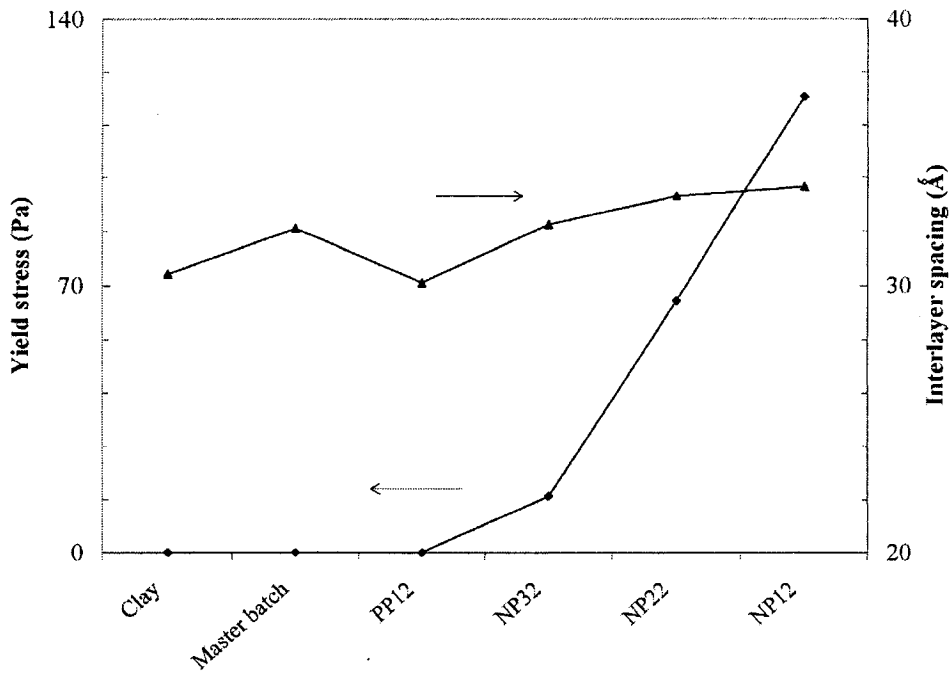

Figure 5.4: Interlayer spacing and yield stress obtained by Eq. (5.1) for samples.

It can be seen that the interlayer spacing of the PP nanocomposite based on P1 without PPMA is slightly lower compared with that of the original clay and, also, the yield stress is zero. For the polypropylene nanocomposite prepared by P1 and PPMA, the interlayer spacing is slightly higher than that of the master batch, while the yield stress has dramatically increased. This suggests that the yield stress of the PP nanocomposites will increase in conjunction with an increase in the interlayer distance of the nanoclay, and by increasing the silicate layers separated from the stack layers.

Figure 5.5 (a) shows the TEM image of the nanocomposite prepared by using the polypropylene (P1) without PPMA.

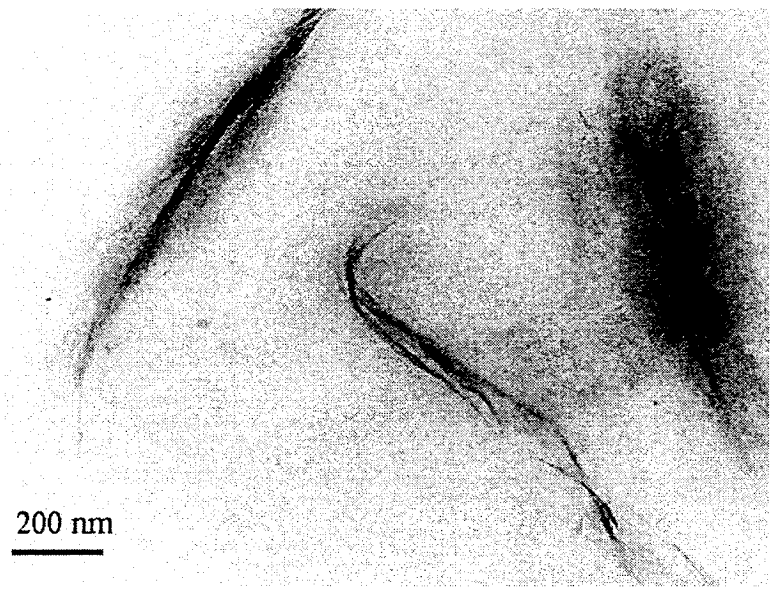

(a)

Figure 5.5: TEM image for (a) PP12.

For the uncompatibilized nanocomposite (PP12) at 2 wt % of the clay, large aggregates of the clay particles can exist as in conventional composites. For the nanocomposite prepared by P1, containing 2 wt % of the clay, the number of the silicate aggregates is diminished by incorporating the PPMA, as shown in Figure 5.5-b. These results are in accordance with the intensity of the XRD patterns observed for the P1 nanocomposite.

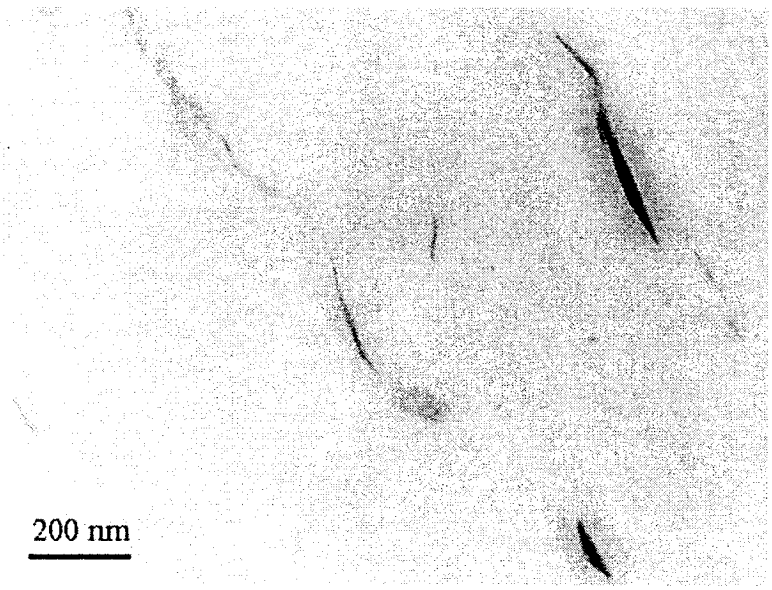

(b)

Figure 5.5: TEM image for (b) NP12.

5.3.2. Effects of PPMA and the viscosity of polypropylene in TPV nanocomposites

Figure 5.6 presents the X-ray diffraction patterns of the original Cloisite 15A, TPV1 20 P and TPV1 20 N. It can be seen that the interlayer distance of the silicate layers is larger in the TPV1 20 P without PPMA ($2\theta = 2.35^{o}$, d = 37.61 Å) than in the original nanoclay, as shown in Figure 5.6-b. We recall that the d-spacing of the PP nanocomposite prepared by P1 without PPMA (PP12) was less than that of the clay (Fig.5.1-c). The XRD pattern of the TPV1 20 N with PPMA presented in Figure 5.6-c shows that the peak position has not changed in comparison with the TPV1 20 P without PPMA, but its intensity has decreased. This is due to the fact that PPMA has a

significant effect on the exfoliation degree of the silicate layers in the PP phase of the TPV nanocomposite (TPV1 20 N).

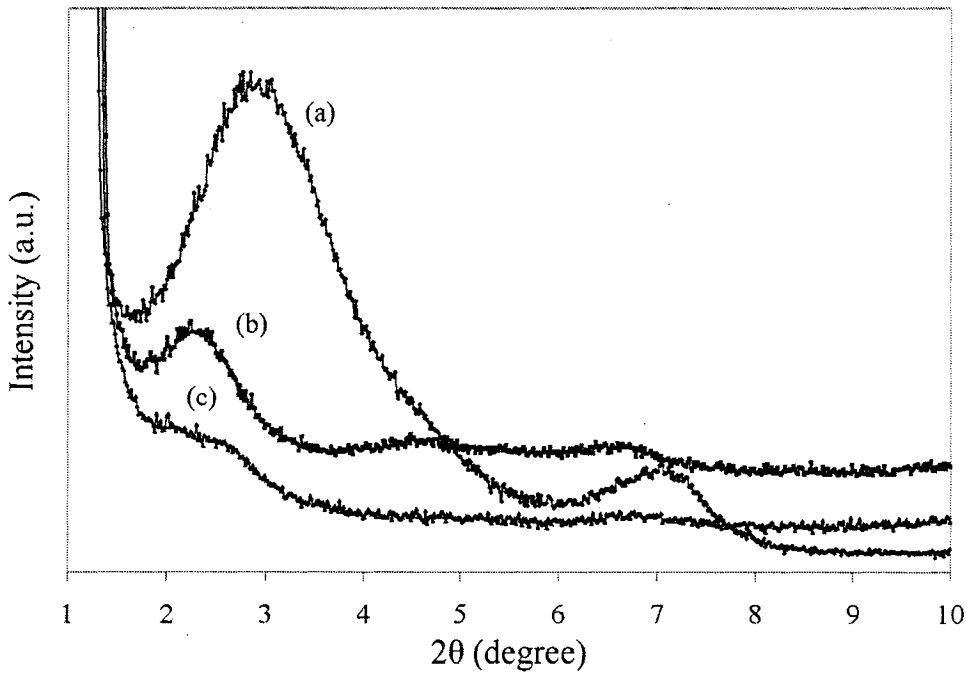

Figure 5.6: X-ray diffraction patterns of (a) nanoclay, (b) TPV1 20 P, (c) TPV1 20 N.

Figure 5.7 shows the X-ray diffraction patterns of the nanoclay, TPV1 20 N, TPV1 40 N, and TPV1 60 N. It is observed that the d_{001} of the clay (d = 38.40 Á) in the TPV nanocomposite prepared with 40 % EPDM increased and also the intensity of the peak decreased in comparison with TPV1 20 N. It can be seen that the first

characteristic peak of the nanoclay has disappeared for the TPV samples prepared with 60 % of EPDM suggesting a nearly exfoliated structure.

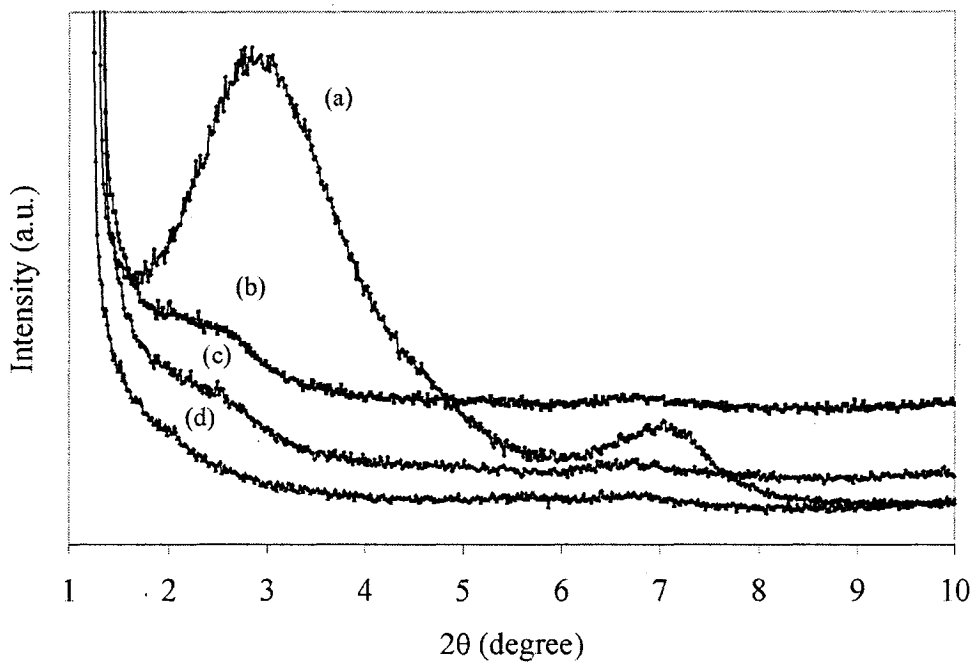

Figure 5.7: X-ray diffraction patterns of (a) Cloisite 15A, (b) TPV1 20 N, (c) TPV1 40 N(d) TPV1 60 N.

Therefore, it was found that the exfoliation degree of the silicate layers increased when the concentration of the rubber phase was increased. This is due to the fact that the dynamic vulcanization of the EPDM phase increased the viscosity of the matrix phase, and thus the shear stress imposed by the matrix during mixing increased, which in turn facilitates the break-up process of the nanoclay agglomerates. Similar

trends were observed in the TPV nanocomposites based on P2 and P3. Figure 5.8 shows the X-ray diffraction patterns of the TPV nanocomposite prepared with different viscosities of polypropylene containing 60 % EPDM.

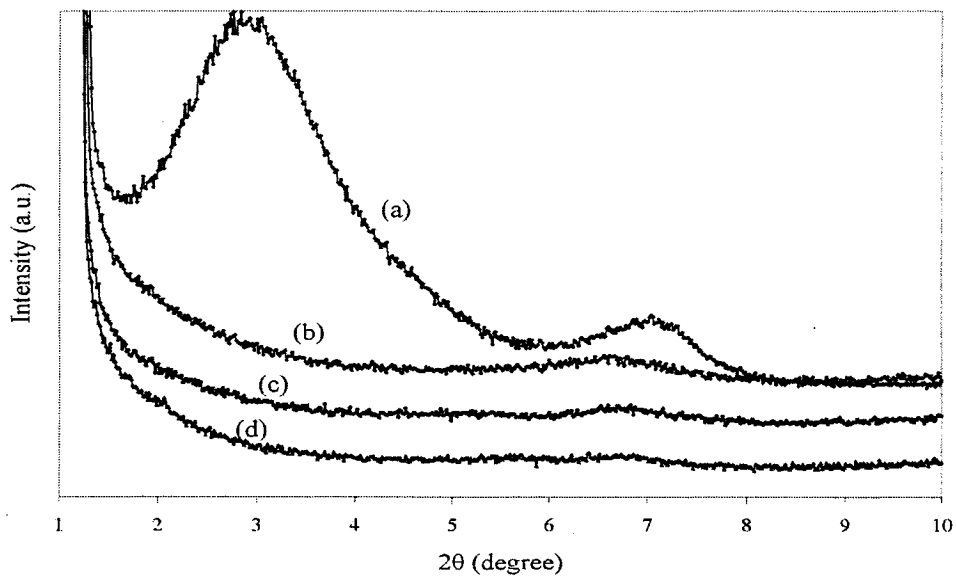

Figure 5.8: X-ray diffraction patterns of (a) nanoclay , (b) TPV3 60 N, and (c) TPV2 60 N(d) TPV1 60 N.

These results can be described through the storage modulus and the viscosity of the TPV nanocomposites. The storage modulus of the TPV1 20 P (without PPMA) has increased in comparison with the similar but unfilled matrix (TPV1 20) as illustrated in Figure 5.9. We recall that the storage modulus of PP nanocomposites without PPMA was found to remain unchanged with respect to the neat polymer.

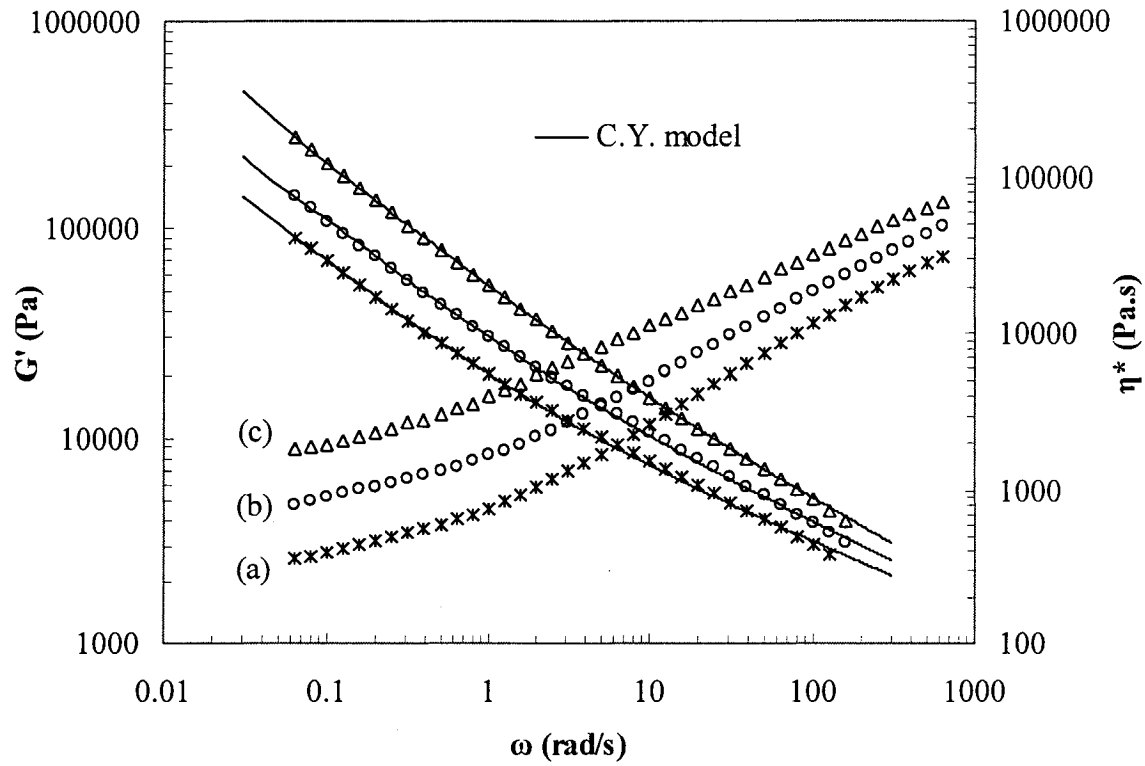

Figure 5.9: Storage modulus and complex viscosity as a function of frequency for (a) TPV1 20, (b) TPV1 20 P, and (c) TPV1 20 N.

It is also observed from Figure 5.9 that the storage modulus of the TPV1 20 N has increased in comparison with the TPV1 20 P due to the effect of the PPMA, as explained above.

The flow behavior and linear viscoelastic properties of the dynamically vulcanized nanocomposite TPVs, based on low viscosity PP and PPMA containing 20, 40 and 60 % EPDM, are shown in Figure 5.10.

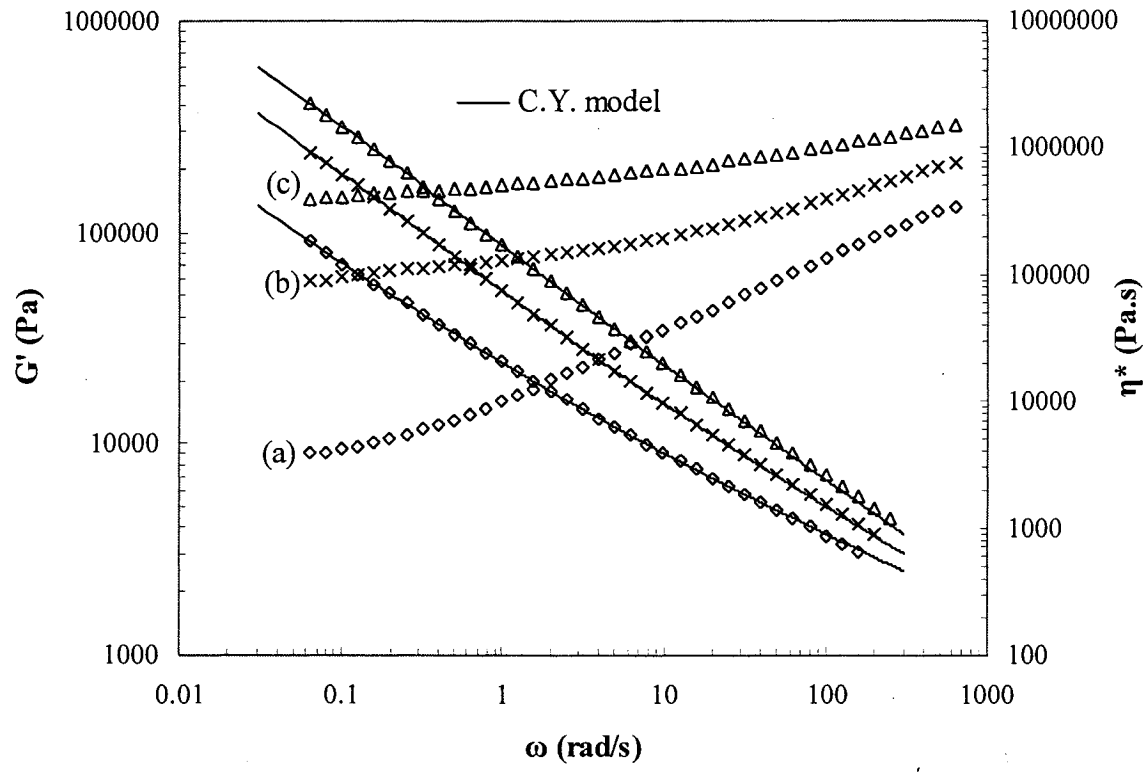

Figure 5.10: Storage modulus and complex viscosity as a function of frequency for (a) TPV1 20 N, (b) TPV1 40 N, and (c) TPV1 60 N.

It can be seen that the TPV nanocomposites exhibited strong elastic modulus that has a tendency to become increasingly independent of frequency (plateau) at low frequencies with the highest extent for the sample having 60 % EPDM.

Similar trends are observed in the complex viscosity of these TPV nanocomposites, as shown in Figure 5.10. It has been reported that TPV materials without nanoclay present a yield stress, which increases sharply in accordance with an increased rubber content [14, 20]. For the present work, the melt yield stress, estimated

by fitting the viscosity data with Eq. (1), increased from 2651 Pa for the TPV without nanoclay and PPMA (TPV1 20), to 3665 Pa for the TPV nanocomposite without PPMA (TPV1 20 P) and, finally, to 5794 for the TPV nanocomposite with PPMA (TPV1 20 N). This is due to the fact that the clay could disperse through the matrix of the sample even without PPMA and, also, a further increase in the degree of dispersion from the incorporation of the PPMA in the TPV nanocomposite. These results are in accordance with the X-ray diffraction peaks obtained for the TPV nanocomposites. The melt yield stress calculated by correlating the viscosity data with Eq. (1) increased from 29250 Pa for the TPV1 40 without nanoclay to 47665 Pa for the TPV1 40 N, and increased from 75260 Pa for TPV1 60 to 121850 for TPV1 60 N. These results can be attributed to strong interfacial interaction between the clay and the nanocomposite matrix and, also, the existence of the physical three-dimensional network structure formed between the cured rubber particles as evidenced by SEM results.

Figure 5.11 shows the scanning electron microscopy of cryogenically fractured and etched surfaces of the dynamically vulcanized nanocomposites prepared by P1 and 20, 40, 60 % EPDM rubber. These results show that the agglomerate formation of the rubber particles increased by the increased rubber aggregate size resulting from the increased rubber content in the samples. It should be also noted that the crosslinked rubber particles covered by a layer of polypropylene are attached together via a joint shell mechanism [21].

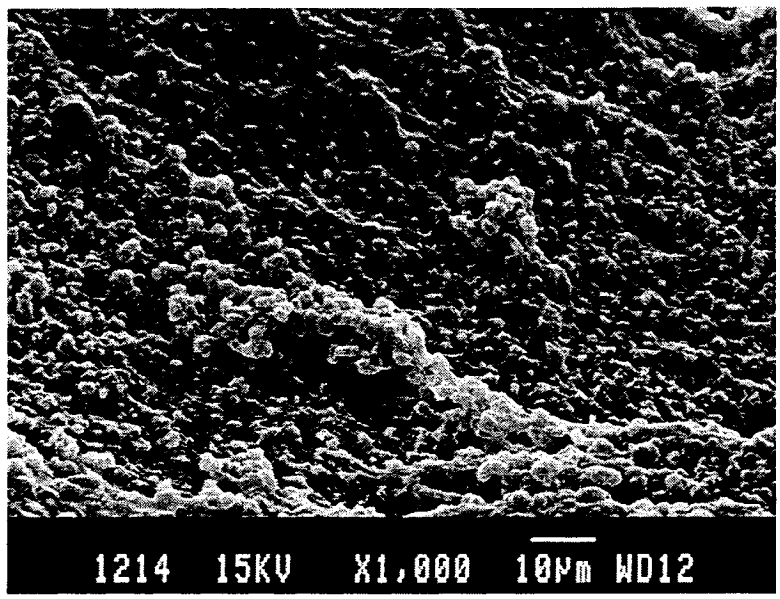

(a)

Figure 5.11: SEM photomicrograph of etched cryo-fractured surface of (a) TPV1 20 N.

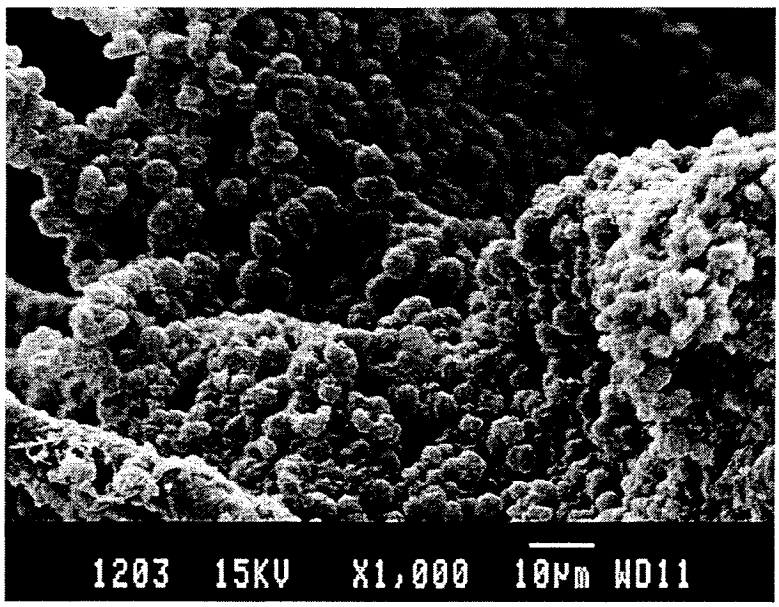

(b)

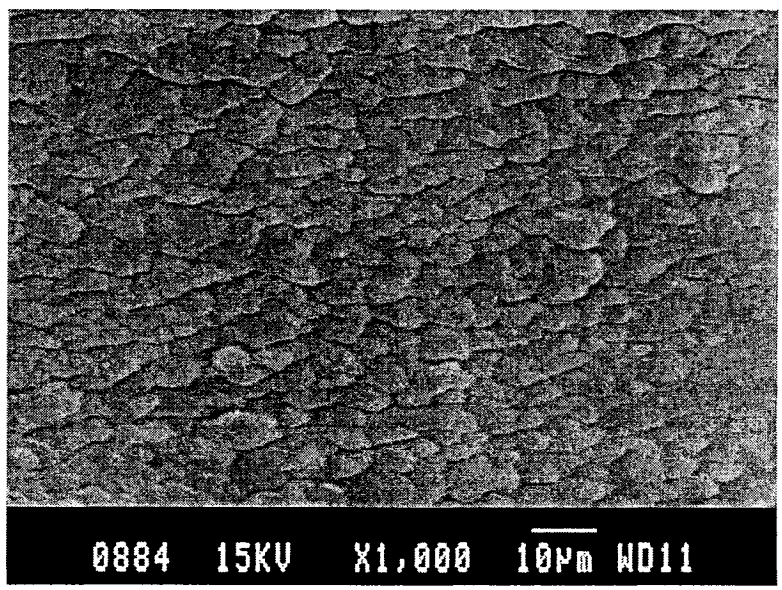

(c)

Figure 5.11: SEM photomicrographs of etched cryo-fractured surface of (b) TPV1 40 N (c) TPV1 60 N.

Similar trends were obtained in the TPV nanocomposites prepared with medium and high viscosity polypropylene containing 20, 40 and 60 % EPDM. Figure 5.12 shows the difference between the yield stresses of the TPV nanocomposites having PPMA and the TPVs prepared by P1, P2 and P3 without clay, at different contents of the rubber.

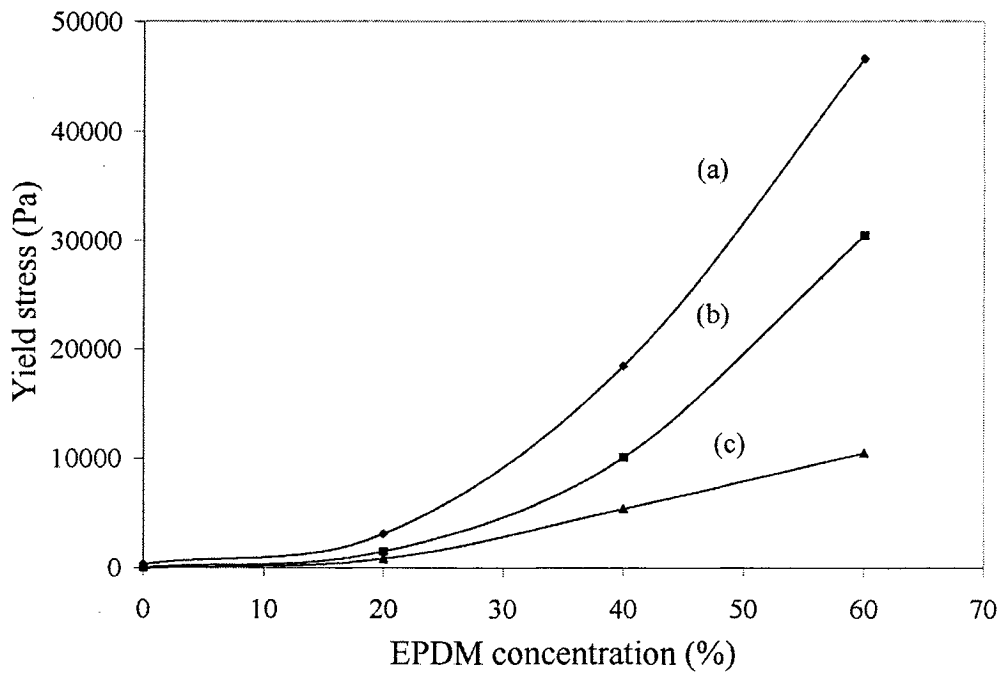

Figure 5.12: Increased yield stress for TPV nanocomposites prepared with (a) P1, (b) P2 and (c) P3.

It can be seen that the yield stress of the prepared TPV nanocomposite, based on a low-viscosity PP, increased more than that of the samples prepared with a medium

and high-viscosity PP. These results suggest that the nanoclay dispersion and exfoliation is better achieved in the TPV nanocomposites prepared based on low-viscous PP compared with the HVP samples at 20, 40, and 60 wt % of the rubber. In order to get a better insight of the nanoclay dispersion, TEM images where taken from these samples as illustrated in Figures 5.13 and 5.14.

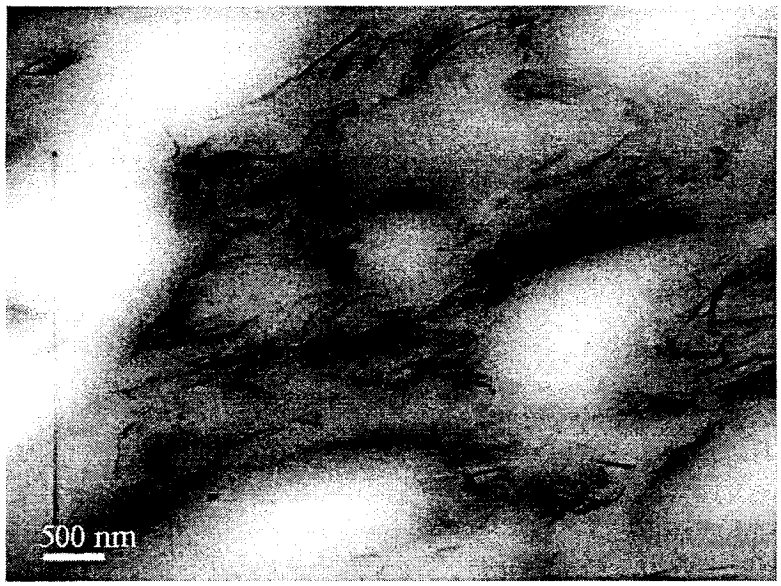

(a)

Figure 5.13: TEM image of TPV1 60 N before EPDM vulcanization (a).

The TEM image of the sample prepared by P1 before EPDM vulcanization is shown in Figure 5.13-a, which shows the silicate layers are dispersed throughout the PP matrix and can not penetrate into the elastomer phase during the mixing process. The rubber phase is white in color, and the silicate layers appear as black lines in the darker polypropylene phase. However, in TPV nanocomposites based on high viscosity PP

before curing the rubber phase, the nanoclays were found to be partly dispersed in the continuous phase, and partly agglomerated at the interfacial boundary between the polypropylene and the rubber phases, as shown in Figure 5.13-b.

(b)

Figure 5.13: TEM image of TPV3 60 N before curing step (b).

TEM images of TPV1 N 60, TPV3 N 60 and TPV1 N 20 after EPDM vulcanization are presented in Figure 5.14. For the TPV nanocomposites containing 60 % EPDM, the XRD results suggested a nearly exfoliated structure. In TPV hybrid based on LVP, a significant fraction of the silicate layers were exfoliated in the PP phase, while a slight amount remained in a more clustered state, as shown in Figures 5.14-a. The agglomerated state of the clay was more pronounced for the high viscosity PP based TPV as illustrated in Figure 5.14-b. The existence of the small peak in the X-

ray diffraction patterns around $2\theta = 7^{o}$ may be attributed to these un-exfoliated silicates. The TEM image of the TPV nanocomposite prepared by low viscosity PP containing 20 % EPDM shows that some silicate layers were present in the matrix as exfoliated layers, while most of the clay remained in clusters as shown in Figure 5.14-c. Therefore, the silicate layers were mainly intercalated rather than exfoliated in the TPV hybrid having 20 wt % of the rubber.

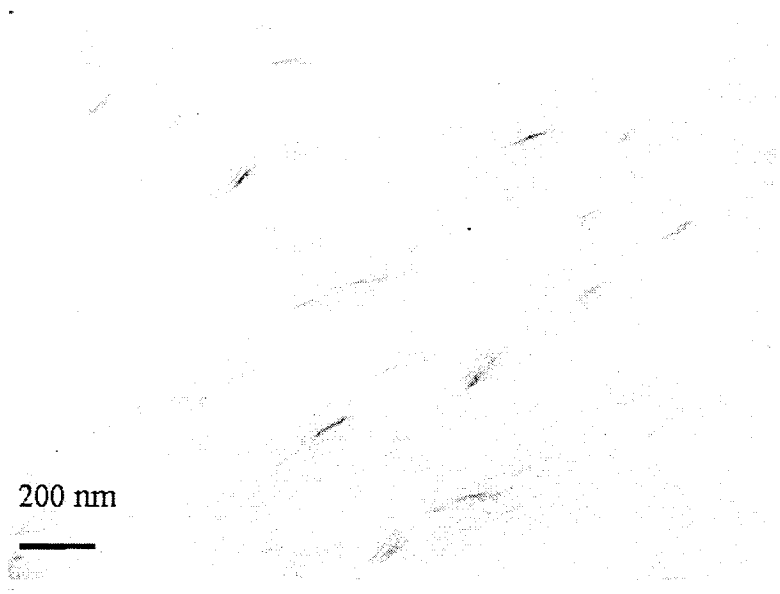

(a)

Figure 5.14: TEM image of (a) TPV1 60 N nanocomposite after EPDM vulcanization.

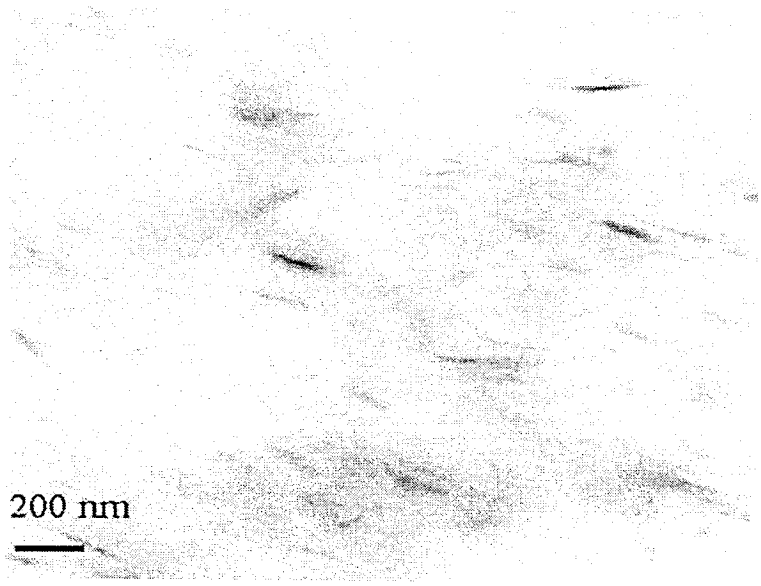

(b)

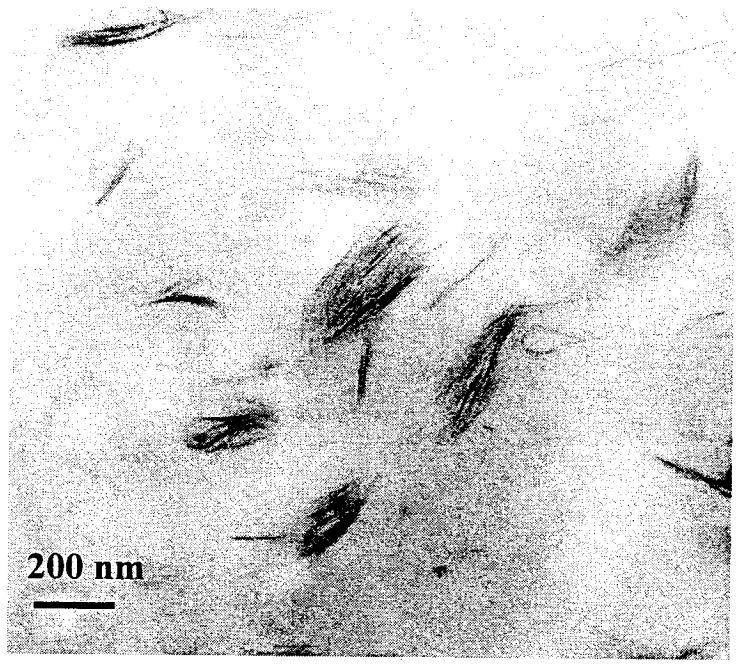

(c)

Figure 5.14: TEM image of (b) TPV3 60 N and (c) TPV1 20 N nanocomposites after EPDM vulcanization.

In this work, after considering these results we attempted to use a suitable linear viscoelastic model to achieve more insight into the relationship between the rheology and morphology of the TPV nanocomposites. Muller et al. [22] reported that, in the Palierne model, when H tends to ½, the model is found to be similar to the Einstein model introduced for diluted suspensions, in the following form:

$$G^*_{susp} = G^*_m \frac{1+3\phi H}{1-2\phi H} \approx G^*_m(1+2.5\phi), H = \frac{1}{2} \quad \text{.....} \quad (5.2)$$

Where ϕ is the dispersed phase concentration, G^*_{susp}, and G^*_m are the complex modulus of the blend and polymer matrix, respectively. Ghoharpy et al. [23] modified the Palierne model for TPV materials based on PP/EPDM, considering that the rubber particles were supposed to be spherical and a maximum packing volume (ϕ_m) of 0.64, as follows:

$$G^*_{susp} = a_1(\frac{\phi}{\phi_m}) + a_2(\frac{\phi}{\phi_m})^2 + G^*_m \frac{1+3\phi H}{1-2\phi H}, H = \frac{1}{2}$$

.....(5.3)

$$a_1 = -7.6E4\,,\ a_2 = 2.3E5$$

The results of the Palierne, the modified Palierne model and the experimental data for the TPV nanocomposites prepared with LVP containing 20, 40, and 60 %

EPDM at 2 wt % of the clay are shown in Figure 5.15. It can be seen that there is a close agreement between the experimental data and the Palierne model at high shear. Likewise, a considerable agreement between the results of the experimental data and the modified model was obtained for the TPV nanocomposite at 60 % rubber with ϕ_m = 0.64 as shown in Figure 5.15-a. However, in the TPV nanocomposites at 40 and 20 % EPDM, a better fit was achieved with ϕ_m = 0.59 and ϕ_m = 0.5, as shown in Figures 5.15-b and c, respectively. It should be noted that the maximum packing volume varies with the particle shape and the state of agglomeration of fillers [24]. Figure 5.16 shows the maximum packing volume obtained by using Eq. (3) in the TPV nanocomposite having 20, 40 and 60 % EPDM. It can be seen that the ϕ_m decreased when the rubber content was decreased in the TPV samples. The decrease in the maximum packing volume in the TPV nanocomposites can be explained due to the fact that the dispersion degree of the clay through the TPV matrix decreased when the EPDM content was decreased, as evidenced by Figure 5.14-c.

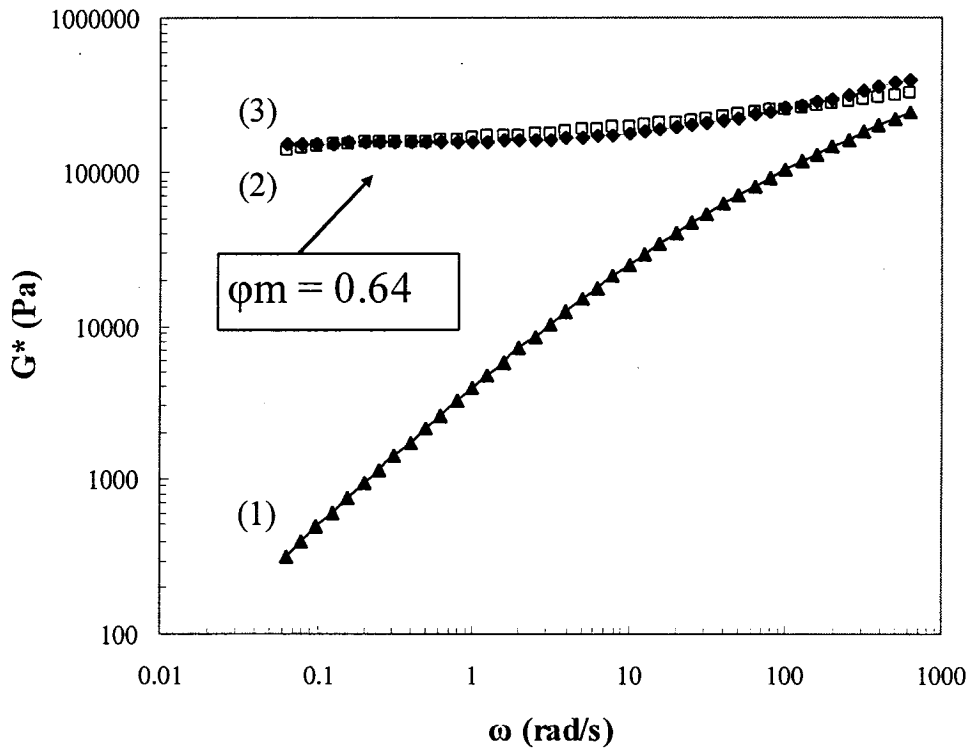

Figure 5.15 (a): Complex modulus vs. frequency obtained from (1) Paliene model, (2) modified Paliene model, and (3) experimental data for TPV1 60N.

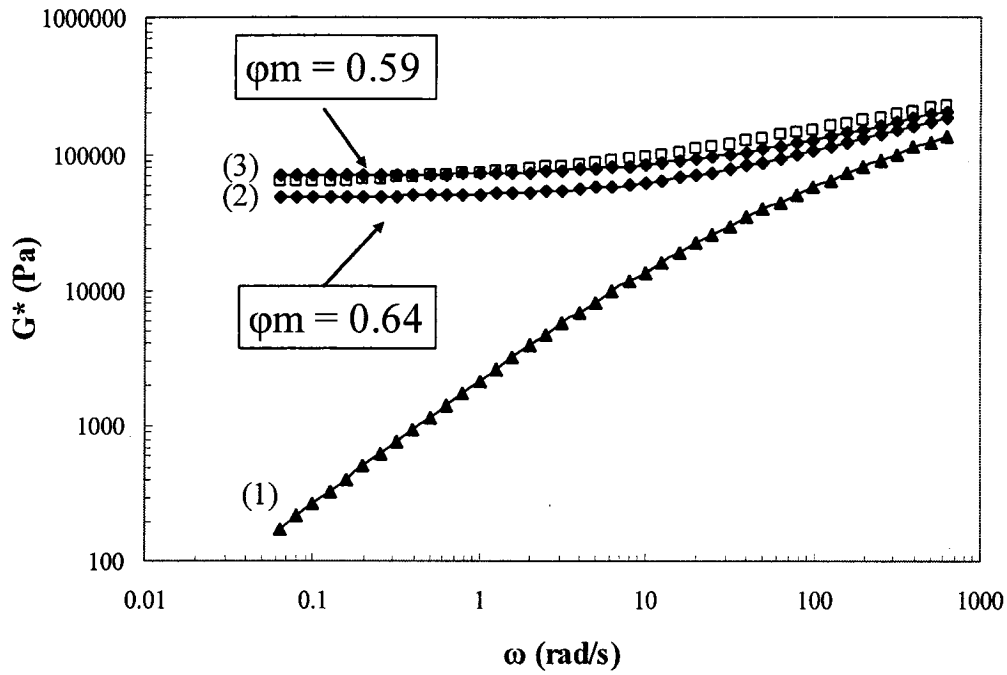

Figure 5.15 (b): Complex modulus vs. frequency obtained from (1) Paliene model, (2) modified Paliene model, and (3) experimental data for TPV1 40N.

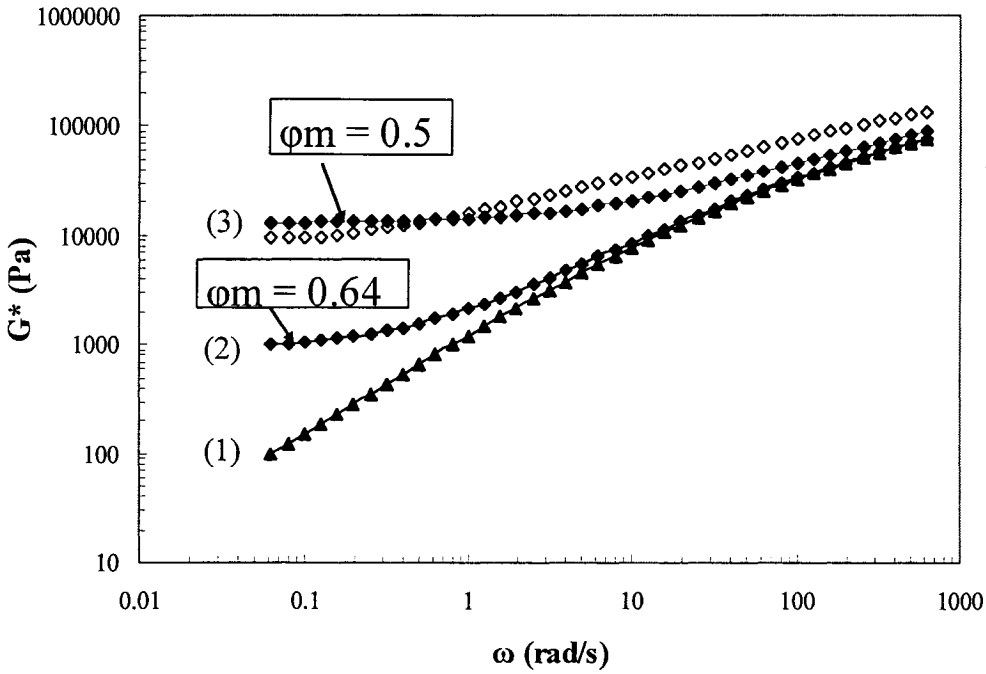

Figure 5.15 (c) : Complex modulus vs. frequency obtained from (1) Paliene model, (2) modified Paliene model, and (3) experimental data for TPV1 20N.

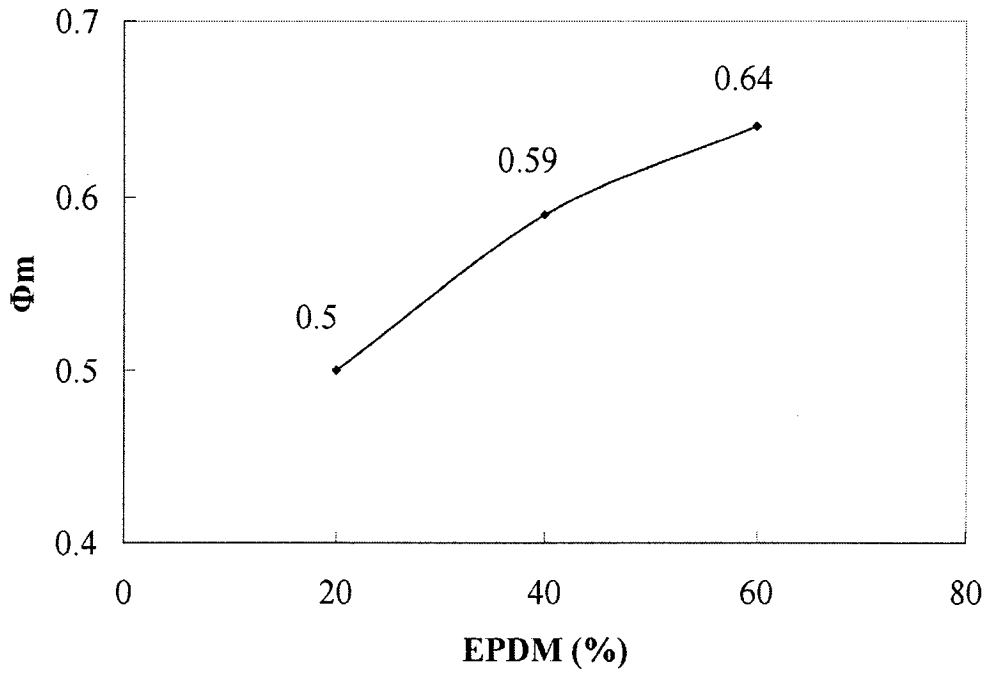

Figure 5.16: Maximum packing volume obtained by using Eq. (5.3) in the TPV nanocomposites prepared with P1 containing 20, 40, and 60 % EPDM.

5.4 Conclusion:

We studied the linear viscoelastic properties and the morphology of the dynamically vulcanized nanocomposite TPEs based on PP/EPDM prepared with different viscosities of PP containing 20, 40 and 60 % rubber, at 2 wt % of the clay. The

study demonstrates that there is a close relationship between the rheology and morphology of the TPV nanocomposites.

In uncompatibilized PP nanocomposites prepared with polypropylene of different viscosities, the PP chains could not penetrate efficiently between the silicate layers of the clay. However, the interlayer distance of the clay increased in the TPV nanocomposites prepared from the same PP, but without PPMA, and containing 20, 40 or 60 % EPDM.

The polypropylene nanocomposite prepared without PPMA demonstrated the storage modulus curve very close to that of the unfilled matrix. However, in the TPV nanocomposite without PPMA, the storage modulus curve significantly increased in comparison with that of the corresponding matrix.

The exfoliation degree of the clay increased with introduction of PPMA for both the PP and TPV nanocomposites. In the TPV nanocomposites prepared with PPMA, the silicate agglomeration considerably decreased with increasing the rubber content.

The yield stress of the prepared TPV nanocomposite, based on low viscosity PP, increased more than that for the TPV hybrid prepared by high viscosity PP.

The TPV nanocomposites containing 20, 40 and 60 % EPDM exhibited strong elastic modulus that tends to plateau out at low shear rates. These results were shown to be due to the strong interfacial interaction between the nanoclay and the TPV matrix and, also, the existence of the physical three-dimensional network structure formed between the cured rubber particles, as evidenced by the morphological features of the samples.

A Carreau-Yasuda law with a yield stress and a linear viscoelastic model, taking into account the maximum packing volume, were used to describe the melt linear viscoelastic properties of the TPV nanocomposites. Considerable agreement was found between the linear viscoelastic model and the experimental data in the TPV nanocomposites, containing 60 % EPDM. In this model, the maximum packing volume increased when the rubber content was increased.

Acknowledgments

This research was supported by the Natural Sciences and Engineering Research Council of Canada (NSERC). The authors acknowledge the generous assistance given by Bayer and Eastman Chemical Products companies in connection with the supply of materials used in this research.

References:

1 U.S. Patent 4130535 (1978), *Coran, A.Y., Patel, R. P.*

2 *Abdou-Sabet, S., Puydak, R.C., Rader, C.P.,*: Rubber Chem. Technol 69, p. 476 (1996)

3 *Naderi, Gh. Razavi Nouri, M.,*: Iran. Polym. J. 8, p. 37, (1999)

4 *Svoboda, P., Zeng, C., Wang, H., Lee, L. J., Tomasko, D. L.,*: J. Appl. Polym. Sci., 85, p.1562, (2002)

5 *Kato, M., Usuki, A., Okada, A.,*: J. Appl. Polym. Sci. 66, p. 1781 (1997)

6 *Hasegawa, N., Okamoto, H., Kawasumi, M., Kato, M. Tsukigase, A. Usuki, A.,*: J. Appl. Polym. Sci., 78, p.1918, (2000)

7 *Hasegawa, N., Kawasumi, M., kato, M., Usuki, A., Okada, A.,*: J. Appl. Polym. Sci. 67, p. 87, (1998)

8 *Alexandre, M., Dubois, P.,*: Mater. Sci. Eng. 28, P. 1, (2000)

9 *Ren, J., Silva, As., Krshnamoorti, R.,*: Macromolecules 33, p. 3739, (2000)

10 *Galgali, G., Ramesh, C., lele, A.,*: Macromolecules 34, p. 852-8, (2001)

11 Yong *T., L., Park, O.O.,*: Rheol. Acta 40, p. 220, (2001)

12 *Gu, S. Y., Ren, J., Wang, Q. F.,*: J. Appl. Polym. Sci. 91, p. 2427, (2004)

13 *Li, J., chixing, Z., Wang, G., Yu, W., Tao, Y.,*: Polymer Composites 24, 3, p. 323, (2003)

14 *Han, P., K., White, J., L.,*: Rubber Chem. Tech. 68, 5, p.728 (1995)

15 *Loppez-Manchado, M.A., Biagiotti, J., Kenny, J.M.,*: J. Appl. Polym. Sci. 81, p. 1, (2001)

16 *Naderi, G., Lafleur, P.G., Dubois, C.,* Polym. Eng. Sci., in press (2006).

17 *Kyu-nam, K., Hyungsu K., Jae-wook, L.,*: Polym. Eng. Sci. 41, p. 1963, (2001)

18 *lertwimolnun, W., Vergnes, B.,*: Polymer 46, p. 3462, (2005)

19 *Berzin, F., Vergnes, B., Delamare, L.,*: J. Appl. Polym. Sci. 80, p. 1243 (2001)

20 *Takumi, A., White, J. L.,*: Polym. Eng. Sci. 38, 4, p.590 (1998)

21 *Goharpey, F., Katbab, A. A., Nazockdast, H.,*: Rubber Chem. Tech. 76, p. 1, (2003)

22 *Muller, R., Graebling, D., Palierne, J.F.,*: Macromolecules 26, p. 320, (1993)

23 *Goharpey, F., Katbab, A.A., Nazockdast, H.,*: Polym. Eng. Sc. 45, p. 84, (2005)

24 *Nielson, L.E., Landel, R.E.,*: Mechanical Properties of Polymers and Composites, 2nd ed., Marcel Dekker, New York, (1994)

CHAPTER 6

The Influence of Matrix Viscosity and Composition on the Morphology, Rheology and Mechanical Properties of Thermoplastic Elastomer Nanocomposites

Chapter 4 and 5 provide comprehensive knowledge of the microstructure, rheological, and mechanical properties in the dynamically vulcanized nanocomposite thermoplastic elastomers (selectively reinforced plastic phase TPV nanocomposites) prepared by a three-step melt mixing process containing different viscosities of PP and EPDM contents of 20, 40, 60 wt%.

The morphology of the TPV nanocomposites before the vulcanization of the rubber phase (selectively filled plastic phase TPE nanocomposites) revealed that the clay dispersed through the PP phase and could not penetrate into the EPDM phase during the mixing process.

One of the important factors affecting the mechanical properties of nanoclay-reinforced TPEs is feeding routes. On the other hand, the final phase morphology of the TPE nanocomposites significantly depends on the phase location of the clay reinforcement, whether it lies in the dispersed rubber phase or in the continuous plastic matrix. In this work, we studied the microstructure, rheology, and mechanical properties of the uncured TPE nanocomposites prepared by a one-step melt-mixing

properties of the uncured TPE nanocomposites prepared by a one-step melt-mixing process. EPDM (20, 40, and 60 wt %), PP (different viscosities), maleic anhydride-modified polypropylene (PPMA), and clay (3 wt %) were compounded in a small laboratory internal mixer. The effects of PP/EPDM viscosity ratio and composition were also investigated.

To study the morphology of the TPE nanocomposite samples, cryogenically fractured surfaces of the samples were etched by n-heptane. The same microstructure and rheology investigation method in the first and second papers were applied here.

This paper is submitted to the journal of Polymer.

The Influence of Matrix Viscosity and Composition on the Morphology, Rheology and Mechanical Properties of Thermoplastic Elastomer Nanocomposites based on PP/EPDM

Naderi Ghasem, Lafleur Pierre G., and Dubois Charles[‡]

Center for Applied Research on Polymers and Composites, CREPEC, Department of Chemical Engineering, Ecole Polytechnique de Montreal, 2900 Edouard Montpetit, P.O. Box 6079, Station Centre-Ville Montreal, QC, Canada, H3C 3A7

Abstract

The morphological and rheological properties were studied in thermoplastic elastomer nanocomposites (TPE nanocomposites) based on different viscosities of polypropylene and EPDM rubber (20, 40, 60 wt %). EPDM, PP, Cloisite 15A and maleic anhydride-modified polypropylene (PPMA) as compatibilizer were compounded by a one-step melt mixing process in a laboratory internal mixer.

The structure of the nanocomposites was characterized with X-ray diffraction (XRD), scanning electron microscopy (SEM), transmission electron microscopy (TEM) and rheometry in small amplitude oscillatory shear.

The distribution state of the clay between the two phases (PP and EPDM) was found to be dependent upon the viscosity ratio of PP to EPDM. In the nanocomposites prepared based on low viscosity PP (LVP) and EPDM, the clay was mostly dispersed

[‡]Correspondence concerning this article should be addressed to C. Dubois
Email address: Charles.Dubois@polymtl.ca .

into the plastic phase and also the dispersed rubber particle size decreased in comparison with similar but unfilled blends. However, the dispersed elastomer droplet size in the high viscosity PP (HVP) blends containing 40, and 60 % EPDM increased with the introduction of the clay. For TPE nanocomposites, the dependence of the storage modulus (G′) on angular frequency (ω) was shown non-terminal behaviors. The increase in the storage modulus and the decrease in the terminal zone slope of the elastic modulus curve were found to be larger in the LVP hybrid in comparison with the HVP sample. The yield stress of the nanoclay-filled blends prepared with LVP increased more than that of the HVP hybrids. The tensile modulus improved for all TPE nanocomposites and obtained higher percent increase in the case of the LVP samples.

Keywords: TPE nanocomposites, polyolefin nanocomposite, morphology, rheology, mechanical properties.

6.1 Introduction

Thermoplastic elastomers (TPEs) based on polypropylene (PP) and ethylene-propylene-diene terpolymer (EPDM) have gained considerable attention due to a combination of rubbery properties along with their thermoplastic nature as well as the simple preparation method. The mechanical properties of the TPEs depend not only on the specifications of individual component in the blend but also on the final phase morphology in the materials [1-3]. Therefore, many reports have been published on the phase morphology of the blends. The concentration of the compounds, processing

condition, viscosity ratio, elasticity ratio, and interfacial tension between two polymers play an important role to control the morphology of the blends [4-7].

However, there is little information available in the literature dealing with the effect of reinforcing fillers on the morphology, microstructure and rheology of the thermoplastic elastomers. The use of nanoclay at a small amount (up to 5 wt %) has received significant attention of scientists and engineers in recent years. This is mainly attributed to the nanoscale dimension of the silicate layers dispersed in polymer matrix, which causes a strong interfacial interaction between the silicate layers and polymer chains, hence the mechanical, thermal stability, barrier, and fire resistance properties of polymer nanocomposites increase in comparison with pristine polymer [8, 9].

TPE nanocomposites are emerging as a new class of industrially important material. While nanocomposites based on PP and EPDM have been prepared by many researchers [10-13], few efforts have been devoted to the study of TPE nanocomposites [14-16].

Lee et al. [14] studied the mechanical properties of PP/EPDM/clay blends prepared without PPMA by direct melt mixing. They reported that the tensile modulus of the blends increased with the introduction of the clay, whereas their tensile strength decreased.

As the morphology of the TPEs plays a very significant role in controlling all characteristics, Mehta *et al.* [15] examined the effect of the clay content on the morphology of thermoplastic olefin (TPO) nanocomposites based on PP/EPDM

(70/30). They observed that the size of the rubber particles dispersed through the plastic phase decreased as the clay concentration was increased.

The final phase morphology in the polymer blends can be affected by the distribution state of the filler particles between the two phases and the interaction of the filler surface with either of the polymeric phases. It has been also reported that the viscosity ratio, feeding routes and the affinity of the filler toward the polymeric phases control the filler distribution [17, 18].

The present study considers the effect of the matrix viscosity and composition on the morphology, rheology and mechanical properties of the thermoplastic elastomer nanocomposites (TPE nanocomposites) based on PP/EPDM.

The results will show how the dispersed rubber particle size is influenced by the clay in TPEs prepared with different viscosities of polypropylene and provide some understanding of the clay dispersion in the PP and EPDM phases.

6.2 Experimental

6.2.1 Materials

The basic specifications of EPDM and the three grades of polypropylene (Basell Co.) employed in this study are reported in Table 1. The EPDM rubber (Buna EP T 6470) was based on ethylene norbornene (ENB) as a termonomer, and was supplied by Bayer Co. The nanoclay used was Cloisite 15A which was a natural montmorillonite modified with a dimethyl dehydrogenated tallow quaternary ammonium having a cation-

exchange capacity (CEC) at 125 meq/100g from Southern Clay Products and has a specific gravity of 1.66. Epolene G3015 (M_w=47000, Acid Number =15, mol of MA/mol of PPMA=6.3, MA~1%) as maleic anhydride-modified polypropylene (PPMA) was obtained from Eastman Chemical.

Table 6.1: Basic specification of PP and EPDM

Materials	Characteristics	
PP (P1)	MFI	14 gr/10 min
	Density	0.91 g/cm^3
	Tm	>160 ^{oC}
	η_0 [1]	1818 Pa.s
PP (P2)	MFI	4 gr/10 min
	η_0 [1]	5000
PP (P3)	MFI	0.5 gr/10 min
	η_0 [1]	27100
EPDM	Mooney Viscosity ML (1+4), 125°C	55
	Ethylen Content	68 %
	Termonomer Content	4.5 % ENB
	Density	0.86 g/cm^3

1- Zero shear viscosity is obtained by C. Y. model $\eta^*(\omega) = \eta_0((1+(\omega\lambda)^a)^{(m-1)/a}$

6.2.2 Sample preparation

TPE nanocomposite samples composed of 80/20, 60/40, 40/60, PP/EPDM (wt/wt) were prepared in a small-scale laboratory internal mixer (Rhemix 600). PP, EPDM, clay powder and PPMA pellet were melt-mixed by a one-step process in the mixer at 180 °C under nitrogen with a rotor speed of 100 rpm for 10 min. For all nanocomposite samples, the PPMA/Cloisite 15A ratio and the clay concentration were kept constant at 3:1 and 3 % wt respectively. For electron microscopic examination, samples were immediately cooled in ice water. The prepared compounds were compression-molded by hot press at 200 °C for 10 min to obtain suitable samples for X-ray diffraction test. The variations of mixing torques and temperatures as a function of time were recorded for all blending processes. For comparison purposes, unfilled but otherwise similar TPEs were also compounded as reference materials. In all instances, the clay had been dried at 80 °C for 24 h prior to processing.

6.2.3 Characterization

In order to evaluate the dispersion of the clay in the polymer matrix, X-ray diffraction (XRD) was performed at room temperature using an X-ray diffractomer (Philips model X'Pert) in the low angle of 2θ. The X-ray beam was a Cu-K_α radiation (λ=1.540598 A°) using a 50 kV voltage generator and a 40 mA current. The basal spacing of silicates was estimated from the position of the plane peak in the WAXD intensity profile using the Bragg's law, $d = \lambda / (2 \sin\theta_{max})$. Specimens for X-ray diffraction were obtained by compression-molded sheets of 2 mm in thickness.

The nanostructure of the clay was observed by a transmission electron microscopy (JEM-2100F, JEOL) with an accelerator voltage of 200 kV. The surface of the samples was first coated with gold and then a thin section of each specimen was prepared by using a focused ion beam (FB-2000A, Hitachi) and also a cryo-microtom equipped with a diamond knife at -100 °C.

To study the morphology of the TPE nanocomposite samples, cryogenically fractured surfaces of the samples were etched by n-heptane. The treated samples were then coated with gold and viewed with a scanning electron microscope model JSM-840 made by JEOL company.

The rheological characterization of samples was carried out using a stress controlled rheometer (AR 2000). The experiments were performed in parallel-plate geometry with a diameter of 25 mm under a nitrogen atmosphere at a temperature of 220 °C and in the range of 0.01-80 Hz frequency.

The stress-strain properties of the composites were determined in accordance with the test procedures set forth in ASTM D412 at room temperature with cross head speed of 50 mm/min using an Instron model 4201.

6.3 Results and discussion

We obtained the linear viscoelastic behavior of the polymers used for preparing the TPE nanocomposites. Figure 6.1 shows the elastic modulus (G′) and complex viscosities (η^*) of EPDM and polypropylenes with different viscosities (P1, P2, and P3) as a function of angular frequency. The polypropylenes exhibited a viscosity that

reaches a constant value at low frequencies; however, the viscosity of EPDM increases indefinitely at low shear rates.

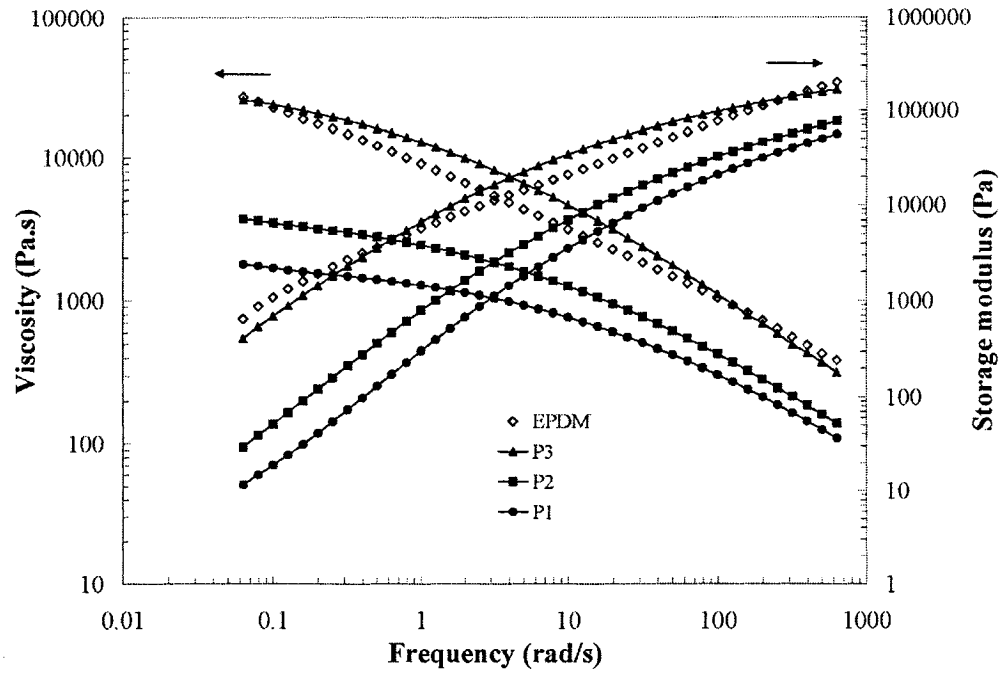

Figure 6.1: Complex viscosity and storage modulus of EPDM and three different types of polypropylene versus angular frequency.

The simplified Carreau-Yasuda (C.Y.) model was used to fit the complex viscosity data of the pure polymers from oscillatory shear measurements. The zero shear viscosity of three grads of PP obtained from C.Y. model, are given in Table 6.1. There was approximately a five-fold difference in zero shear viscosity between high

and medium-viscous PP and, also, a fifteen-fold difference between high and low-viscous PP.

The X-ray diffraction scans of the clay (Cloisite 15 A) and the TPE nanocomposites prepared with LVP and 20, 40, 60 % EPDM are shown in Figure 6.2.

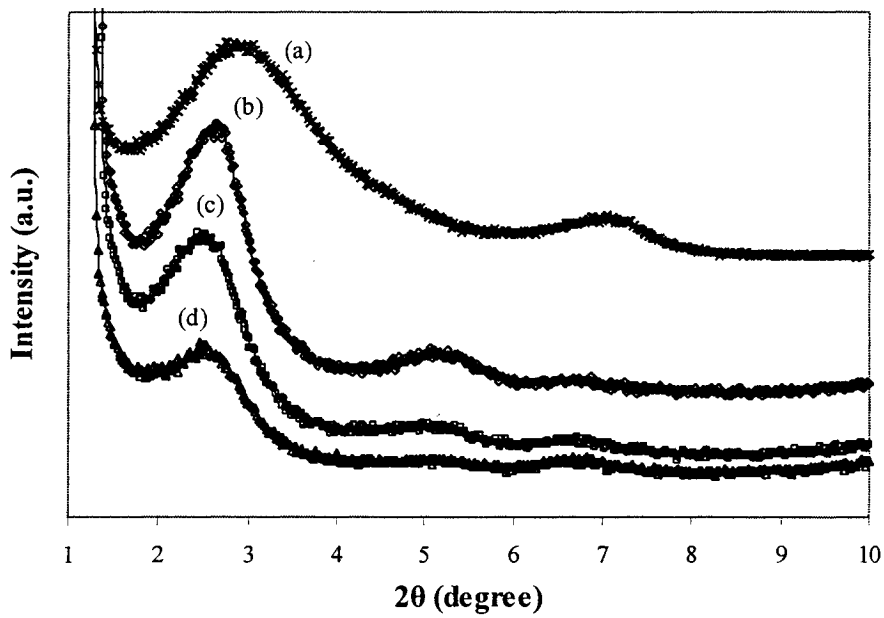

Figure 6.2: X-ray diffraction patterns of (a) Cloisite 15A and TPE nanocomposites based on P1 with (b) 60 %, (c) 40 %, and (d) 20 % EPDM.

It is observed from Fig. 6.2(a) that the diffraction peak corresponding to the (001) plane of the clay appeared at 2.9 ° (d = 30.44 Á) before mixing with PP and EPDM while the TPE sample containing 20 % EPDM showed a diffraction peak at 2θ = 2.55 °, which corresponds to an interlayer spacing of 34.62 Á, as shown in Fig. 6.2(d).

This is attributed to the intercalation of the polymer chains and the compatibilizer (PPMA) inside the silicate layers. In the TPE nanocomposites containing 40 and 60 % EPDM, the basal spacing of the clay was 33.95 Á and 32.69 Á respectively.

It is also shown from Fig.6.2 that the intensity of the XRD peaks increased when the EPDM concentration was increased. These results suggest that the clay tends to disperse into the low viscosity polypropylene (LVP) in the samples containing 20, 40 and 60 % rubber. Since P1 is a low-viscous material compared with the elastomer; consequently, the silicate layers remain into the LVP phase and can not penetrate into the rubber phase during mixing process.

We recall that the concentration of the clay was kept constant at 3 wt % for all TPE nanocomposites containing different contents of the elastomer. It is well known that the intensity of XRD peak of nanocomposites prepared based on a nonpolar polymer matrix increases with increasing the clay content due to the influence of the packing density, rending more difficult the penetration of the polymer chains between the silicate layers [10, 11]. Therefore, it is reasonable to say that the clay concentration increases in the polypropylene phase of the TPE nanocomposite when EPDM content is

increased. On the other hand, the interlayer spacing of the clay in the samples decreased when the rubber content was increased. Therefore, higher nanoclay intercalation was achieved in the TPE nanocomposite prepared with 20 wt % of the elastomer, the higher intercalation means higher disordering of the layered silicate structure, consequently decreasing the peak intensity of the clay in the sample [19].

Figure 6.3 shows the XRD patterns of the original clay and the samples prepared from medium viscosity polypropylene (MVP) at different contents of the rubber (20, 40 and 60 % EPDM).

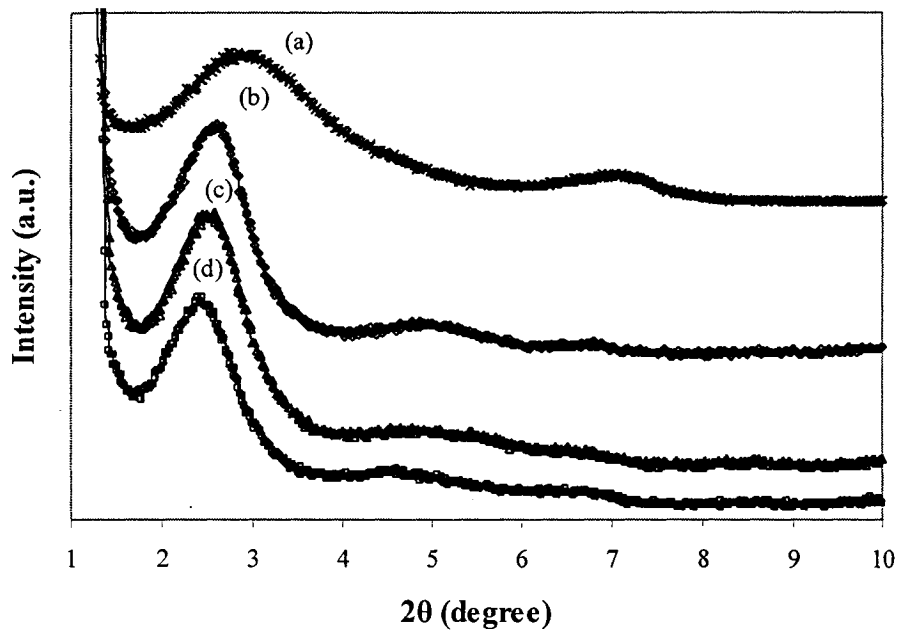

Figure 6.3: X-ray diffraction patterns of (a) Cloisite 15A and TPE nanocomposites based on P2 with (b) 60 %, (c) 40 %, and (d) 20 % EPDM.

It can be seen that the XRD peaks of the TPE nanocomposites were shifted to lower angles in comparison with the clay showing an intercalated structure in the samples. It is also observed that the intensity of the peaks was almost similar in shape for the samples [14]. These results suggest that the clay disperses into the PP phase but some silicate layers diffuse into the EPDM phase as the rubber content is increased. The XRD peaks also show that the interlayer distance of the clay in the samples decreased as the elastomer content was increased.

In the TPE nanocomposites prepared from high viscosity PP (HVP) and 20, 40, 60 % EPDM, similar trends were observed for the peak position of the XRD patterns, which indicate the intercalation of the silicate layers by the polymer chains. However, the intensity of the XRD peaks in the TPE nanocomposites decreased when the rubber content was increased as illustrated in Figure 6.4.

These results suggest that the clay disperses into both the PP and the EPDM phases and that the clay concentration would increase in the rubber phase with increasing the elastomer content. The decrease in the intensity of the XRD peaks for the HVP samples is attributed to the increase of the shear stress imposed by the EPDM phase which in turn facilitates the break-up process of the nanoclay agglomeration in the rubber phase [10, 14]. Therefore, it is reasonable to say that the concentration of the clay in the rubber phase of the TPE based on HVP is more than that for the sample prepared from MVP.

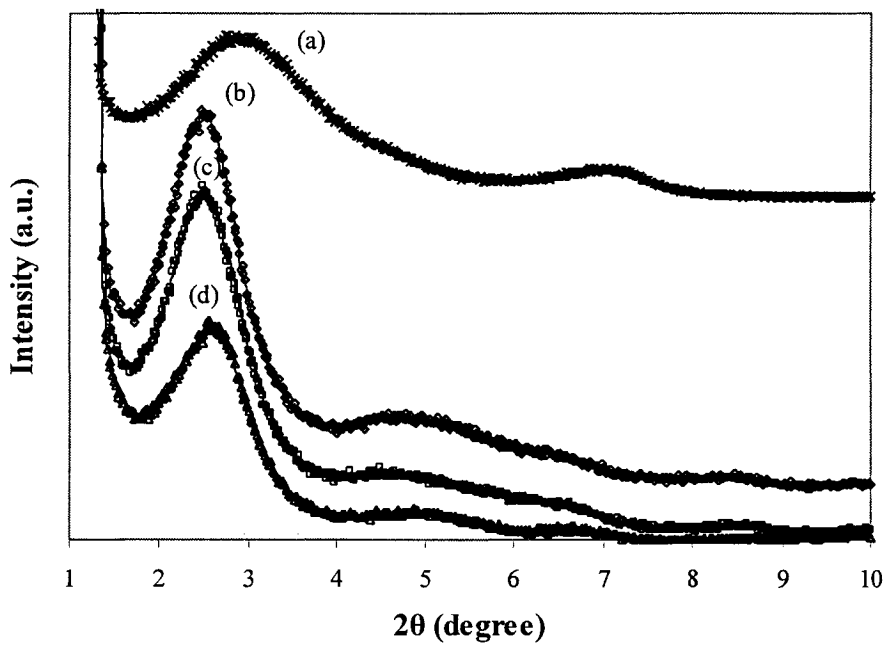

Figure 6.4: X-ray diffraction patterns of (a) Cloisite 15A and TPE nanocomposites based on P3 with (b) 20 %, (c) 40 %, and (d) 60 % EPDM.

SEM micrographs presented in Figures 6.5, and 6.6 stress the difference observed between the samples prepared with the low and high viscosity polypropylene having 40 and 60 wt % of the rubber. The rubber droplets, which have been removed by selectively etching in n-heptane, were displayed as the dark holes. The SEM

photomicrographs of the etched cryogenic fractured surfaces of the unfilled samples prepared based on PP/EPDM (60/40) show that the size of the rubber droplets decreased when the viscosity of the PP phase was increased as illustrated in Figures 6.5-a and 6.6-a respectively.

It is well known that, fine dispersions could be achieved if the viscosity ratio value of plastic/rubber is near unity in PP/EPDM blends [20].

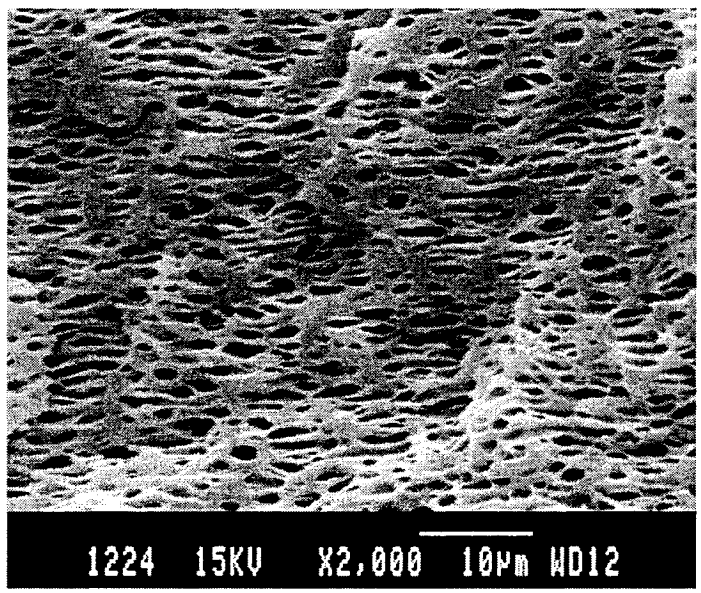

(a)

Figure 6.5: SEM micrograph of TPE based on (a) unfilled P1/EPDM (60/40)

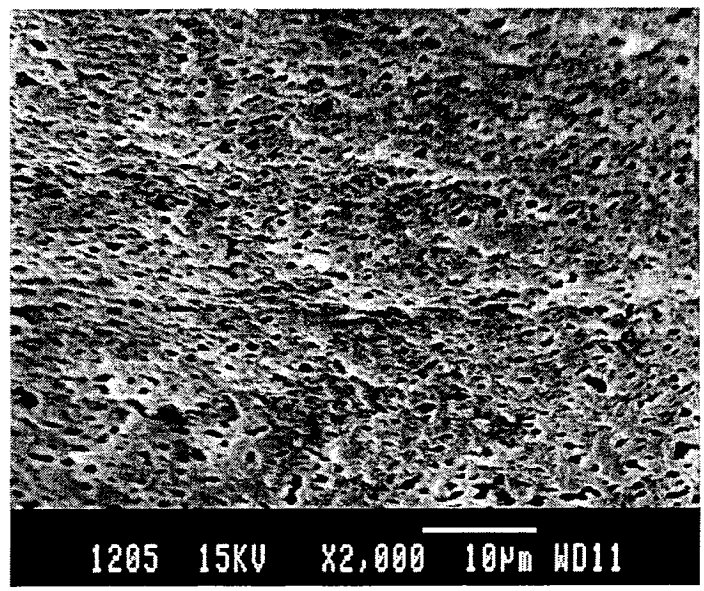

(b)

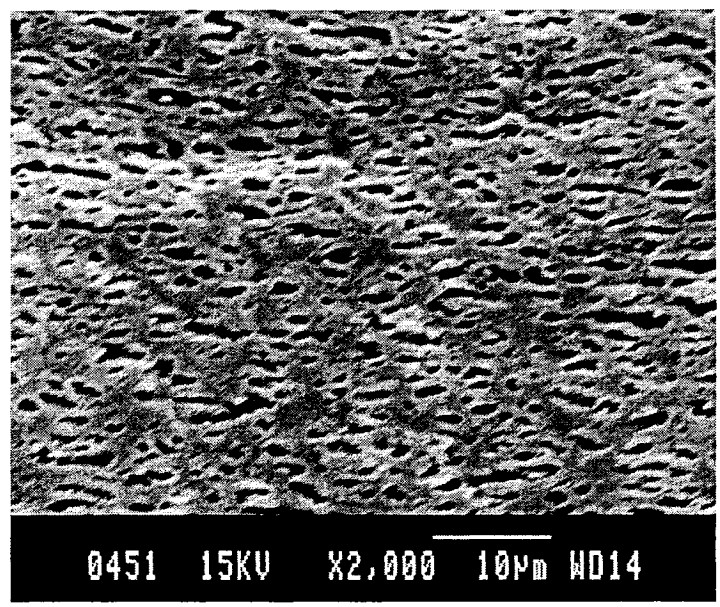

(c)

Figure 6.5: SEM micrograph of TPE based on (b) nanoclay-filled P1/EPDM (60/40), (c) nanoclay-filled P1/EPDM (60/40) without PPMA.

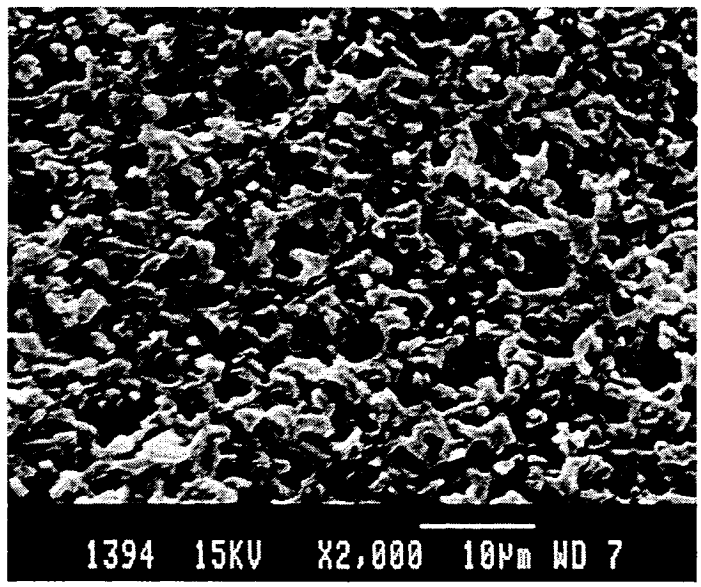

(d)

Figure 6.5: SEM micrograph of TPE based on and (d) unfilled P1/EPDM (40/60).

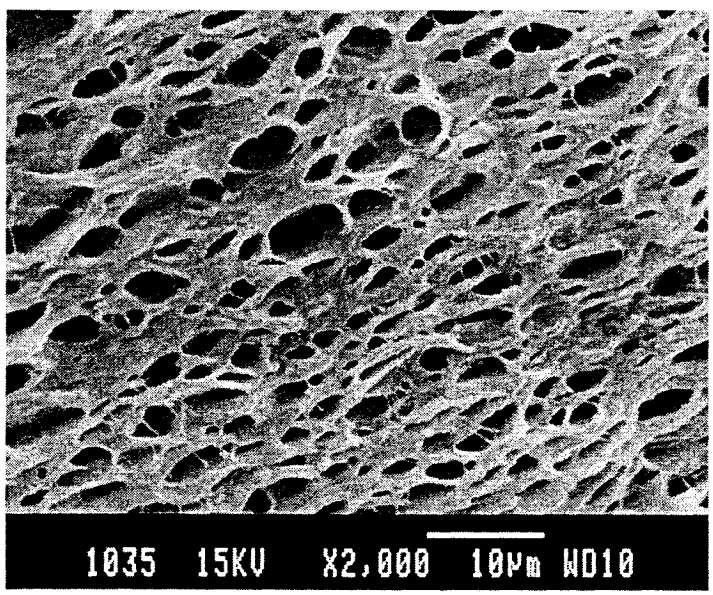

(e)

Figure 6.5: SEM micrograph of TPE based on (e) nanoclay-filled P1/EPDM (40/60).

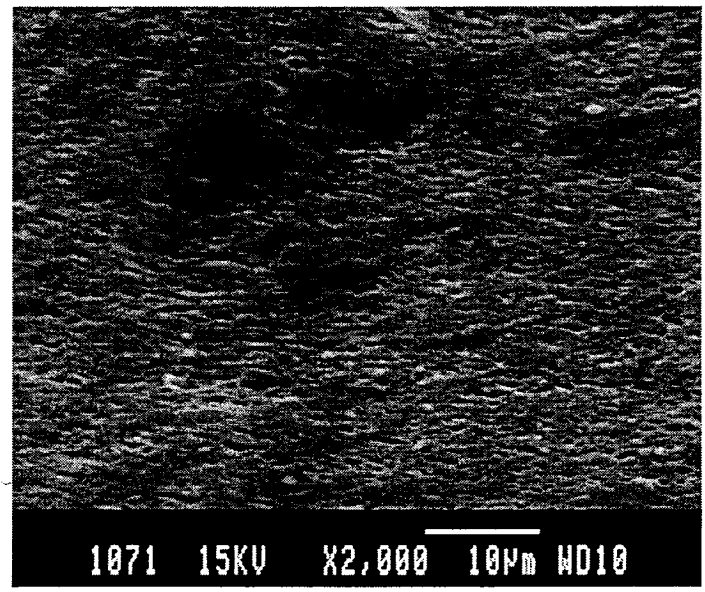

(a)

Figure 6.6: SEM micrograph of TPE based on (a) unfilled P3/EPDM (60/40).

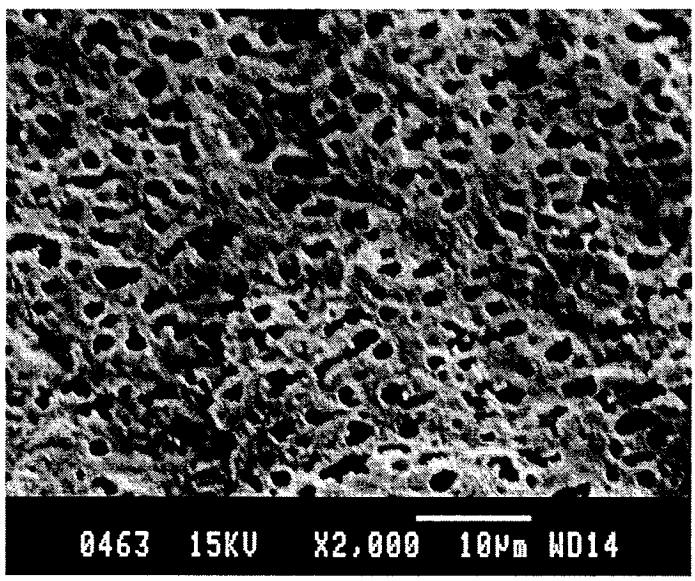

(b)

Figure 6.6: SEM micrograph of TPE based on (b) nanoclay-filled P3/EPDM (60/40).

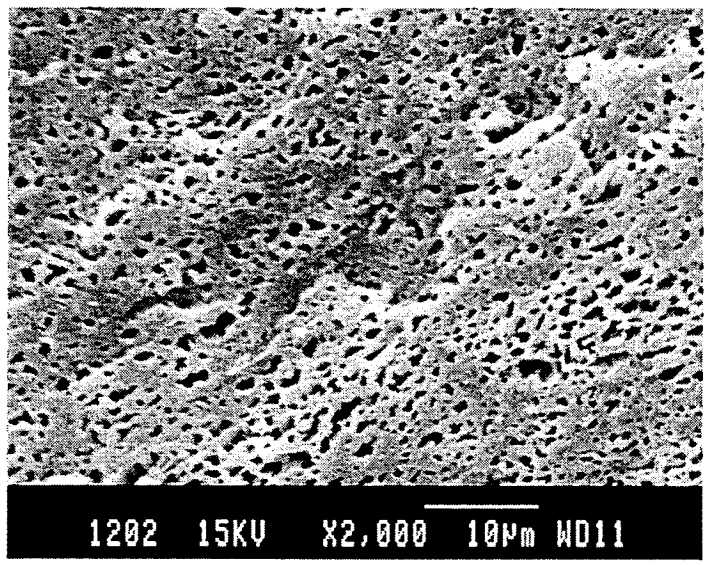

(c)

Figure 6.6: SEM micrograph of TPE based on (c) unfilled P3/EPDM (40/60).

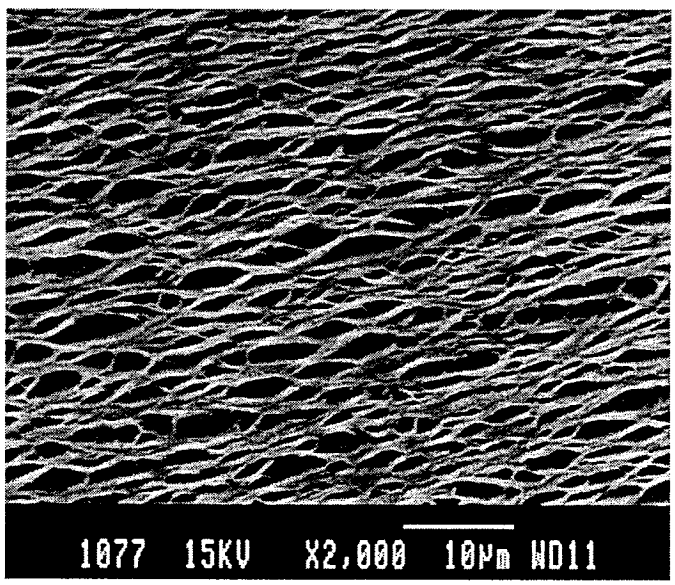

(d)

Figure 6.6: SEM micrograph of TPE based on (d) nanoclay-filled P3/EPDM (40/60).

The decrease in the volume average diameter (dv) of the rubber droplets with increasing the viscosity of PP phase in the unloaded blends having 20, 40 and 60 % EPDM is shown in Figure 6.7. One can also see that the size of the rubber droplets increased when the rubber content was increased in the unfilled samples demonstrating the significant role of coalescence in increasing the dispersed rubber droplet size as a result of increasing the rubber concentration [20].

Sigma scan software connected to a digitalization table was applied to measure the volume average diameter of the dispersed rubber phase. The dv refer to the volume average diameter of a corresponding volume sphere for the elongated rubber phase. In this latter case, we also measured the length and the width of the deformed EPDM phase particles in the same way. We utilized several micrographs to analyze an average of 200 particles for each sample. The SEM photomicrographs of the etched cryogenic fractured surfaces of both the unfilled sample and the nanocomposite prepared based on P1/EPDM (60/40) and 3 wt % of the clay are presented in Figures 6.5-a, and 6.5-b.

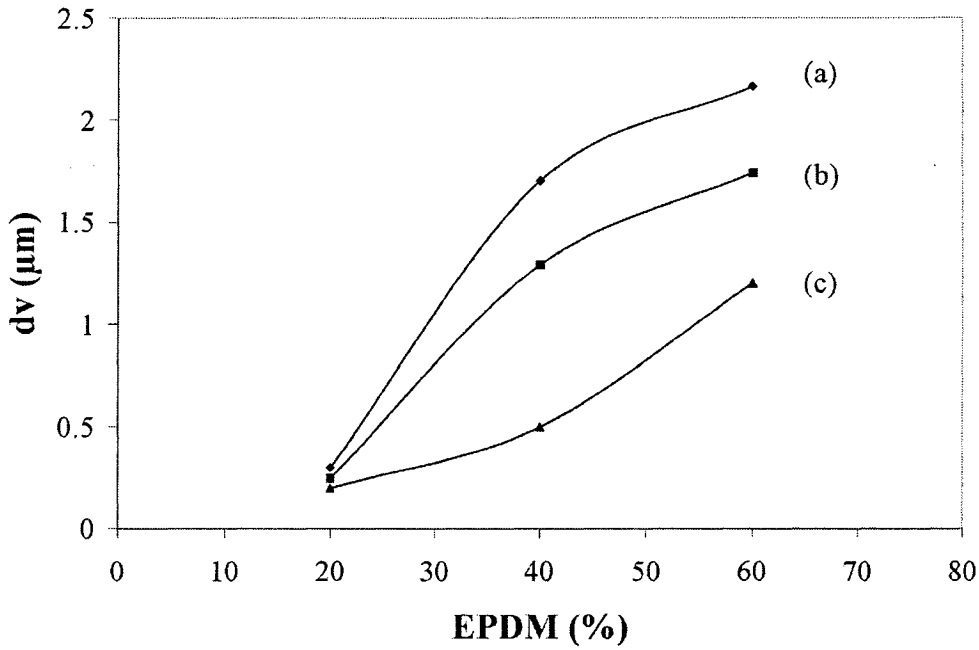

Figure 6.7: Volume average diameter of rubber droplets in unfilled TPEs based on (a) P1, (b) P2 and (c) P3.

The dispersion of the EPDM droplets throughout the PP matrix is clearly seen in both the unfilled and the nanoclay-filled samples indicating a matrix-dispersed type of morphology is developed in these blends. In the case of the unfilled sample based on LVP as presented in Figure 6.5(a), the dispersed elastomer droplets were appeared larger in size compared with similar nanoclay-filled sample as shown in Fig. 6.5(b).

In agreement with the observations of Mehta *et al.* [15], this may be related to the increase of the melt viscosity of the plastic phase which led to decrease the viscosity difference between the two phases.

We prepared a sample [P1/EPDM/clay (57/40/3)] without PPMA with the purpose of determining if the reduction of the rubber particle size is owing to the PPMA or the nanoclay itself. The results demonstrated that the clay itself can diminish the elastomer droplet size; however, the decrease of the rubber particles in the sample prepared with PPMA was more than in the sample without compatibilizer as shown in Fig. 6.5 (c). This is related to better dispersion of the clay with PPMA resulting in more increase of the viscosity of the plastic phase.

The unloaded-LVP sample prepared with 60 % EPDM tends to show a random co-continuous morphology as illustrated in Fig. 6.5(d). However, the rubber particles were dispersed through the plastic matrix in the nanoclay-filled sample based on P1/EPDM (40/60) as shown in Fig. 6.5 (e).

In the nanocomposite prepared based on P3/EPDM (60/40) at 3 wt % of the clay, the dispersed rubber droplets were showed larger in size and more elongated by nanoclay in comparison with similar but unloaded sample as illustrated in Figures 6.6-a, and 6.6-b respectively. This is attributed to the existence of the clay in the elastomer phase and hence the increase of the viscosity difference between the two phases, consequently, the formation of large rubber droplet.

The rubber particles were dispersed through the polypropylene matrix in the unfilled blend prepared from HVP and 60 % EPDM as shown in Figure 6.6-(c) [18,

21]. However, the size of the rubber particles increased with the introduction of the clay in the TPE nanocomposite based on HVP/EPDM (40/60) as illustrated in Figure 6.6-(d).

Therefore, we can conclude that the distribution state of the clay between the two phases (PP, and EPDM) and the rubber particle size in the samples strongly depend on the viscosity ratio of the polypropylene to the rubber phase.

The volume average diameter of the rubber droplets in the nanoclay-filled blends prepared with low and high viscosity PP is presented and compared with the similar but unloaded samples containing 20, 40, and 60 % EPDM as shown in Figure 6.8. These results are in agreement with the intensity of the XRD patterns for the TPE nanocomposites.

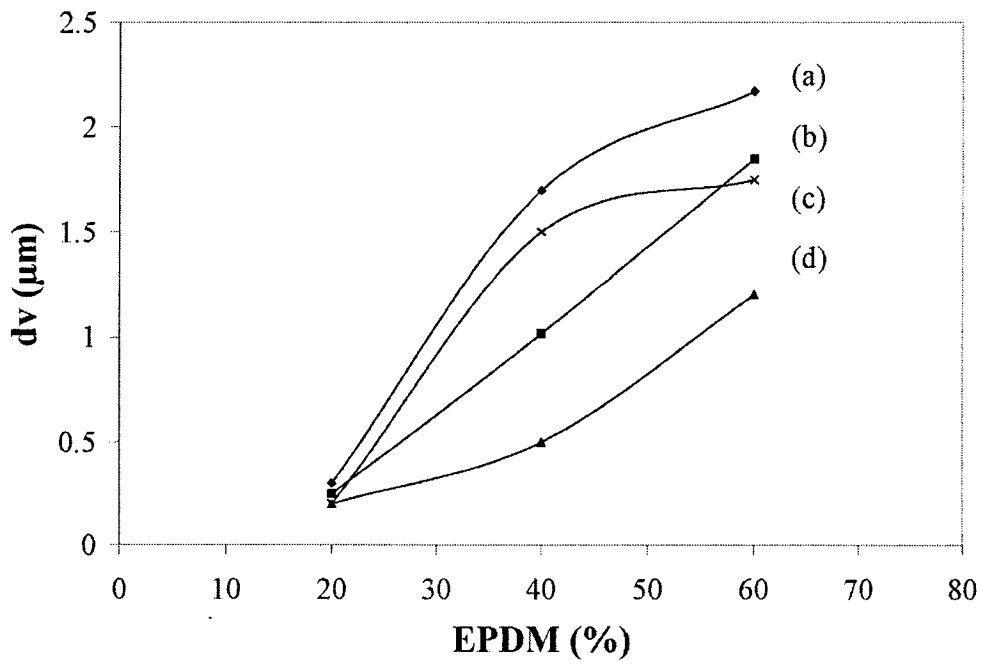

Figure 6.8: Volume average diameter of rubber droplets in TPE based on (a) unfilled P1, (b) nanoclay-filled P1 (c) nanoclay-filled P3, and (d) unfilled P3 .

The TPE nanocomposites prepared with low and high viscosity PP having 60 % EPDM were further characterized using TEM as contrasted in Figure 6.9. TEM images confirmed the intercalation of the polymers inside the Cloisite 15 A. It is obvious from the TEM image of the sample prepared based on P1/EPDM (40/60) that the silicate layers dispersed through the low viscosity polypropylene matrix phase and hardly exist in the dispersed elastomer phase as shown in Figure 6.9-a.

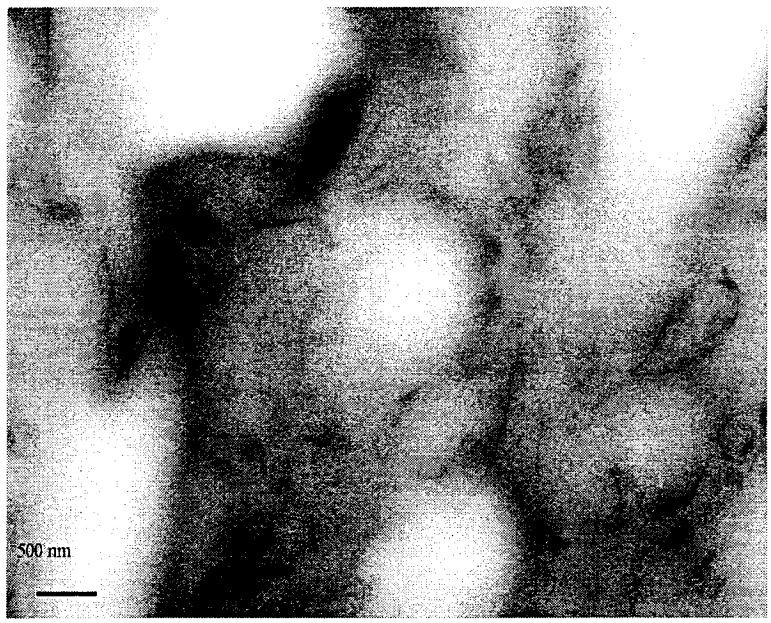

(a)

Figure 6.9: TEM image of nanoclay-filled TPE based on (a) P1/EPDM (40/60).

The rubber phase is white in color, the silicate layers appear as black lines in the darker polypropylene phase. In TEM image illustrated in Figure 6.9-b for the TPE nanocomposite based on P3/EPDM (40/60), the silicate layers were found to be partly agglomerated at interfacial boundary between the polypropylene and rubber phases and partly dispersed into the EPDM phase.

(b)

Figure 6.9: TEM image of nanoclay-filled TPE based on (b) P3/EPDM (40/60).

Both the rheological and mechanical properties of the samples are dependent on the morphology of the TPE nanocomposites as discussed below. Figure 6.10 plots the elastic modulus and the complex viscosity dependence as a function of angular frequency in the nanocomposites prepared with different viscosities of PP containing 40 wt % of the rubber and their matrix at 220 ^{o}C and strain amplitude of 0.5 %.

Several trends in Fig. 6.10 (a) should be noted. Firstly, the storage modulus of the TPE nanocomposite prepared with low viscosity PP tends to a plateau beginning at low shear rates. Secondly, a dramatic increase in the storage modulus (G′) of the blend based on LVP is observed over its matrix.

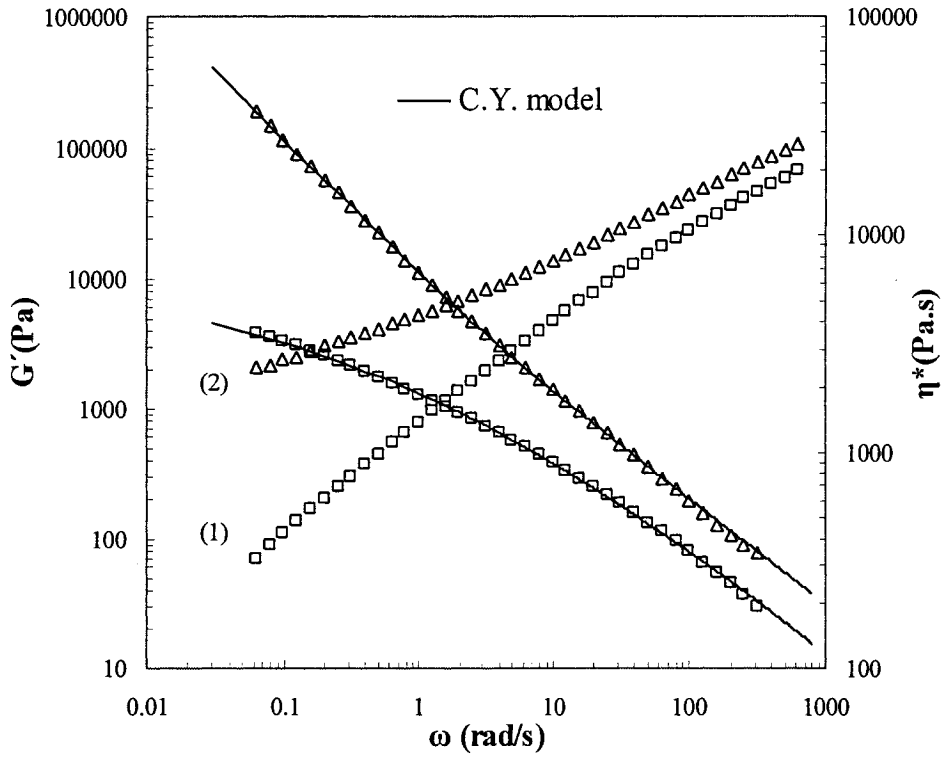

Figure 6.10 (a): Storage modulus and complex viscosity as a function of frequency in TPE based on (1) unfilled P1/EPDM (60/40), and (2) nanoclay-filled P1/EPDM (60/40).

It is also observed from Figures 6.10 (a) and 6.10 (c) that at 1 rad/s, the G′ of the nanoclay-filled blend prepared from LVP is 669 % higher than that of its equivalent matrix, however, in the nanoclay-loaded sample with HVP, it is 232 % higher that it's pristine matrix.

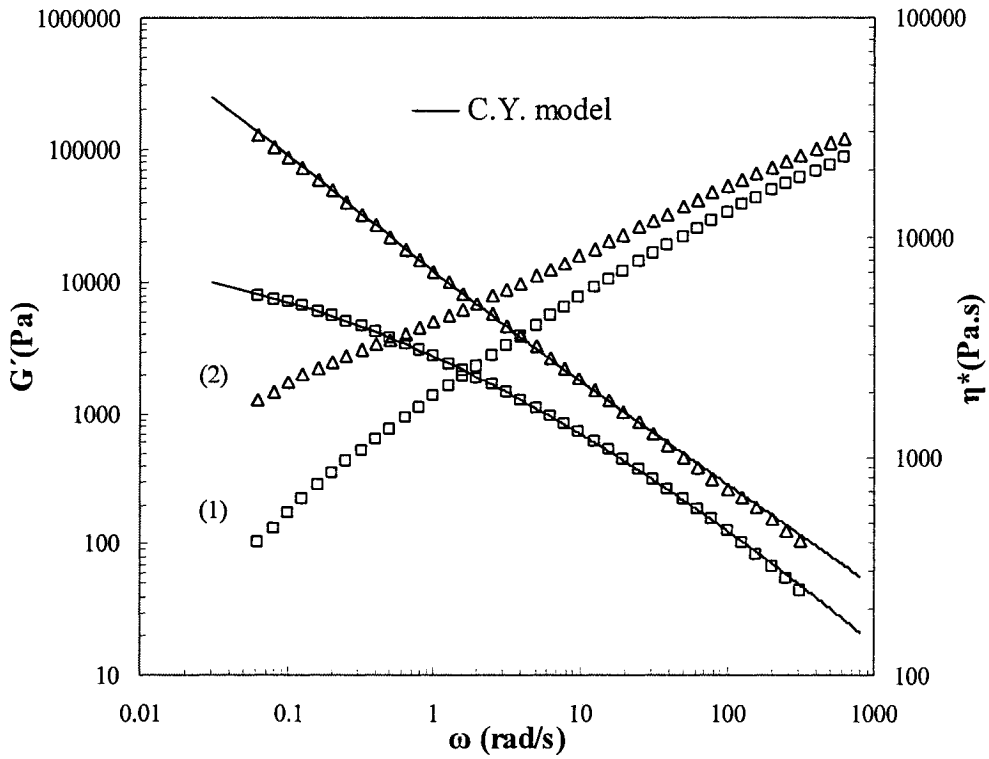

Figure 6.10 (b): Storage modulus and complex viscosity as a function of frequency in TPE based on (1) unfilled P2/EPDM (60/40), and (2) nanoclay-filled P2/EPDM (60/40).

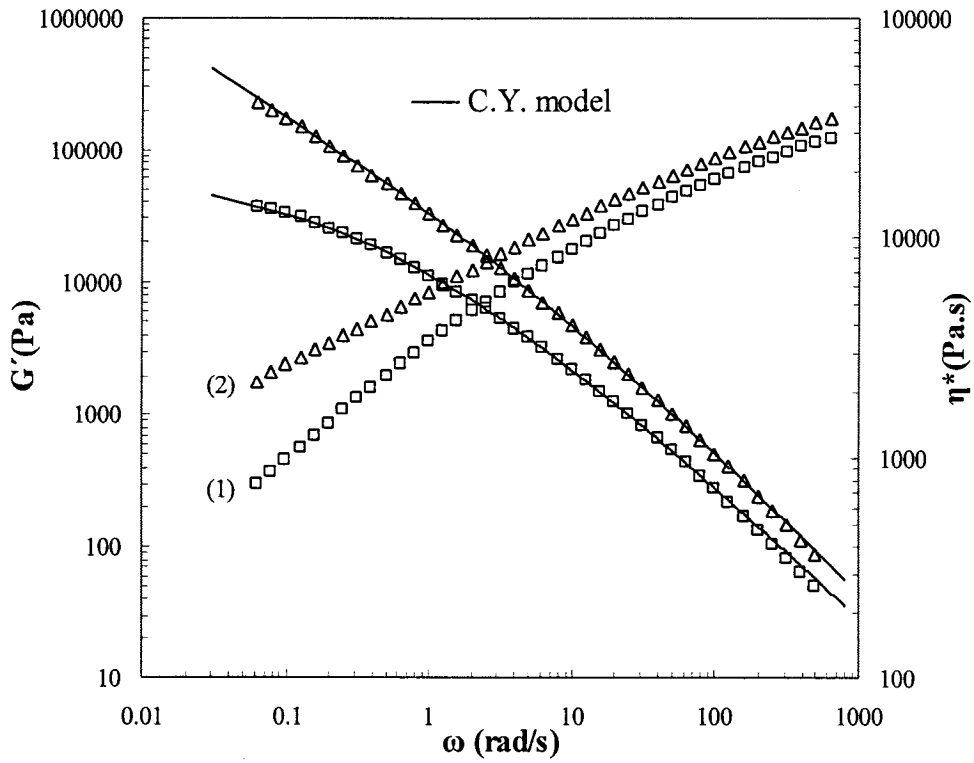

Figure 6.10 (c): Storage modulus and complex viscosity as a function of frequency in TPE based on (1) unfilled P3/EPDM (60/40), and (2) nanoclay-filled P3/EPDM (60/40).

Table 6.2 reports the terminal zone slopes of the samples containing 40 % EPDM which were calculated at low ω region. The non-terminal behavior of the blends was significantly smaller than 2. In addition, a gradual reduction was obtained in the power-law dependence of the storage modulus with decreasing the viscosity of the

polypropylene phase in the TPE nanocomposites as shown in Table 6.2. The terminal zone slope of the storage modulus (G′) is two ($G' \alpha \omega^2$) for typical bulk polymers [22].

Table 6.2: Terminal slopes of G′ versus ω and viscosity of TPEs and their nanocomposites at 220 °C

Sample PP/EPDM (60/40)	G′ (Pa)	Complex viscosity (at 1 rad/s) (Pa.s)
P1/EPDM	0.635	1858
Nano (P1/EPDM)	0.272	6723
P2/EPDM	0.6	2882
Nano (P2/EPDM)	0.333	7073
P3/EPDM	0.589	6722
Nano (P3/EPDM)	0.394	11380

Similar trends are observed in the complex viscosity of these nanocomposites, as presented in Figure 10. The non-terminal flow behavior of the TPE nanocomposites at low frequency is comparable to those reported for the block copolymer, highly concentrated particulate composites, and smectic liquid-crystalline small molecules exhibiting a yield stress [22, 23]. A Carreau-Yasuda (C.Y.) model [12, 24] with a yield stress can be used to describe the behavior of the TPE nanocomposites as follows:

$$\eta_{(s)}(\omega) = \frac{\sigma_0}{\omega} + \eta_0[1 + (\lambda\omega)^a]^{(m-1)/a} \quad \text{.....(6.1)}$$

Where σ_0 is the yield stress, η_0 is the zero shear viscosity, λ is the time constant, a is the Yasuda parameter and m is the dimensionless power law index.

Figure 6.11 shows the increased yield stress [obtained by Eq. (6.1)] for samples prepared with different viscosities of polypropylene having 20, 40 and 60 % EPDM.

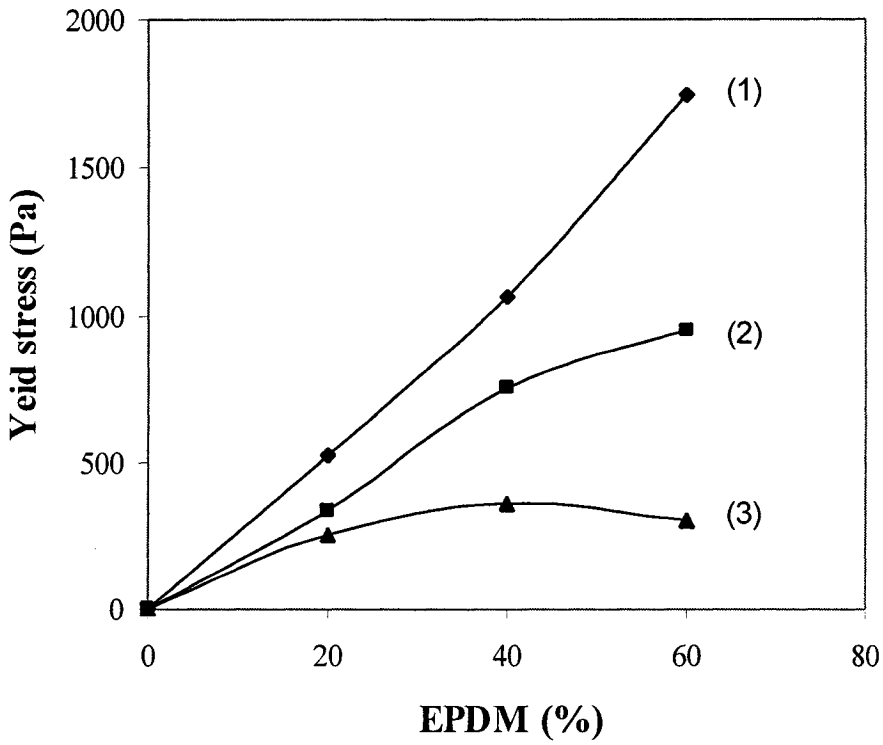

Figure 6.11: Yield stress obtained by Eq. (6.1) in TPE nanocomposites based on (1) P1, (2) P2 and (P3).

One can see that the yield stress in the samples prepared with low-viscous PP is higher than that of the medium and high viscosity PP samples. These results can be attributed to higher interaction between the nanoclay and the LVP matrix (better dispersion) as well as smaller rubber particles with higher specific surface area in the TPE nanocomposites based on LVP compared with the samples prepared from MVP and HVP. These rheological results are in accordance with the XRD peaks and the morphological features of the samples.

In further characterization of these materials, the mechanical properties for the TPEs and their nanocomposites have been obtained. Figure 6.12 shows the tensile modulus of the unfilled blends prepared with low viscosity PP having 20, 40 and 60 % EPDM and their nanocomposites.

It is observed that the tensile modulus of the nanoclay-reinforced TPE samples improved in all compositions compared with similar but unfilled blends. There is an inverse relation between the tensile modulus and the EPDM content in the samples. This is due to the fact that the semicrystalline polypropylene content decreases and also the dispersed rubber particle size increases when the EPDM concentration is increased [25].

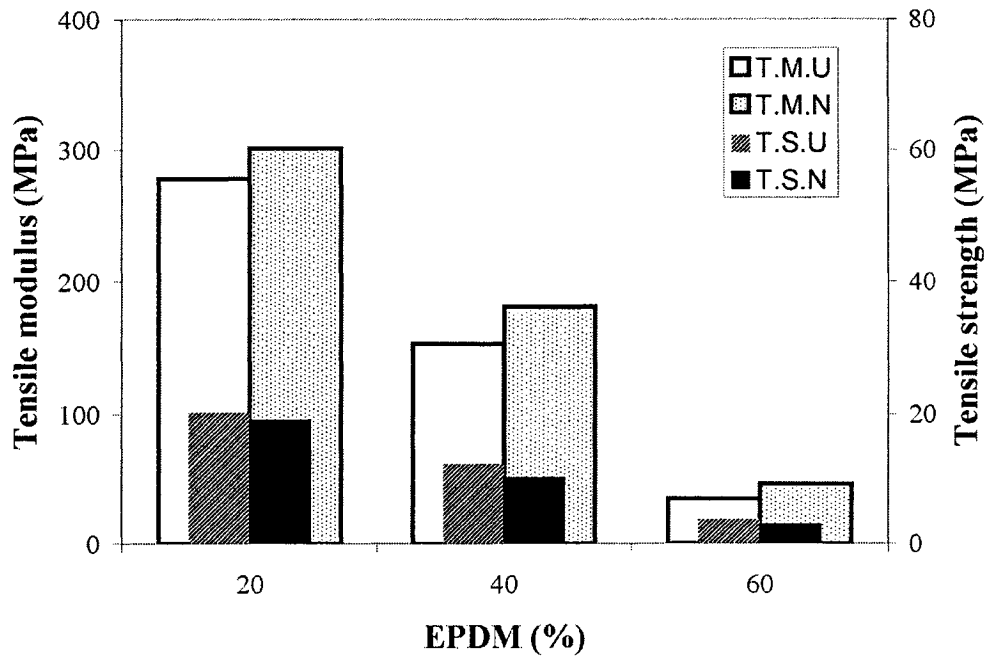

Figure 6.12: Tensile strength and modulus of TPEs and their nanocomposites based on P1, (Tensile Modulus =T.M., Tensile Strength=T.S, Unfilled=U, Nano=N).

Table 6.3 show the effect of different viscosities of the polypropylene phase on the tensile strength and modulus of the TPE nanocomposites prepared with 3 wt % of the clay containing different contents of EPDM rubber. The reported mechanical properties are an average of 5 measurements. The mechanical properties were consistent with the morphological structure observed by the SEM and TEM. As reported in Table 6.3, the tensile properties of the unfilled blends containing 20, 40, and

60 % rubber increased with increasing the viscosity of the polypropylene phase. This is attributed to smaller rubber droplets size with higher specific surface area in the unloaded TPEs prepared from HVP in comparison with the samples having MVP, and LVP [26].

The tensile modulus of the blends increased with the introduction of the clay. The most significant increase in the tensile modulus is obtained for the TPE nanocomposite prepared with low-viscous PP. The nanoclay-reinforced sample prepared with LVP having 60 % EPDM presented the highest percent increase in the tensile modulus.

Table 6.3 also shows the effect of the clay on the tensile strength of the TPE nanocomposites. In the PP/EPDM blends having low, medium and high viscous-PP, the tensile strength decreased with the introduction of the clay. With the addition of the particulate fillers, the tensile strength of plastics generally decreases at lower concentration [27].

Table 6.3: Mechanical properties of PP/EPDM blends and their nanocomposites

EPDM /PP	Properties	P1		P2		P3	
		TPE	nano-TPE	TPE	nano-TPE	TPE	nano-TPE
20/80	T. M.	278	301.4 (8%)	291	311.2 (7%)	317.5	337 (6%)
	T. S.	20.2	19.5	24.9	23.8	27.3	26
40/60	T. M.	153	180.5(18%)	160	179(12%)	172	184(7%)
	T. S.	12.3	11.9	13.5	13.6	14.5	13.7
60/40	T. M.	35	46.5 (32%)	36	42.5(18%)	38.1	40 (5%)
	T. S.	3.8	3.1	4	4.1	4.5	4.5

6.4 Conclusion

We examined the morphological, rheological and mechanical properties of the nanoclay-reinforced thermoplastic elastomers (TPE nanocomposites) prepared with different viscosities of polypropylene at 20, 40 and 60 % EPDM and compared with similar but unfilled blends.

X-ray results and TEM image showed an intercalated structure in the TPE nanocomposites. The microstructure of the nanoclay-reinforced PP/EPDM blends was affected by the distribution state of the clay between the two phases.

The size of the dispersed rubber particles was shown to be larger for the nanoclay-filled blends prepared with HVP at 40 and 60 % EPDM in comparison with similar unfilled samples.

The yield stress of the TPE nanocomposites based on LVP increased more than that of the TPE hybrids prepared with HVP. The increase in the storage modulus and the decrease in the terminal zone slope of the melt storage modulus were found to be larger for the LVP nanocomposites in comparison with the HVP sample.

Mechanical properties were consistent with the microstructure observed by SEM and TEM in the TPE hybrids. The tensile modulus improved in all TPE nanocomposites and obtained higher percent increase in the case of LVP samples.

Acknowledgments

This research was supported by the Natural Sciences and Engineering Research Council of Canada (NSERC). The authors acknowledge the generous assistance given by Bayer and Eastman Chemical Products companies in connection with the supply of materials used in this research.

References

1- A.Y. Coran, in ''Thermoplastic Elastomers, '' N. R. Legge, G, Holden, H. E. Schroeder, Eds., Hanser Publishers, New York, 1987.

2- B. Bucknall, Toughened Plastics, Applied Science Publisher,London, 1977.

3- A. Y. Coran and R. P. Patel, *Rubber Chem. Technol.*, **54**, 116, (1982).

4- G. N. Avgeropoulos and F. C. Weisser, *Rubber Chem. Technol.*, **49**, 93, (1976).

5- Wu, s., *Polym. Eng. Sci.*, **27,** 241, (1987).

6- Karges-Kocsis, K., Csikai, I., *Polym. Eng. Sci.*, **27,** 241, (1987).

7- S. Wu, Polymer **27**, 335, (1987).

8- Darrell M., and Krishnamurthy, J., *Ind. Eng. Chem. Res.*, **41**, 6402, (2002).

9- S. Hambir, N. Bulakh and P. Jog, *Polym. Eng. Sci.*, **42,** 1800, (2002).

10- K. Kyu-nam, K. Hyungsu and L. Jae-wook, *Polym. Eng. Sci.*, **41**, 1963, (2001).

11- P. Svoboda, C. Zeng, H. wang, L. J. Lee, D. L. Tomasko, *J. Appl. Polym. Sci.*, **85**, 1562, (2002).

12- *lertwimolnun, W., Vergnes, B.,*: *Polymer* **46**, p. 3462, (2005)

13- Konstantinos, G., Jozsef K., *Polymer,* **46**, 3069, (2005).

14- K.Y. Lee, L. A. Goettler, *Polym. Eng. Sci.*, **44,** 1103, (2004).

15- S. Mehta, F. M. Mirabella, K. Rufener, A. Bafna, *J. Appl. Polym. Sci.,* **92,** 928, (2004).

16- J.K. Mishra, K.J. Hwang, C.S. Ha, *Polymer*, **46**, 1995, (2005).

17- Shuster, R. H., *Rubber Chem Technol.*, **69**, 5, (1996).

18- Bazgir, S., Katbab, A.A., Nazockdast, H. *Rubber Chem Technol.* **77**, 176, (2004).

19- RA.Vaia, DP. Giannelis, Macromolecules, **30**, 8000, (1997).

20- O. Chung, A.Y. Coran, *Rubber Chem Technol.,* **70**, 5, 781, (1997).

21- F. Goharpay, A.A. Katbab, H. Nazokdast, *J. Appl. Polym. Sci.,* **81**, 2531, (2001)

22- Gu S., Ren J., Wang Q.,: *J. Appl. Polym. Sci.,* **91**, 2427, (2004).

23- Rosedale, J. H., Bates, F.S., *Macromolecules,* **23**, 2329, (1990).

24- Berzin, F., Vergnes, B., Delamare, L.,: *J. Appl. Polym. Sci.* **80**, p. 1243 (2001)

25- Katbab A., Nazockdast H., Bazgir S., *J. Appl. Polym. Sci*, **75**, 1127, (2000).

26- Goharpey, F., Katbab, A. A., Nazockdast, H., *Rubber Chem. Tech.* 76, 1, 239, (2003).

27- Nassar N., Utracki L. A., Kamal M. R., *Intern. Polym. Process*, **4**, 423, (2005).

CHAPTER 7

SUMMARY AND RECOMMENDATIONS

7.1 CONCLUSIONS AND DISCUSSIONS

Dynamically vulcanized nanocomposite thermoplastic elastomers (TPV nanocomposites) were prepared by a three-step melt mixing process containing different viscosities of PP and EPDM at different contents of the clay. The effects of matrix viscosity and composition on the morphology, rheology and mechanical properties of the uncured nanocomposite blends (TPE nanocomposites) prepared using a one-step melt mixing process are studied as well.

The TPV nanocomposites show higher steady state value of the mixing torque in comparison with similar but unloaded TPVs prepared with PPMA. The increased torque value is an indirect evidence of strong interaction between the TPV matrix and the nanoclay. The X-ray diffraction peaks corresponding to the (001) plane of the clay in the TPV nanocomposites prepared based on PP/EPDM (40/60) with different viscosities of PP shift toward lower angles in comparison with the original clay. It was also observed that the intensity of the XRD peaks significantly decreases compared with Cloisite 15A. This is explained due to the fact that the dynamic vulcanization of EPDM phase increases the viscosity of the blend and hence the shear stress imposed by the matrix during the mixing increases, which in turn facilitate the break-up process of

the clay agglomerates. The first characteristic peak of the organo-clay disappears for the TPV nanocomposites containing different viscosities of PP and 60 % EPDM when post processing is applied to these samples. The absence of the diffraction peak suggests that the compression molding process could contribute to the further exfoliation of the silicate layers in the TPV nanocomposites. The silicate layers disperse throughout the polypropylene phase before the vulcanization of the rubber phase in the TPV nanocomposites prepared from low viscosity PP (LVP) and can not penetrate into the EPDM phase during the mixing process. This is due to the initial placement of the clay in the polypropylene phase (selectively reinforced plastic phase in the TPV nanocomposites). In the uncured TPV nanocomposites having high viscosity PP (HVP), the clay partly disperses in the continuous phase and partly agglomerates at interfacial boundary between the polypropylene and the rubber phases. It is found that the microstructure of the TPV nanocomposites is sensitive to the viscosity ratio of the two phases (PP and EPDM) and the clay content. The clay is nearly exfoliated and randomly distributed into the PP matrix of the TPV sample prepared with LVP at 60 % rubber and 2 wt % of the clay. The rubber particles disperse into the plastic matrix in form of aggregate and their size increases with the introduction of the clay in the TPV materials prepared from 60 % EPDM. The increase in the rubber particle size of the TPV nanocomposites is explained by the modified rheology of the nanocomposites. It is accepted that the size of the dispersed rubber phase in unfilled TPV materials based on PP/EPDM (without clay) depends on the viscosity ratio and interfacial interactions between the two phases. In the case of the TPV nanocomposites, the clay plays an

important role to determine the morphology of the samples. Initially, the clay can not penetrate into the rubber phase but after adding accelerators such as TMTD, the rubber phase become more polar. Therefore, it is possible that some clay goes to the EPDM phase before the completion of the curing cycle. This changes the viscosity ratio between the two phases, and consequently, the size of the rubber phase increases. The tensile modulus of the TPV nanocomposites having 60 % rubber significantly improves from 20 to 90 % depending on the organo-clay concentration and the viscosity difference between PP and EPDM phases. The exfoliation of 2 wt % Cloisite 15A in the low viscosity PP based TPV nanocomposite having 60 % rubber increased the tension modulus by 92 %, while the similar addition of 2 wt % the clay to the TPV based on high viscosity PP resulted in only a 23 % increase in tension modulus over the unfilled TPV. This would tend to confirm that the clay dispersion and exfoliation is better achieved in the former composition. The exfoliated structure of the TPV nanocomposites resulted in reduction of the degree of crystallinity and increase of the polymer crystallization temperature because the dispersed silicate layers act as nucleating agents. The oxygen permeability of the TPV hybrids based on PP/EPDM (40/60) and 2 wt % of the clay decreases by as much as 20 % as compared with the pristine TPV.

It is found that the interlayer distance of the clay in PP nanocomposites prepared with different viscosities of polypropylene at 2 wt % clay (without PPMA as compatibilizer) decreases compared with the pristine clay (Cloisite 15A). This indicates that the polypropylenes can not penetrate into the interlayer of the organo-clay, even

when modified by a dimethyl dehydrogenated tallow quaternary ammonium at the shear stress imposed by the matrix. However, the interlayer distance of the clay increases in the TPV nanocomposite prepared from the same PP, but without PPMA, and containing 20, 40 or 60 % EPDM. The polypropylene nanocomposites prepared without PPMA at 2 % clay demonstrate the storage modulus curves very close to the corresponding matrix storage modulus curves. But, the storage modulus curves of the TPV nanocomposites without PPMA at 2 wt % of the clay significantly increase in comparison with those of the equivalent matrix. As already mentioned, the dynamic vulcanization of the rubber phase increased the shear stress imposed by the matrix which in turn facilitates the break-up process of the clay agglomerates resulting in strong interaction between the clay and the TPV matrix. The dispersion of the clay improved with introduction of PPMA in the PP nanocomposites. A dramatic increase in the storage modulus curve with the onset of a plateau at a low frequency observes in the PP nanocomposite prepared from LVP and PPMA at 2 % clay compared with similar but unfilled matrix. In contrary, the PP hybride based on HVP and 2 % clay with PPMA show a storage modulus curve similar to the equivalent matrix. This is for the reason that the LVP can more readily penetrate between the silicate layers in comparison with the HVP. Therefore, the PP-nanoclay interaction in the polypropylene nanocomposite prepared from LVP is stronger than that for the hybrid based on HVP. It is found that the yield stress of the PP nanocomposites at 2 % clay increases as the viscosity of the matrix is decreased. On the other hand, the yield stress of the PP hybrids increases when the interlayer distance of the clay is increased in the samples. It

is also found that the intensity of the XRD peaks in the TPV samples prepared with PPMA decreases in comparison with the similar TPV hybrids prepared without PPMA. This is due to the fact that the compatibilizer (PPMA) can improve the dispersion of the clay through the matrix of the TPV samples. The intensity of the X-ray diffraction peaks decreases when the rubber concentration is increased in the TPV nanocomposites. The decrease in the intensity of the XRD peaks is attributed to the increase of the shear stress imposed by the matrix phase leading to break-up the agglomeration of the clay particles. Therefore, the dispersion of the silicate layers in the polypropylene phase of the TPV samples increases as the EPDM content is increased. It is observed that the TPV nanocomposites exhibit strong elastic modulus that tends to become increasingly independent of frequency (plateau) at low shear rates with the highest extent for the sample containing 60 % of the EPDM. The yield stress of the TPV nanocomposites remarkably increases when the rubber content is increased. This is attributed to the strong interfacial interaction between the clay and the nanocomposite matrix as well as the existence of the physical three-dimensional network structure formed between the cured rubber particles. SEM results evidenced that the rubber particle agglomeration increased by the increased rubber aggregate size resulting from the increased rubber content in the TPV samples. The yield stress of the TPV nanocomposite prepared based on low viscosity PP increases more than that of the similar hybrids prepared from medium and high viscosity PP. These results are explained due to the fact that the nanoclay dispersion and exfoliation is better achieved in the TPV nanocomposites prepared based on LVP. The melt linear viscoelastic

properties of the TPV nanocomposites are described by a Carreau-Yasuda law with a yield stress and also a linear viscoelastic model (modified Palierne model), tacking into account the maximum packing volume (ϕ_m). There is a considerable agreement between the results of the experimental data and the modified model for the TPV nanocomposite at 60 % EPDM with ϕ_m = 0.64. However, in the TPV nanocomposites at 40 and 20 % EPDM, a better fit (between experimental and model) is obtained with ϕ_m = 0.59 and ϕ_m = 0.5 respectively. The decrease in the maximum packing volume in the TPV nanocomposites can be explained by the fact that the dispersion degree of the clay decreases in the TPV nanocomposites when the rubber content is decreased. On the other hand, the silicate agglomeration considerably decreases with increasing the rubber content in the TPV nanocomposites.

It is found that the uncured thermoplastic elastomers (TPE nanocomposites) prepared by a one-step melt mixing process containing 20, 40, and 60 % EPDM and 3 wt % of clay show an intercalated structure. In the TPE nanocomposites having LVP and 3 % clay, the intensity of the XRD peaks increases when the rubber concentration is increased. These results are due to the fact that the clay tends to disperse into the low viscosity phase (polypropylene (P1)) in the TPE samples (20, 40 and 60 % EPDM). As the P1 is a low-viscous material compared with EPDM; consequently, the silicate layers stay in the LVP phase and can not penetrate into the rubber phase during mixing process. On the other hand the clay concentration increases in the polypropylene phase of the TPE nanocomposite when EPDM content is increased. It was found that the

interlayer spacing of the clay in the TPE samples decreases with increasing the rubber content. The intensity of the XRD peaks is almost similar in shape for the uncured blends prepared from medium viscosity polypropylene (MVP) and 20, 40, 60 % EPDM at 3 % clay. This similarity in the XRD patterns is for the reason that the silicate layers disperse in the PP phase but some clay diffuses into the EPDM phase with increasing the rubber content. In TPE nanocomposites prepared using high viscosity PP (HVP) and 20, 40, 60 % EPDM at 3 % clay, similar trends are observed for the peak position of the XRD diffraction patterns, however, the intensity of the peaks decreases as the rubber content is increased. We can say that the clay disperses into both the PP and the EPDM phases and that the clay concentration would increase in the rubber phase with increasing the elastomer content. The decrease in the intensity of the XRD peaks for the HVP samples can be attributed to the increase of the shear stress imposed by the EPDM phase which in turn facilitates the break-up process of the clay agglomerates in the rubber phase. Therefore, we can say that the concentration of the clay in the rubber phase of the high viscosity PP samples is more than in the TPE nanocomposite prepared with MVP. In the unfilled blends prepared based on PP/EPDM (80/20, 60/40, 40/60), the size of the EPDM droplets decreases when the viscosity of PP phase is increased. In fact, the dispersed rubber particle size decreases as the viscosity difference between the rubber and plastic is decreased. Moreover, in the unfilled blends prepared with different viscosities of PP, the size of the rubber droplets increases when the rubber content is increased. This shows the significant role of the coalescence in increasing the dispersed rubber droplet size as a result of increasing the rubber content.

The blend based on LVP/EPDM (60/40) at 3 % clay exhibits a reduction in the size of the rubber particles compared with the similar but unfilled blend. The reduction in the elastomer particle size is related to the increase of the melt viscosity of the blend. The unloaded-LVP based sample prepared with 60 % EPDM shows a random co-continuous morphology, however, a dispersed rubber droplet type of morphology is obtained in the nanoclay-filled sample counterpart. In the nanocomposite prepared based on HVP/EPDM (60/40) and 3 % clay, the dispersed rubber droplets become larger in size and more elongated by nanoclay compared with the equivalent unloaded blend. This is attributed to the existence of the clay in the elastomer phase which leads to increase the viscosity difference between the two phases and hence the formation of large rubber droplet. The rubber particles are dispersed into the plastic matrix in the unloaded blend based on HVP/EPDM (40/60). However, the size of the rubber particles increases with the introduction of the clay in the TPE nanocomposites prepared from HVP and 60 % EPDM. We conclude that the distribution state of the clay between the two phases and also the rubber particle size of the TPE samples strongly depend on the viscosity ratio of the PP to EPDM. The storage modulus (G′) of the TPE nanocomposite prepared with LVP containing 40 % rubber at 3 % clay shows a plateau beginning at low shear rates. The G′ of the filled LVP based blend at 1 rad/s is 669 % higher than that of the equivalent matrix, however, in the loaded HVP based sample, it is 232 % greater than it's pristine. The terminal zone slopes of the storage modulus curve in the TPE samples prepared with 40 % rubber and different viscosities of PP, at 3 % clay are measured. A gradual reduction is obtained in the power-law dependence of

the storage modulus with decreasing the viscosity of the polypropylene phase in the TPE nanocomposites. The yield stress in the hybrid prepared with low-viscous PP and 3 % clay is higher than that of the medium and high viscosity PP sample counterpart. These results are attributed to stronger interaction between the nanoclay and the matrix as well as smaller rubber particle size with higher specific surface area in the TPE nanocomposite based on LVP in comparison with the equivalent samples prepared with MVP and HVP. The mechanical properties of the TPE hybrids are consonant with the morphological features observed by SEM and TEM. There is an inverse relation between the tensile modulus and EPDM content in the samples. This is due to the fact that the semicrystalline polypropylene decreases and the dispersed rubber particle size increases when the EPDM concentration is increased. The tensile properties of the non-reinforced blends increase as the viscosity of the polypropylene phase is increased. The tensile modulus of the nanoclay-reinforced samples improves in comparison with the similar but unfilled blends. The most significant increase in the tensile modulus is for the nanocomposite prepared with low-viscous PP. The nanoclay-reinforced sample having 60 % EPDM prepared with LVP at 3 % clay presents the highest percent increase in the tensile modulus. In the uncured PP/EPDM blends having low, medium and high viscous-PP, the tensile strength decreases with introduction of the clay.

7.2 RECOMMENDATIONS

We suggest the following recommendations for future works.

1- Preparation and characterization of the TPV and TPE nanocomposites based on PP/EPDM by using a twin screw extruder (TSE).

2- The effect of elongational flow mixer (EFM) on the microstructure and the mechanical properties of the nanocomposites.

3- The influence of molecular weight and percentage of maleic anhydride (MA %) of the compatibilizer (PPMA) on microstructure, rheology, and mechanical properties of the nanocomposites.

4- The effect of different kinds of clay and compatibilizer on the final state and rate of cure in the TPV nanocomposites prepared with selectively reinforced rubber phase.

5- Comparative studies of the microstructure, rheological behavior, and mechanical properties between dynamically vulcanized nanocomposites prepared by a one-step and a three-step melt mixing process in TSE.

REFERENCES

Abdou-Sabet S., Fath M.A., (1982). Thermoplastic elastomer blends of olefin rubber and polyolefin resin. *U.S. Patent* 4, 311, 628

Abdou-Sabet, S., Patel, R. P., (1991). Morphology of elastomeric alloys, *Rubber Chem. Tech*, 64, 769

Abdou-Sabet S., Puydak R.C., rader C.P. (1996). Dynamically vulcanized thermoplastic elastomers. *Rubber Chem. Tech*, 69, 3, 476

Abdou-Sabet S., Datta S., (2000). Thermoplastic Vulcanizates, in '*Polymer Blends*' edited by Paul D.R. Bucknal C.B. John Wiley, sons Inc., Vol. 2: Performance, Ch. 35, 517

Acharya H., Pramanik M., Srivastava S.K., Bhowmick, (2004). Synthesis and evaluation of high-performance ethylene propylene diene terpolymer organoclay nanoscale composites, *J. Appl. Polym. Sci.*, 93, 2429

Ahmadi S.J., Huang Y., Li W., (2005). Fabrication and physical properties of EPDM organoclay nanocomposites, *Composites Sci. Tech.*, 65, 1069

Ajayan P. M., Schadler L. S., Braun P. V., (2003). Nanocomposite science and technology, Weinheim Wiley, pp.77

Alexandre, M., Dubois, P., Sun, T., Graces, JM. Jerome, R. (2002). Polyethylene-layered silicate nanocomposites prepared by the polymerization-filling technique: synthesis and mechanical properties, *Polymer*, 43, 2123

Alexandre M., Dubois, P. (2000). Polymer-layered silicate nanocomposites: Preparation, properties and uses of a new class of materials, *Mater. Sci. Eng.*, 28, 1

Anil K. J., Neeraj K. G., N agpal, A. K. (2000). Effect of dynamic cross-linking on melt rheological properties of PP/EPDM, *J. Appl. Polym. Sci.* 77, 1488

Aranda P., Ruiz-Hitzky E. (1992). Poly (ethylene oxide) silicate intercalation materials, *Chem. Mater.*, 4, 1395

Ashish L., Malcolm M., Girish G. (2002). In situ rheo x ray investigation of flow induced orientation in layered silicate syndiotactic PP nanocomposite melt, *J. Rheol.* 46, 1091

Avgeropoulos G. N., Weisser F. C., (1976). Heterogeneous blends of polymer, rheology and morphology, *Rubber Chem. Tech.*, 49, 93

Balakrishnan S., Start P.R., raghavan D., Hudson S.D., (2005). The influence of clay and elastomer concentration on the morphology and fracture energy of preformed acrylic rubber dispersed clay filled epoxy nanocomposites, *Polymer*, 46, 11255

Baranov A.O., Erina, N.A Medintseva, T.I. Kuptsov S.A., Prut, E.V. (2003). Interphase layer formation in iso-tactic polypropylene/ethylene-propylene rubber blends, *J. Appl. Polym. Sci.*, 89, 1, 249

Baranov A.O., Erina, N.A Medintseva, T.I. Kuptsov S.A., Prut, E.V. (2001). The influence of the Interphase layer on the properties of iso-tactic polypropylene ethylene propylene rubber blends, *Polym. Sci.* 43, 11, 1177

Bazgir S., Katbab A.A., Nazockdast H., (2003). Microstructure-properties correlation in silica-reinforced dynamically vulcanized EPDM/PP thermoplastic elastomers, *Rubber Chem. Tech.*, 76, 176

Bazgir S.,Katbab A.A., Nazockdast H., (2004). Silica-reinforced dynamically vulcanized ethylene-propylene-propylene-diene monomer/polypropylene thermoplastic elastomer, morphology, rheology and dynamic mechanical properties, *J. Appl. Polym. Sci.*, 92, 2000

Berzin F., Vergnes B., Delamare L., (2001). Rheological behavior of controlled-rheology polypropylenes obtained by peroxide-promoted degradation during extrusion: comparison between homo-polymer and copolymer, *J. Appl. Polym. Sci.*, 80, 1243

Bhowmick A.K., Inoue T., (1993). Structure development during dynamic vulcanization of hydrogenation nitrile rubber/nylon blends, *J. Appl. Polym. Sci.*, 49, 11, 1893

Bories M., Huneault M.A., Lafleur P.G., (1999). Effect of twin screw extruder design and process conditions on ultrafine $Caco_3$ dispersion into PP, *Inter. Polym. Process.*, 3, 234

Bucknall B., (1977). Toughened plastics, Applied Science Publisher, London, 359 pp.

Carreau P. J., De Kee D., Chhabra R. P., (1997)., Rheology of polymeric systems: Principles and applications" Munich, Hanser Publishers,

Bureau M. N., Ton-That M.-T., Perrin-Sarazin F., (2003). Polyolefin nanocomposites, essential work of fracture analysis, *international symposium on polymer nanocomposites science and technology,* Boucherville, Quebec, Canada, October 6, 8

Chan C., Wu J., Li J., Cheung Y., (2002). Polypropylene calcium carbonate nanocomposites, *Polymer,* 43, 2981

Chang Y., Yang Y., Ryu S., nah C., (2002), Preparation and properties of EPDM organomontmorillonite hybrid nanocomposites, *Polym. Int.* , 51, 319

Chang S.H., Kim S., (1986). Structure and properties of dynamically cured EPDM-PP blends, *J. Appl. Polym. Sci.*, 32, 6281

Chung O., Coran A. Y., (1997). Morphology of rubber/plastic blends *Rubber. Chem. Tech.*, 70, 781

Chung O., Nadella H. P., (2001). Phase morphology and cure state characterization of soft thermoplastic vulcanizates (TPVs) by using atomic force microscopy, *ANTEC*, 2926

Chung O., Coran A. Y., White J.L. (1997). Melt rheology of dynamically vulcanized rubber plastic blends, *ANTEC,* 1997

Coran A.Y., Patel R. P. (1978).Thermoplastic vulcanizates of olefin rubber and polyolefin resin , *U.S. Patent 4,130,535*

Coran A. Y., Patel R., (1980). Rubber-thermoplastic compositions Part 1 EPDM-polypropylene thermoplastic vulcanizates, *Rubber chem. tech*, 53, 141

Coran A. Y., Patel, R. P. (1982). Rubber-thermoplastic compositions 5 selecting polymers for thermoplastic vulcanizates, *Rubber Chem. Tech.*, 55, 1,116

Coran A.Y., (1987). In ''Thermoplastic elastomers, '' N. R. Legge, G, Holden, H. E. Schroeder, Eds., Hanser Publishers, New York

Cox W.P., Merz E.H., (1958). Correlation of dynamic and steady flow viscosities. *J. Polym. Sci.,* 28, 619

Damour A., Salventat D., (1847). Et analyses sur un hydrosilicate d'alumine trouve a montmorillon, *Ann. Chim. Phys. Ser.* 21, 376

Danesi S., Porter R.S., (1978). Blends of iso-tactic polypropylene and ethylene propylene rubber: rheology, morphology, and mechanics, *Polymer*, 19, 448

Darrell M., Krishnamurthy J., (2002). Strategies for optimizing polypropylene-clay nanocomposite *Ind. Eng. Chem. Res.*, 41, 6402

Dennis H.R., Hunter D.L., Chang D., Kim S., White J.L., Cho J.W., Paul D.R. (2001). Effect of melt processing conditions on the extent of exfoliation in organoclay-based nanocomposites, *Polymer*, 42, 9513-9522

Fisher W. K., (1974). Dynamically partially cured thermoplastic blend of mono-olefin co-polymer rubber and polyolefin plastic, *U. S. Patent* 3,806,558, April 23

Fornes T.D., Yoon P., Kesskkula H., Paul, D.R. (2001). Nylon 6 nanocomposites: the effect of matrix molecular weight, *Polymer*, 42, 9929

Fortelny I., Kovar J., (1992). Effect of the composition and properties of components on the phase structure of polymer blends, *Eur. Polym. J.,* 28, 1, 85

Galgali G., Ramesh C., lele A., (2001)., A rheological study on the kinetics of hybride formation in polypropylene nanocomposites, *Macromolecules*, 34, 4, 852

Garces, J. Moll, D., Bicerano, J., Fibiger, R. (2000). Polymeric nanocomposites for automotive applications, *Adv Mater*, 12, 1835

Gessler A. M., Haslett W. H., Process for preparing a vulcanized blend of crystalline polypropylene and chlorinated butyl rubber (1962). *U.S. Patent* 3,037,954, June 5

Ghoreishy M.H.R., Razavi-Nouri M., Naderi, G. (2000). Finite element analysis of flow of thermoplastic elastomer melt through axisymmertric die with slip boundary condition, *Plastic Rubber and Comp.*, 29, 5, 224

Gianelli W., Ferrara G., Camino G., Pellegatti G., Rosenthal J., Trombini R.C., (2005). Effect of matrix feature on polypropylene layered silicate nanocomposites, *Polymer*, 46, 7037

Giannelis E.P., Krishnamoorti R., Manias E., (1999). Polymer silicate nanocomposites, *Adv. Polym. Sci.*, Vol. 138, 107

Goettler L.A., Richwine J.R., Wille F.J., (1982). The rheology and processing of olefin based thermoplastic vulcanizates, *Rubber Chem. Tech.*, 55, 1448

Goharpey F., Katbab A. A., Nazockdast H., (2001). Mechanism of morphology development in dynamically cured EPDM/PP I. state of cure, *J. Appl. Polym. Sci.*, vol. 81, 2531.

Goharpey F., Katbab A. A., Nazockdast H., (2003). Formation of rubber particle agglomerates during morphology development in dynamically crosslinked EPDM/PP thermoplastic elastomers, part 1: effect of processing and polymer structural parameters, *Rubber Chem. Tech.*, 76, 1, 239

Goharpey F., Katbab A.A., Nazockdast H., (2005). Relationship between the rheology and morphology of dynamically vulcanized thermoplastic elastomers based on EPDM/PP, *Polym. Eng. Sci.* 45, 84

Gonzalez-Montiel A., Keskkula H., Paul D. R., (1995). Morphology of nylon 6 polypropylene blends compatibilized with maleated polypropylene, *J. Polym. Sci. Part. Polym. Phys.*, 33, 1751

Gopakumar T.G., Lee J.A., Kontopoulou M., Parent J.s., (2002). Influence of clay exfoliation on the physical properties of montmorillonite/polyethylene composites, *Polymer*, 43, 5483

Gu S. Y., Ren J., Wang Q. F., (2004). Rheology of poly(propylene)/clay nanocomposites, *J. Appl. Polym. Sci.*, 91, 2427

Gupta A., kumar P., Ratnam B., (1991). Glass fiber reinforced polypropylene EPDM blend, melt rheological properties, *J. Appl. Polym. Sci.*, 42, 2611

Hambir S., Bulakh N., Jog P. (2002). Polypropylene/clay nanocomposites: Effect of compatibilizer on the thermal, crystallization and dynamic mechanical behavior, *Polym. Eng. Sci.*, 42, 1800

Han P. K., White J. L., (1995). Rheological studies of dynamically vulcanized and mechanical blends of polypropylene and ethylene-propylene rubber, *Rubber Chem. Tech.* 68, 5, 728

Hasegawa N., Okamoto H., Kawasumi M., Kato M., Tsukigase A., Usuki A. (2000). polyolefin clay hybrids based on modified polyolefin and organoclay, *Macromolecular Mater. Eng.*, 280, 281, 76

Hasegawa N., Usuki A., (2004). Silicate layer exfoliation in polyolefin clay nanocomposites based on maleic anhydride modified polypropylene and organophilic clay, *J. Appl. Polym. Sci.*, 93, 464

Hasegawa N., Okamoto H., Kawasumi M., Kato M., Tsukigase A., Usuki A., Preparation and mechanical properties of polypropylene-clay hybrids based on modified polypropylene and organophilic clay (2000). *J. Appl. Polym. Sci.,* 78, 11, 1918

Hasegawa N., Kawasumi M., kato M., Usuki A., Okada A., (1998). Preparation and mechanical properties of polypropylene-clay hybrids using a maleic anhydride-modified polypropylene oligomer, *J. Appl. Polym. Sci.,* 67, 1, 87

Hernandez-Luna A., Anne N. (2002). Creep and tensile behavior of polypropylene nanocomposite, ANTEC, 1461

Hua Z., Yong Z., zohglin P., Yinxi Z., (2004). A comparison between cure systems for EPDM/montmorillonite nanocomposites, 12, 3, 197

Jain A. K., Nagpal A. K., Singhal R., Gupta N. K., (2000). Effect of dynamic crosslinking on impact strength and other mechanical properties of PP/EPDM , *J. Appl. Polym. Sci.*, vol. 78, 2089

Jeon H., Jung, H. Hudson, (1998). Morphology of polymer/silicate nanocomposites: High density polyethylene and a nitrile copolymer, *Polym. Bulletin*, 41, 107

Jian L., Chixing Z., Wang G., (2003). Study on nonisothermal crystallization of maleic anhydride grafted polypropylene/montmorillonite nanocomposite, *Polym. Tes.,* 22, 2, 217

Jisheng M., Zongneng Q., Youliang H., (2001). Synthesis and characterization of polypropylene clay nanocomposites, *J. Appl. Polym. Sci.*, 82, 3611

Jisheng M., Zhang Z., Zongneng Q., Youliang H., (2002). Crystallization behaviors of polypropylene/montmorillonite nanocomposites *J. Appl. Polym. Sci.,* 83, 9, 1978-1985

Joubert C., Cassagnau P., Michel A., (2002). Influence of the processing conditions ona two phase reactive blend system, EVA/PP thermoplastic vulcanizate, *Polym. Eng. Sci.,* 42, 11, 2222

Kamal M., (2003). Melt processing of PA66/clay HDPE/clay and HDPE/PA66/clay, International symposium on polymer nanocomposites science and technology Boucherville, Quebec, Canada, October 6, 8

Kaempfer D., Thomann R., Mulhaupt R., (2002). Melt compounding of syndiotactic polypropylene nanocomposites containing organophilic layered silicates and in situ formed core/shell nanoparticles, *Polymer*, 43, 2909-16

Karges-Kocsis K., Csikai I., (1987). Skin-core morphology and failure of injection-molded specimens of impact-molded polypropylene blends, *Polym. Eng. Sci.,* 27, 4, 241

Karger-Kocsis A., Kallo A., Kuleznev V., (1984). Phase structure of impact-modified polypropylene blends, *polymer*, 25, 279

Katbab A.A., Nazockdast H., Bazgir H., (2000). Carbon black-reinforced dynamically cured EPDM/PP thermoplastic elastomers, I. morphology, rheology, and dynamic mechanical properties, *J. Appl. Polym. Sci.,* 75, 9, 1127

Kato M., Usuki A., Okada A., (1997). Synthesis of polypropylene oligomer-clay intercalation compounds, *J. Appl. Polym. Sci.* 66, 9, 1781

Kato M., Matsushita M., Fukumori K. (2003). Development of a new production method for a polypropylene clay nanocomposite, *international symposium on polymer nanocomposites science and technology,* Boucherville, Quebec, Canada, October 6, 8

Kawasumi M., Hasegawa N., Kato M., Usuki A., Okada, A. (1997). Preparation and mechanical properties of polypropylene-clay hybrids, *Macromolecules*, 30, 20, 6333-6338

Kim Y., Cho W., Ha C. Kim W., (1995). The control of miscibility of PP-EPDM blends by adding ionomer and applying dynamic vulcanization, *Polym. Eng. Sci.*, 35, 20, 1592

Kim K., Kim H., Lee (2001). Effect of interlayer structure, matrix viscosity and composition of a functionalized polymer on the phase structure of polypropylene-montmorillonite nanocomposites, J., *Polym. Eng. Sci.*, 41, 1963

Kodgire P., Kalgaonkar R., Hambir S., Bulakh N., Jog J. (2001). PP/clay nanocomposites: effect of clay treatment on morphology and dynamical properties, *J. Appl. Polym. Sci.* , 81, 1786

Kolarik J., (1992). Ternary composites of polypropylene elastomer calcium carbonate, effect of functionalized components on phase structure and mechanical properties, *Polymer*, 33, 4961

Konstantinos G., Jozsef K., (2005). Effects of primary and quaternary amine intercalants on the organoclay dispersion in a sulfur-cured EPDM rubber, *Polymer,* 46, 9, 3069

Konstantinos G.G., Thomann R., Karger-kocsis J., (2004). Characteristics of ethylene propylene diene monomer rubber-organoclay nanocomposites resulting from different processing conditions and formulations, *Polym. Int.* 53, 1191

Kornmann X. (2000). Synthesis and characterization of thermoset-clay nanocomposites, Lulea University of technology, Sweden

Kresge E.N., (1978). in "Polymer blend," Paul D.R., Newman S., Eds., academic press, New York, Vol. 2, Ch. 20

Krulis Z., Fortelny I., (1997). Effect of dynamic crosslinking on rheological properties of molten polypropylene ethylene propylene elastomer blends, *Eur. Polym. J.,* 33, 4, 513

Kresge E.N., (1990). Polyolefin thermoplastic elastomer blends, *Rubber Chem. Tech.* 64, 469

Lan T., Kaviratna P. D., Pinnavaia T. J., (1995). Mechanism of clay tactoid exfoliation in epoxy-clay nanocomposites, *Chem. Mater.*, 7, 2144

Laokijcharoen P., Coran A.Y., (1998). The evaluation of morphology in NR/HDPE blends part I. microscopy for unvulcanized blends, *Rubber Chem. Tech.*, 71, 5, 966

Larson R.G., Winey K.I., Patel S.S., Watanabe H., Bruinsman R., (1993). *Rheol Acta,* 32, 245

Le H.H., Lupke T., Pham T., Radush H.J., (2003). Time dependent deformation behavior of thermoplastic elastomers, *Polymer*, 44, 4589

Lee K. Y. Goettler L. A., (2004). Structure-property relationship in polymer blend nanocomposite, *Polym. Eng. Sci.*, 44, 6, 1103

Lee Y. L., Goettler L. A., (2004). Synthesis and properties of polymer blend nanocomposites, *ANTEC*, 1709

Lee H. L., Fasulo P. D., Rodgers W. R., paul D. R., (2004). Properties and morphology of TPO-based nanocomposites, *ANTEC*, 1513

Lertwimolnun W., Vergnes B., (2005). Influence of compatibilizer and processing conditions on the dispersion of nanoclay in a polypropylene matrix, *Polymer,* 46, 3462

Lertwimolnun W., Vergnes B., (2006). Effect of processing conditions on the formation of polypropylene organoclay nanocomposites in a twin screw extruder, *Polym. Eng. Sci.*, 46, 314

Li J., Chixing Z., Wang G., Yu W., Tao Y., (2003). Preparation and linear rheological behavior of polypropylene/MMT nanocomposites, *Polymer Composites,* 24, 3, 323-331

Li J., Ma P. L., Favis B. D., (2002). The role of the blend interface type on morphology in co-continuous polymer blends, *Macromolecules,* 35, 2005

Li J., Ton-That M.T., Tsai S.J., (2005). PP based nanocomposites with various intercalants types and intercalants coverage, *International symposium on polymer nanocomposites science and technology*, Boucherville, Quebec, Canada, 28

Li J., Zhou C., Wang G., Zhao D.,(2003). Study on rheological behavior of polypropylene/clay nanocomposites, *J. Appl. Polym. Sci.*, 89, 3609

Li W., Huang Y.D., Ahmadi S. J., (2004). Preparation and properties of ethylene-propylene-diene rubber organomontmorillonite nanocomposites, *J. Appl. Polym. Sci.*, 94, 440

Liu B., Ding Q., He Q., Cai J., Hu B., Shen J., (2006). Novel preparation and properties of EPDM montmorillonite nanocomposites, *J. Appl. Polym. Sci.*, 99, 2578

Liu X., Wu Q., (2001). PP/clay nanocomposites prepared by grafting-melt intercalation, *Polymer,* 42, 25, Sep 17, 10013

Liu L.M., Qi Z.N., Zhu, X.G. (1999). Studies on nylon 6/clay nanocomposites by melt-intercalation process, *J. Appl. Polym. Sci.*, 71, 1133

Lopez-Manchado M. A., Arroyo M., Herrero B., Biagiotti J., (2003). Vulcanization kinetics of natural rubber-organoclay nanocomposites, *J. Appl. Polym. Sci.*, Vol. 89, 1-15.

Lopez-Manchado M.A., Biagiotti J., Kenny J.M., (2001). Rheological behavior and processability of polypropylene blends with rubber ethylene propylene diene ter-polymer, *J. Appl. Polym. Sci.* 81, 1

Makadia C. M., (2000). Nanocomposites of polypropylene by polymer melt compounding approach, University of Massachusetts

Makoto, K., Usuki A., Okada A., (1997). Synthesis of polypropylene oligomer clay intercalation compounds, *J. Appl. Polym. Sci.,* 66, 1781

Manias E., Touny A., Wu L., Lu B. Strawhecker, K., Gilman, JW., Chung, TC., (2000). Polypropylene silicate nanocomposites, synthetic routes and materials properties, *Polym Mater Sci Eng*, 82, 28.

Mehrabzadeh M., Kamal, M.R. (2004). Melt processing of PA-66/clay, HDPE/PA-66/clay nanocomposites, *Polym. Eng. Sci.,* 44, 6, 1152

Mehta S., Mirabella F., M. Rufener, K. Bafna, (2004). Thermoplastic olefin/Clay nanocomposites: morphology and mechanical properties, *J. Appl. Polym. Sci.,* 92, 2, 928

Martin P., Carreau P. J., Favis B. D., (2000). Investigating the morphology rheology interrelationships in immiscible polymer blends, J. Rheol., 44, 3, 569

Mighri F., Huneault M.A., Ajji A., Ko G.H., Watanabe F., (2001). Rheology of EPR-PP blends, *J. Appl. Polym. Sci.,* 82, 2113

Mishra J. K., Hwang K., Ha, C. (2005). Preparation, mechanical and rheological properties of a thermoplastic polyolefin (TPO)/organoclay nanocomposite with reference to the effect of maleic anhydride modified polypropylene as a compatibilizer, *Polymer*, 46, 1995

Mishra J. K., Ryou J., Kim G., Hwang K., Kim N., Ha C., (2004). Preparation and properties of a new thermoplastic vulcanizate (TPV)/organoclay nanocomposite using maleic anhydride functionalized polypropylene as a compatibilizer, *Mater. Letter.,* 58, 3481

Motomatsu M., Takahashi T., Nie H., Mizutani W., Tokumoto H, (1997). Microstructure study of acrylic polymer-silica nanocomposite surface by scanning force microscopy. *Polymer*, 38, 177

Munstedt H., (1981). Rheology of rubber modified polymer melts, *Polym. Eng. Sci.*, 21, 5, 259

Muller R., Graebling D., Palierne J.F., (1993). Linear viscoelastic behavior of some incompatible polymer blends in the melt, interpretation of data with a model of emulsion of viscoelastic liquids, *Macromolecules,* 26, 320

Naderi G., Razavi Nouri M., (1999). Studies on dynamic vulcanization of PP/NBR thermoplastic elastomer blends, *Iran. Polym. J.*, 8, 1, 37

Naderi G., Lafleur P.G., Dubois C., submitted to *Polym. Eng. Sci.*

Nam PH., Maiti P., Okamoto M., Kotaka T., Hasegawa N., Usuki A., (2001). A hierarchical structure and properties of intercalated polypropylene clay nanocomposite, *Polymer*, 42, 9633

Nassar N., Utracki L. A., Kamal M. R., (2005). Melt intercalation in montmorillonite polystyrene nanocomposites, *Intern. Polym. Process*, 4, 423

Neeraj K., Jain A., Singhal R., Nagpal A., (2000). Effect of dynamic crosslinking on tensile yield behavior of PP/EPDM, *J. Appl. Polym. Sci.*, vol.78, 2104

Nielson L.E., Landel R.E., (1994). Mechanical properties of polymers and composites, 2nd ed., Marcel Dekker, New York

Pantoustier N., Lepoittevin B., Alexandre M., Kubies D., Calberg C., Jerome R., Dubois P., (2002). Biodegradable polyester layered silicate nanocomposites based on polycaprolactone, *Polym. Eng. Sci.*, 42, 1928

Parija S., nayak S.K., Verma S.K., Tripathy S.S., (2004). Studies on physico-mechanical properties and thermal characteristics of polypropylene layered silicate nanocomposites, *Polym. Composite*, 25, 6, 646

Perrin-sarazin F., Ton-that M., Bureau M.N., Denault J., (2005). Micro- and nano-structure in polypropylene clay nanocomposites, *Polymer,* 46, 1

Perrin-Sarazin F., Ton-That M.-T., Cole K. C., Bureau M. N., Denault J. (2003). Polyolefin nanocomposites, Micro-nanostructure analysis, *international symposium on polymer nanocomposites science and technology,* Boucherville, Quebec, Canada, October 6, 8

Qin Z., Yong W., Qiang F., (2003). Shear induced change of exfoliation and orientation in PP MMT nanocomposites, *J. polym. Sci.: part B polym. Phys.*, 41, 1

Ren J., Silva As., Krshnamoorti R., (2000). Linear viscoelasticity of disordered polystyrene-poly-isoprene block copolymer based layered-silicate nanocomposites, *Macromolecules,* 33, 10, 3739

Rosedale J. H., Bates F.S., (1990). Rheology of ordered and disordered symmetric poly(ethylene-propylene)-poly(ethyl-ethylene) di-block copolymer, *Macromolecules,* 23, 2329

Schuster R. H., (1996). Selective interactions in elastomer, a base for compatibility and polymer-filler interactions, *Rubber Chem. Tech.,* 69, 5, 769

Shafiei S. S., Nazockdast H., Katbab A., (2004). Study on parameters affecting the morphology development of dynamically vulcanized thermoplastic elastomers based on EPDM/PP in a co-rotating twin screw extruder, *Rubber Chem. Tech.,* 77, 847

Shing-Chung W., Ling C., (2002). Mechanical and fracture properties of nanoclays filled polypropylene, *ANTEC* 1466

Silva A. N., Rocha M. C.G., Coutinho F.M.B., (2002). Study of rheological behavior of elastomer polypropylene blends, *Polym. Test.*, 21, 289

Solomon M.J., Almusallam A. S., Seefedt K.F., Somwangthanaroj A., Varadan P., (2001). Rheology of polypropylene/clay hybride materials, *Macromolecules,* 34, 1864

Sun T., Garces JM., (2002). High-performance polypropylene-clay nanocomposites by in-situ polymerization with Metallocene-clay catalysts, *Adv. Mater.,* 14, 128

Suprakas S. R., Masami O., (2003). Polymer/layer silicate nanocomposites: A review from preparation to processing, *Prog. Polym. Sci.*, 28, 11, 1539

Svoboda P. Zeng, C. Wang H. Lee L. J., Tomasko, D. L. (2002). Morphology and mechanical properties of polypropylene/organoclay nanocomposites *J. Appl. Polym. Sci.,* 85, 7, 1562

Takekoushi T.,Khouri F.F., Cambell J.R., Jordan T.C., Dai K.H., (1996). Layered minerals and compositions comprising the same, *U.S. patent* 5, 530, 052

Takumi A., White J. L., (1998). Shear viscosity of rubber modified thermoplastics: dynamically vulcanized thermoplastic elastomers and ABS resins at very low stress, *Polym. Eng. Sci.* 38, 4, 590

Thakkar H., Lee K. Y., Goettler L. A., (2003). Phase reinforcement effects in TPV nanocomposites, *ANTEC,* 3009

Tidjani A., Wald O., Pohl M., (2003). Polypropylene graft maleic anhydride nanocomposites: I Characterization and thermal stability of nanocomposites produce under nitrogen and air, *Polym. Deg. Stab.,* 82, 133

Ton-That M.-T., Perrin-Sarazin F., Cole K. C., Bureau M. N., Denault J. (2003). Polyolefin nanocomposites formulation and development, *international symposium on polymer nanocomposites science and technology,* Boucherville, Quebec, Canada, October 6, 8

Toshio I., Tokuhito S. (1995). Selective crosslinking reaction in polymer blends, *J. Appl. Polym. Sci.*, Vol. 56, 1113

Usuki A., Kawasumi M., Kojima Y., Okada A., Kurauchi T. (1993). Swelling behavior of montmorillonite cation exchanged for amino acids by caprolactam, *J. Mater. Res.*, Vol. 8, No. 5, 1174

Usuki A., Kato M., Okada A., Kurauchi T., (1997). Synthesis of polypropylene- clay hybrid., *J. Appl. Polym. Sci.*, 63, 137

Usuki A., Tukigase M., Kato M., (2002). Preparation and properties of EPDM-clay hybrids, *Polymer*, 43, 2185

Utracki L. A., Shi Z. H., (1992). Development of polymer blend morphology during compounding in a twin screw extruder, *Polym. Eng. Sci.*, vol. 32, no. 24, 1824

Vaia R. A., Ishii H., Giannelis E.P., (1993). Synthesis and properties of two-dimensional nanostructures by direct intercalation of polymer melts in layered silicates, *Chem. Mater.,* 5, 1694

Vaia RA., Giannelis DP., (1997). Polymer melt intercalation in organically-modified layered silicates: model predictions and experiment, *Macromolecules,* 30, 8000

Wang Z., Pinnavaia T. J., (1998). Hybrid organic Inorganic nanocomposites: exfoliation of magadiite nanolayers in an elastomeric epoxy polymer, Chem. Mater., 10, 1820

Wang Y., Chen F., Wu K., (2004). Shear rheology and melt compounding of compatibilized polypropylene nanocomposites, *ANTEC*, 1033

Wang Y., Chen F., Wu K., (2005). Effect of the molecular weight of maleated polypropylene on the melt compounding of polypropylene organoclay nanocomposites, *J. Appl. Polym. Sci.*, 97, 1667

Weibing X., Guodong L., Hongbo Z., Shupei T., Gopei H., Wei P., (2003). Preparation and crystallization behavior of PP/PP-g-MAH/Org-MMT nanocomposite, Europe. Polym. J., 39, 1467

Wolf D., Fuchs U., Wagenknecht u., Krezchmar B., Jehnichen D., Haussler L. (1999). Nanocomposites of polyolefin clay hybrids, in: processing of the Euro filler 99, Lyon-Villeurbanne, September 6, 9

Wu T., Chu M., (2005). Preparation and characterization of thermoplastic vulcanizate silica nanocomposites, *J. Appl. Polym. Sci.*, 98, 2025

Wu S., (1987). Formation of dispersed phase in incompatible blends: interfacial and rheological effects, *Polym. Eng. Sci.*, 27, 5, 335

Xiao H., Huang S., Jiang T., (2004). Morphology, rheology, and mechanical properties of dynamically cured EPDM/PP blends, effect of curing agent does variation, *J. Appl. Polym. Sci.*, 92, 357

Xu W., Liang G., Wang W., Tang S., He P., Pan, W. (2003). PP-PP-g-MAH-Org-MMT nanocomposites, I. Intercalation behavior and microstructure, *J. Appl. Polym. Sci.*, 88, 14, 3225

Yong T. L., Park O.O., (2001). Phase morphology and rheological behavior of polymer/layered silicate nanocomposites, *Rheol. Acta*, 40, 220

Yamaguchi M., (2001). Rheological properties of linear and crosslinked polymer blends, relation between crosslink density and enhancement of elongational viscosity, *J. Polym. Sci. Polym. Phys.*, 39, 228

Zheng H., Zhang Y., Peng Z., Zhang Y., (2004). Influence of clay modification on the structure and mechanical properties of EPDM montmorillonite nanocomposites, *Polym. Testing*, 23, 217